IChF
Institute of Physical Chemistry PAS

Scaling model for macroscopic viscosity analysis of polymer solutions.

Doctoral thesis

Airit Agasty

Supervisor: prof. dr hab. Robert Hołyst

The dissertation was prepared within the International PhD Studies at
the Institute of Physical Chemistry of the Polish Academy of Sciences
Department of Soft Condensed Matter and Fluids
Kasprzaka 44/52, 01-224 Warsaw

May 26, 2021

Declaration of Authorship

I, Airit Agasty, declare that this thesis titled, "Scaling model for macroscopic viscosity analysis of polymer solutions." and the work presented in it are my own. I confirm that:

- This work was done wholly or mainly while in candidature for a research degree at the Institute of Physical Chemistry, Polish Academy of Sciences.
- I state that I have exercised care to ensure that the work is original and contains no previously published material or written by another person, except where citations have been made in the text. To the best of my knowledge, the content provided here does not violate any copyrights.
- I accept that the Polish Academy of Sciences has the right to use plagiarism detection software to ensure the thesis's legitimacy.
- I certify that no part of my thesis has been or will be submitted for obtaining a degree or diploma by the Institute of Physical Chemistry, Polish Academy of Science, or any other educational institution.
- This thesis's copyright rests with me and no information derived from it may be published without my consent.

Signed: 

Date: 28.05.2021

Funding Sources

The present research was financed by:

- The European Union Horizon 2020 Research and Innovation Programme under the Marie Skłodowska-Curie grant agreement no. 711859 and the Polish Ministry of Science and Higher Education for implementing an international co-financed project in the years 2017–2021, grant agreement no. 3549/H2020/COFUND/2016/2.
- The Polish National Science Centre, for the Maestro grant, no. 2016/22/A/ST4/00017.

Abstract

Scaling model for macroscopic viscosity analysis of polymer solutions.

by Airit Agasty

Processing of polymeric materials in different types of industries require precise control over the flow of polymer solutions/ melts. This kind of control is possible when the material flow is properly characterized and investigated for internal structure-property relationships. Such relationships for complex liquids like polymer solutions contain internal length-scales (e.g., the radius of gyration or correlation length) influencing their rheological properties. Because of this internal structure, the viscosity of polymer solutions depend on the flow length-scale. Previous studies of nanoprobe diffusion in different polymer systems defined the effective viscosity experienced by those probes as a function of the probe size, the concentration of the system, the molecular weight of the polymers and the temperature of the surroundings. However, it was observed that when the probes had sizes extremely larger than the coil radius of the polymer, the flow was governed by the macroscospic viscosity instead of the nanoviscosity. The effective viscosity defined through the studies on various complex liquids such as: colloidal solutions, protein solutions, micellar solutions, cytoplasm of HeLa cells and E.coli, was still relevant to the study of macroviscosity. In this work, our goal was to use the effective viscosity to derive the macroscopic viscosity for different polymer systems that are commonly used: polydimethylsiloxane (PDMS) in ethyl acetate, hydroxypropyl cellulose (HPC) in water, polymethylmethacrylate (PMMA) in toluene, and polyacrylonitrile (PAN) in dimethyl sulfoxide (DMSO). Our experiments involved measurements of viscosity by rheometer for a wide range of polymer concentrations at different temperatures, hydrodynamic radii by dynamic light scattering (DLS), and molecular weight distributions and polydispersity index by gel permeation chromatography (GPC). We have extended the scaling model to cover concentrations from dilute to concentrated in solution; obtained relations between the coil dimensions as a function of concentrations; explained its applicability for commercial or standard polymers with diverse molecular weight distributions; clarified the reasons and means for the validity of this model regardless of the polydispersity of the polymer samples; and provided a final consolidated information about all the different parameters in our models. Rheology of polymer solutions suffers from the lack of a viscosity model applicable across wide range of variable parameters. Our characterization method provides the possibility to use a length-scale based polymer investigation technique based primarily on easily affordable viscosity measurements. Crucially, this technique will be effective for a wide variety of applications, both at the nanoscale and the macroscale.

Acknowledgements

The road to my Ph.D. has been the most challenging and yet the most rewarding experience of my life. I started my journey without knowing what FCS, confocal microscopy, or nanoscale viscosity was. And now here I am, writing a doctoral thesis for the completion of this degree. I owe this knowledge to the many incredible people I always had around me, and I would like to express my gratitude towards them.

Firstly, I would like to thank my guide, mentor and supervisor - Prof Robert Holyst, without whom I would not even had any Ph.D. I would like to thank him for all of his scientific ideas, discussion, counsel, and support in every matter, research related or personal. His open, kind, and friendly, yet strict attitude created a delightful atmosphere that allowed for effective timely communication, one of the key ingredients for my success. His inputs have shaped me into a better scientist, better scientific writer, better public speaker and into an overall more confident personality. I am truly grateful for having had this opportunity to work with him.

Next, I would like to thank my colleague Agnieszka Wisniewska for all her help and expertise regarding experiments, manuscript writing, and many more. She was always there for any discussion I needed to verify my work, and her approval of the research work was always a confidence builder. I thank her for putting me on to the right track every time I strayed away. I would also like to thank Dr. Tomasz Kalwarczyk for helping me out with crucial scientific discussion from the very first day, in spite of his busy schedule. Whether it was the theories related to any experiment, or the matter of learning scientific writing, he was always there to guide me with an open door and a smile. I would like to thank and acknowledge Prof. Hans-Jurgen Butt for providing the opportunity, invaluable advice during my stay at the Max Planck Institute in Mainz, Germany.. Of course, my time there would not have been successful without the guidance of my supervisor, Dr. Kaloian Koynov. I was incredibly lucky to have had the chance to work under him, and he always shared his tremendous expertise and provided an enjoyable and productive working environment at the MPIP.

I would like to thank my two colleagues and close friends, Dr. Krzysztof Sozanski and Krzysztof Bielec, without whom my life in Poland would have been incomplete. They always helped me out regarding any issues of technical knowledge, or theories, as well as providing me a social life. I would like to thank Patrycja Kuzma for helping me out with all the administrative issues for the duration of my Ph.D, professionally or personally. I am highly indebted to her. I would like to take this time to thank the different members of the Soft Matter group at IChF who over the years have helped me one way or another - Lukasz, Ying, Kasia, Grzegorz, Karina, Xuzhu, and Yirui, as well as all the members of the Physics at Interfaces group at the MPIP - Andreas Best, Andreas Hanewald, Sascha, Valeria and Lijun. I am grateful for the many laughs, beers, parties, and stories that we enjoyed together.

Finally, I would like to acknowledge the most important people in my life who live miles away, and yet without whose support and love I would not be who I am today - my parents. Their sacrifices, selfless patience, compassion, love, and guidance have shaped my career, and all my successes are credited to them.

List of Publications

Publications related to this thesis:

- **Agasty, A.**, Wisniewska, A., Kalwarczyk, T., Koynov, K. and Holyst, R., 2020. Scaling equation for viscosity of polydimethylsiloxane in ethyl acetate: From dilute to concentrated solutions. Polymer, 203, p.122779.
- **Agasty, A.**, Wisniewska, A., Kalwarczyk, T., Koynov, K. and Holyst, R., 2021. Macroscopic Viscosity of Polymer Solutions from the Nanoscale Analysis. ACS Applied Polymer Materials.

Other publications:

- Basu, D., **Agasty, A.**, Das, A., Chattopadhyay, S., Sahu, P. and Heinrich, G., 2020. Phase changing stearate ions as active fillers in multifunctional carboxylated acrylonitrile–butadiene composite: Exploring the role of zinc stearate. Journal of Applied Polymer Science, 137(2), p.48271.

Contents

List of Figures

List of Tables

List of Abbreviations

DMSO	dimethyl sulfoxide
DLS	dynamic light scattering
GPC	gel permeation chromatography
HPC	hydroxypropylcellulose
PAN	polyacrylonitrile
PDMS	polydimethylsiloxane
PEG	polyethylene glycol
PEO	polyethylene oxide
PMMA	polymethylmethacrylate
SSE	Stokes-Sutherland-Einstein

Physical Constants

Avogadro's number	$N_A = 6.022\ x\ 10^{23}$ mol^{-1}
Boltzmann constant	$k = 1.38064852\ x\ 10^{-23}$ m^2 kg s^{-2} K^{-1}
Gas constant	$R = 8.3145$ J mol^{-1} K^{-1}

List of Symbols

η	viscosity	Pa s
η_0	solvent viscosity	Pa s
ξ	correlation length	nm
γ	activation energy	kJ/mol
β	mean field theory exponent	
a	scaling parameter	
c	concentration	g/ml
c^*	overlap concentration	g/ml
c^{**}	2nd crossover concentration	g/ml
R_g	gyration radius	nm
R_h	hydrodynamic radius	nm
T	absolute temperature	K

Dedicated to my parents

Chapter 1

Introduction

1.1 Polymer Fundamentals

For long times, the attention of scientists, and chemists, in particular, were engaged towards an indefinable class of materials, referred to by Graham as 'colloids' in 1861. They were different from crystalline organic materials with a varying range of molecular weights. Chief amongst them were natural substances such as Gum-Arabic which were common as early as the 9th century, and was soluble in water but could not pass through a semi-permeable membrane. Another common example of such materials was natural rubber, used in applications such as waterproofing textiles. Yet, it was only at the start of the twentieth century that the idea of these materials having large molecular weights due to a widespread internal network of repeating units was advocated strongly by Staudinger. Over time, such materials came to be known as **polymers**, derived from the Greek words 'polus' (meaning 'many' or 'much') and 'meros' (meaning 'part').

Polymers have been researched in great depth over the last few decades, resulting in numerous applications for every sphere of life. Polymers consist of several structural repeating units connected by a chemical bond, which are usually covalent in nature. One of the most common examples of polymer in everyday use is polyethylene, a linear chain structure commonly represented as:

$$-CH_2CH_2CH_2 - or[-CH_2CH_2-]_n \tag{1.1}$$

where the repeating unit is [-CH_2CH_2-] and n represents the number of repeating units in the polymer chain. n is also known as the degree of polymerization and represents the chain length of the polymer. Such polymers are usually synthesized chemically through reactions of the smaller individual organic molecules, also termed as **monomers**. For example, the monomer used for synthesis of polyethylene as shown above in Eq1.1 is ethylene. In order to perform such synthesis of polymers, the monomeric materials should have reactive functional groups, or have unsaturated bonds (double or triple bonds) in their chemical structure. They ensure the necessary reactionary pathways for the linkage between the repeating units.

Polymers can be classified under a wide number of categories:

- Molecular structures - Depending upon the orientation of the polymer chains, they can be either linear, branched or network.
- Monomer type - Depending upon the type of repeating unit in the chains, polymers can be classified as homopolymers, copolymers or graft copolymers.
- Polymerization mechanism - Depending upon the reaction mechanism for synthesis of the polymers, they can be classified as addition polymers or condensation polymers.

- Polymerization technique - Based upon the technique used for their synthesis, polymers can be divided under emulsion, solution, suspension, etc.
- Physical properties - Finally, depending upon the glass transition temperature, T_g, of the polymers, their physical properties vary, and this allows to classify them as:

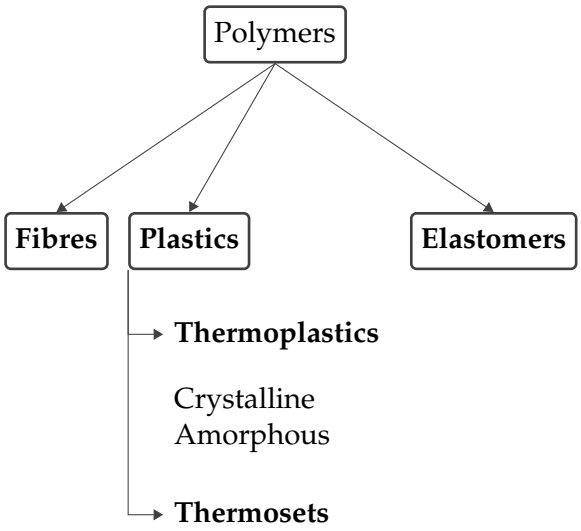

Polymer characterization and differentiation through thorough analytical methods is therefore a necessity, since no other class of materials can rival them in terms of property diversity, processing flexibilities and costs. In an impressive array of applications, polymers showcase high quality of performance which is an essential and extremely challenging feature for any material. The importance of polymers is key to any material development and require detailed studies which are discussed in the following sections.

1.2 Rheology of polymers

The field of rheology ranges in material characteristics from perfectly viscous fluids (Newtonian fluids) to perfectly elastic solids (Hookean solids). In a perfect world, these two extremes are emphasized by two models - the Euclidean solid, which depicts infinite modulus, and the Pascalian fluid, which flows perfectly and has a zero viscosity. Most real world materials straddle between these two unrealistic extremes and are therefore termed as viscoelastic materials. This is because when complex materials such as polymers are deformed, there are elements of both elastic and viscous forces in such deformations. In 1929, Eisenschitz et al [1] introduced a triangular coordinate system depicting the rheological boundaries. They proposed that the total energy in rheological considerations consists of three components - the kinetic energy, the stored energy due to elastic nature, and the loss of energy due to dissipative viscous forces. It was simply an easy way of describing the state existing inside a body through its total energy. In this triangular representation, boundaries of elasticity, viscosity and the corresponding relaxation forces represents the different rheological properties which are crucial to the study of any polymeric materials.

1.2.1 Types of fluid flows

All fluid flows can be broadly categorized into two types:

- Newtonian fluids - The first person to ever discuss the property of resistance to motion in fluids, thereafter known universally as **viscosity**, was Sir Isaac Newton. He spoke of layers of fluid 'slipping' over each other and the resistance that occurs between the layers due to lack of this slipping ability. This internal friction of the fluid layers is proportional to the distance between the layers. For a simplified system of two parallel plates representing the two layers of

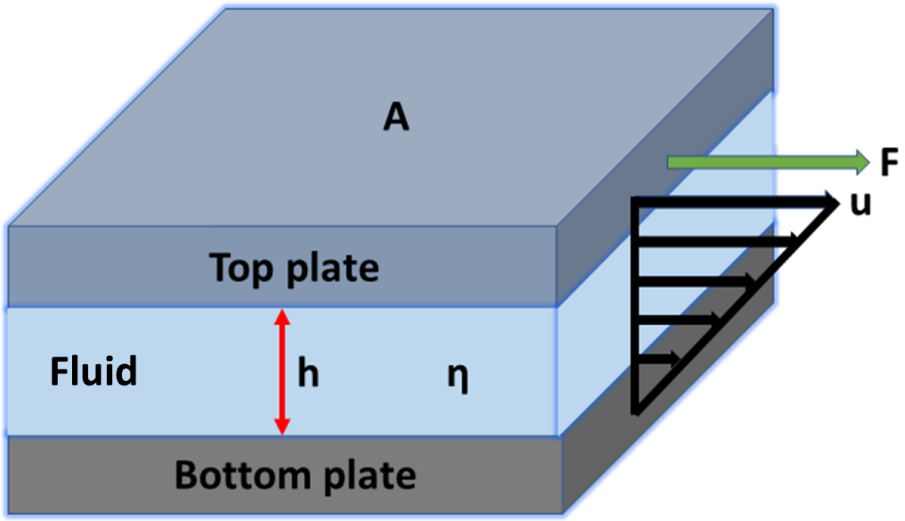

FIGURE 1.1: Simple shear flow

fluid, separated by a distance h, the top plate is pulled in one direction by a force F to maintain motion between the two plates, and is proportional to the velocity difference between the plates u, the plate cross-sectional area A, and inversely proportional to the distance h. From this proportionality arises the parameter η known as the viscosity of the fluid and is commonly calculated as:

$$\eta = \frac{F/A}{u/h} \tag{1.2}$$

where the viscosity η has units of Pa.s. The ratio $\frac{u}{h}$ is the derivative of the fluid speed in the direction perpendicular to the plates, and is the rate of shear deformation or shear velocity. If the velocity does not change in a linear manner as h increases, then the appropriate generalization is:

$$\eta = \frac{\tau}{\frac{\partial u}{\partial h}} \tag{1.3}$$

where τ=F/A is the shear stress, and $\frac{\partial u}{\partial h}$ is the local shear velocity or shear rate. This expression is known as the Newton's law of viscosity. This is a constitutive equation: it is not a fundamental law of nature but an approximation, and therefore it is valid for certain materials while it completely fails for others. Materials that obey the Newton's law are known as Newtonian fluids while those that do not are known as non-Newtonian fluids.

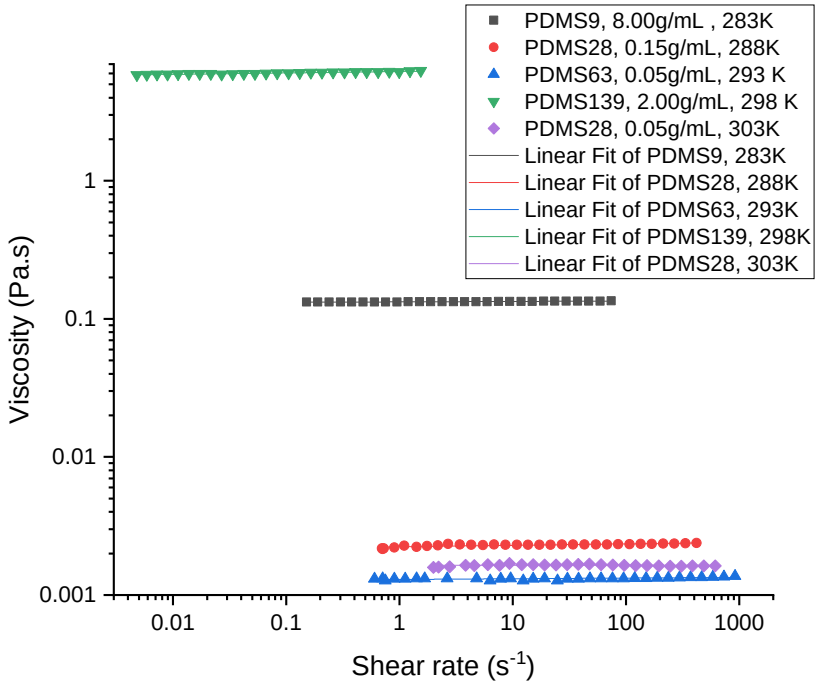

FIGURE 1.2: Checking the Newtonian nature of our studied PDMS-ethyl acetate system. Results taken from the supplementary information of our published results [2].

Common examples of fluids with Newtonian characteristics being used in everyday life include water (η = 0.89 mPa s at 25°C), rice bran cooking oil (η = 40 mPa s at 38°C) and honey or corn syrup (η = 2000-3000 mPa s at 22°C).

- Non-Newtonian fluids - In any three-dimensional flow, the stress components can be identified across all three planes xy, yz and zx when investigated across a cartesian coordinate system. In Newtonian fluids, this shear stress is present across only one plane, with all other components of stress being equal to 0. For many polymeric systems in applications, this simple shear data relating the shear stress to the shear rate does not start from 0, or is not a linear relationship, or both. For this reason, the viscosity η is not a constant parameter due to shearing forces. It also depends on the type of fluid being studied and its kinematic history. Ideally, for such behaviour, these fluids can be further sub-classified into different types, depending upon their nature. However non-Newtonian fluids are not the subject of our study, and so is not discussed in any great detail here.

Fig 1.2 shows that the polymer-solvent systems studied in this research exhibited Newtonian nature in their flow characteristics across a varying range of shear rates. The Newtonian nature of the other polymer systems studied are shown later in Chapter 4. The following chapters will also deal with the development of a scaling model based on these Newtonian viscosities.

1.2.2 Importance of viscosity studies

As already mentioned, **viscosity** is a measure of the resistance experienced by any fluid due to its flow. The higher the internal friction of a fluid, the more resistance it

provides to any deforming forces, and the higher is the viscosity of the given fluid. The viscosity of different fluids is usually studied through the field of rheology, the part of science that describes the flow of materials. Of course rheology is not only about the study of viscosity, but also about the other crucial behaviour exhibited by many complex liquids, namely their **elasticity**. This expression of the elastic nature leads to the term 'soft matter' being used for description of complex fluids such as polymers.The method of identifying the type of behaviour seen from different types of polymer flows, even simple linear flows, is by their rheological measurements. However, the elastic nature is not a source of concern for us, as our studied viscosities were completely Newtonian.

Aside from such complex behaviour, the common viscosity measurements of different fluids suffers from a lack of understanding of the length-scale. For simple fluids such as water, it is not a problem. But for fluids such as polymers, there also exists one of the simplest and most important characteristic - an observable microscopic time scale. The time scales of molecular motion in regular liquids like water are in the order of 10^{-15} s, and are associated with molecular translation. Apart from this microscopic time scale, polymeric liquids have another important scale that correlates their larger internal or external motions in solution with another liquid. This time scale ranges from microseconds to minutes. The ratio of these time scales becomes significant since many physically visible and processing time scales are of similar order. The elastic nature of polymeric liquids is usually associated with large scale microscopic motions. Even though our studies are not concerned about the elastic nature of polymeric objects, it is still crucial to study the different scales existing within a wide variety of polymers. As a result, it is critical to obtain well-defined scaling laws that describe polymers appropriately.

1.2.3 Generalized Newtonian fluid models for non-Newtonian fluids

A generalized Newtonian fluid (GNF) is an idealized fluid in which the shear stress is a function of shear rate at a given time but not of deformation history. The constitutive equation of this type of fluid is a generalized form of the Newtonian fluid, despite the fact that it is non-Newtonian (i.e. non-linear) in nature. There are numerous available GNF models describing the dependence of polymer viscosity on the variations of shear rates, temperatures and pressures [3]. These include the Power law model [4, 5], the Bird-Carreau-Yasuda model [6, 7], the Cross-WLF model [8], the Bingham model and the Herschel-Bulkley model. They are very similar in their description, and are useful for numerical simulations or any application involving higher shear rates. However, as our results have shown that the viscosity studied is not dependent on the shear rates, our study will not involve any of these GNF models.

1.3 Necessity of scaling models

Our understanding of the behavior of long, coiled, flexible macromolecules is based on important scaling concepts. With increase of the chain length or molecular weight M to sufficiently larger quantities, there occurs enhancement of multiple internal properties. This includes properties such as coil dimensions and relaxation times. These changes occur regardless of the chemical composition of the different polymers. Such enhanced internal properties affect the characteristics of a polymer, one

of the most important one being their viscosity. Therefore study of viscosity for polymer solutions usually require certain scaling laws. The reasons for the necessity of having such scaling laws are:[9]:

- Individual coil statics - The first problem that arises in polymer physics is due to the construction of linearly connected flexible individual polymer coils from multiple monomer units. As well as being connected, the units will also have interactions which are not specific to adjacent members of the sequence: whether it be the excluded volume constraint that two monomers cannot be at the same place, Van der Waals forces (longer ranged and canonically attractive) between monomers in pure polymers, or in solution systems where there are energies of solvation, monomer-monomer contacts differing in energy from monomer-solvent ones, etc. Such a system of interaction is represented in Fig 1.3.

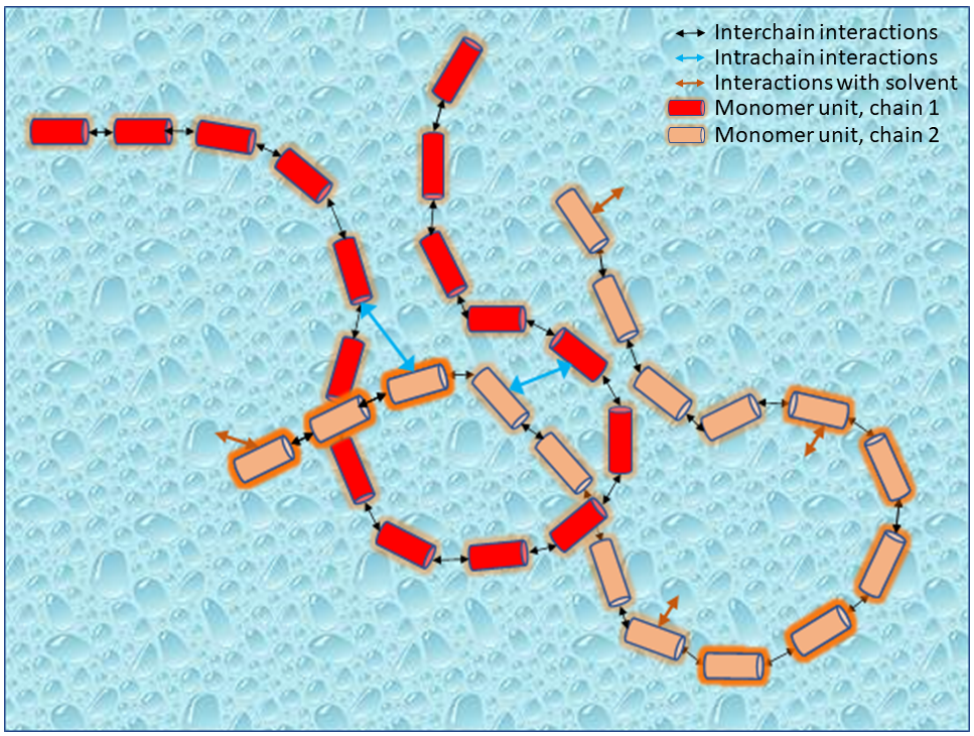

FIGURE 1.3: Individual polymer coils in solution.

- Coil swelling - Flory[10] addressed the problem of polymer chain conformations by considering the case of a polymer in a good solvent. The corresponding model allowed to obtain the chain's total free energy without the need to count every possible chain conformation. An estimate of the chain's optimum end-to-end distance could be determined from the minimum free energy of the chain. Flory's theory also assumed that ideal chains have a Gaussian distribution of the end to end distance, which can be summarized as:

$$\langle r^2 \rangle^{\frac{1}{2}} = N^{\frac{1}{2}} l \tag{1.4}$$

where r is the end to end distance, N is the number of monomers, and l is the contour length of the chain. The corresponding description of the free energy

for a monomer of length b was:

$$\Delta E = k_B T \frac{r^2}{Nb} \tag{1.5}$$

where k_B is the Boltzmann contant, and T is the temperature in the absolute scale. However, it was later observed that this approach needed to be changed for swollen systems[11, 12]. Larger polymer coils are spread over larger volumes, and thus they rarely occur as a dilute state in solution. When chains have repulsive interactions, they no longer remain ideal. The chains have an effective repulsion between the surrounding monomers that tend to swell the polymer chain. The entropy loss that occurs due to such a deformation resulting from the swelling acts as a balance to the monomeric repulsions. Therefore, studies of polymer solutions require detailed investigation to describe their characteristics during flow. The Fig 1.4 shows the simple state of polymer coils in the presence of a solvent, while the Fig 1.5 shows an example of an ideal Gaussian chain.

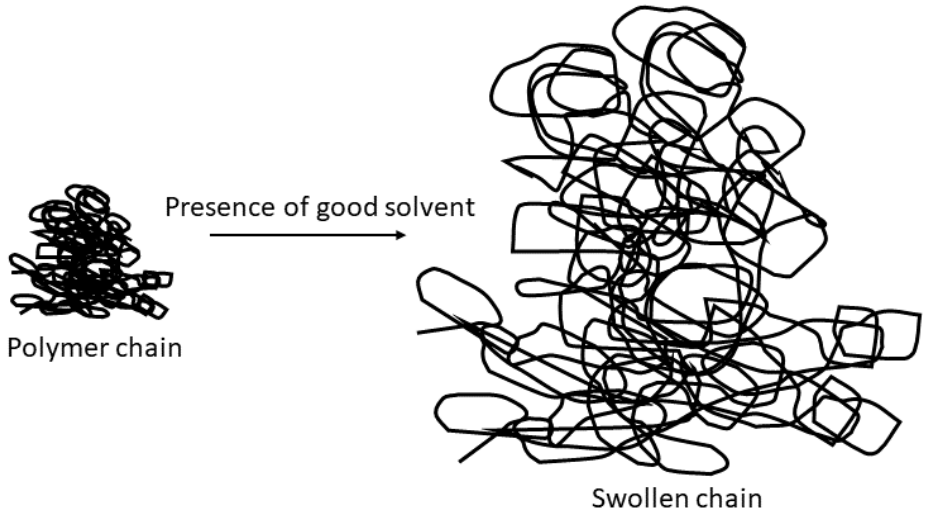

FIGURE 1.4: Coil swelling in the presence of a good solvent.

- Entanglements due to solution concentrations - When the concentration of polymer coils in a solution increase, they start to overlap and then intertwine with each other. Looking at the entangled zone, it turns out that this regime requires proper investigation in terms of a blob scaling picture. Physically, the blob size ξ may be identified as a correlation length of the polymer density variations. This semi-dilute behaviour does not extend all the way to the polymer melt because eventually ξ comes down to the scale of the screening length. Screening cannot then further reduce coil dimensions and there exists a concentrated regime where the chain conformations are fairly independent of concentration. In the concentrated regimes, as the monomer concentration becomes larger, other higher order effects take over. The following Fig 1.6 shows the internal characteristics of an entangled system. Such a system affects the viscosity, and requires proper description.

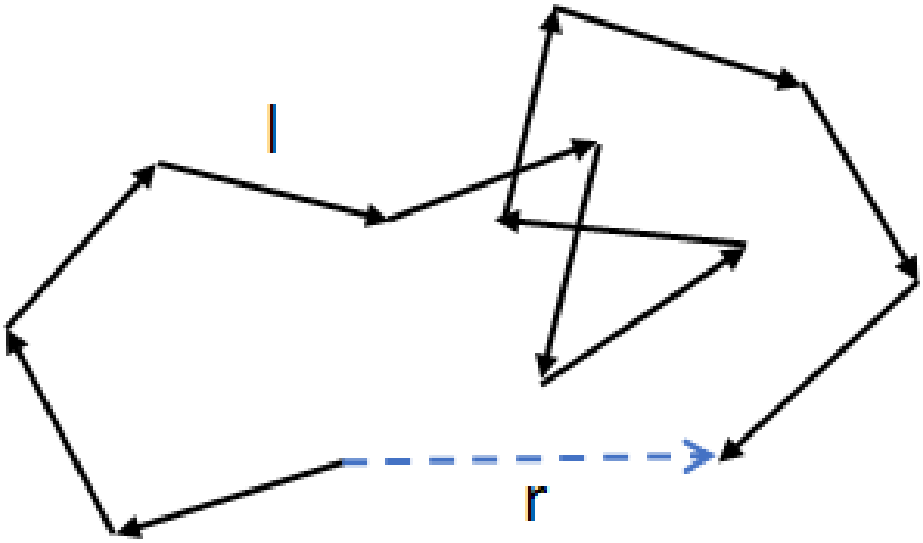

FIGURE 1.5: An ideal Gaussian chain of end-to-end distance r.

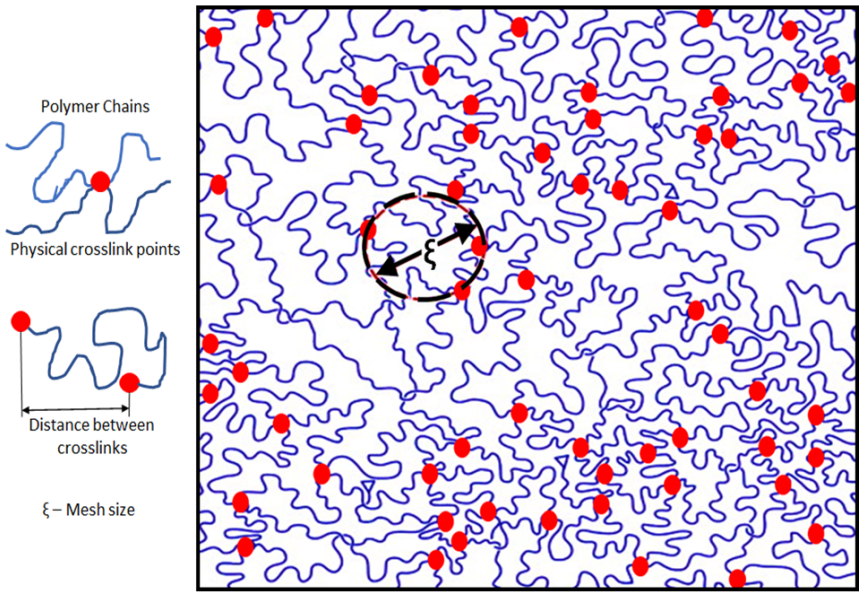

FIGURE 1.6: Entanglement network inside a polymer solution.

- Molecular-weight effects - Viscosity is also greatly affected by the change in the molecular weight of the polymer studied. The greater the molecular weight of the polymer chains, the greater is the resulting entanglements inside the polymer solutions. Due to increased amount of entanglements, the motion of the chains becomes more hindered accordingly, leading to corresponding changes in the flow nature. This is represented by Fig 1.7. Thus a core problem for polymer scaling is the molecular weight exponent of the viscosity, as well as the difficulties of measuring high viscosities.

Based on the above considerations, a number of theoretical models have been developed over the years that predicts the viscosity of polymer solutions. Some of the

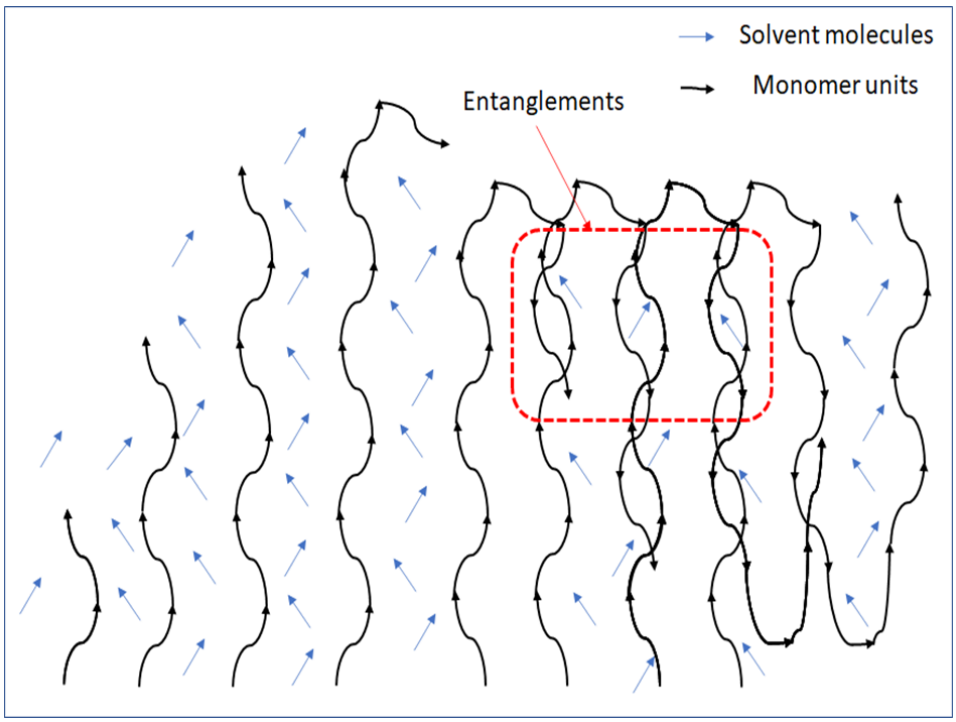

FIGURE 1.7: Simplified view of molecular weight effect in polymer solutions. As the number of monomers and hence the molecular weight of the chains increase, the number of entanglements increase. Consequently, it becomes harder for the chains to move under the influence of the solvent.

more relevant models in relation to our work have been discussed in the following sections.

1.4 Influence of polymer motion on the viscosity

Before studying the models that describe the flow characteristics of polymer solutions, it is important to get an idea about how the polymer chain motion affects their viscosity. Many theoretical models have been developed over the years for the description of polymer chain motion. Some of the common models on the motion of polymer chains are described in this section.

1.4.1 Single chain models of Rouse and Zimm

Rouse defined a model describing the viscosity of polymer chains based on defining single polymer chain dynamics. In his approach, he considered the macromolecules as represented by linear chains of "beads" connected by Hookean "springs" [13]. In such cases, all local chemical details such as energy of interactions for different monomers were completely avoided[14]. This allowed a simple polymer chain description using a small number of parameters. Such chains were basically treated as ideal ones, and could be described either discretely or continuously. One such discrete method involved dividing the contour length of the polymer chains L into different segments N known as **Kuhn** segments [15], with each of a constant length b, such that:

$$L = Nb \tag{1.6}$$

The representation is shown accurately in Fig 1.8. The solvent molecules surround-

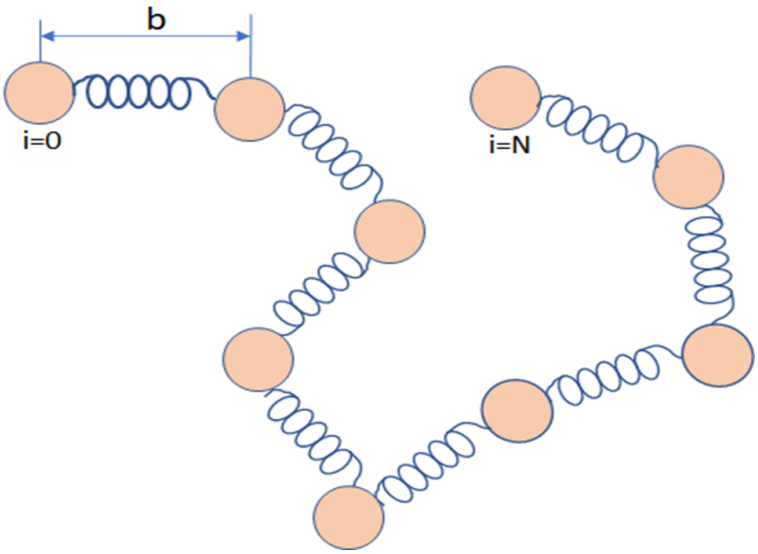

FIGURE 1.8: Simplified representation of the Rouse model for polymer chains.

ing such polymer chains in solution were studied through some effective interactions, due to their collision with the polymer molecules. Such collisions resulted in Brownian motion of the polymer molecules. By studying the random motion, the viscosity of the polymer solution was determined. It was assumed that the different separated parts of chain did not have any hydrodynamic interactions between them. This allowed the studied flow to be assumed as a Stokes flow. As described by George Stokes, such a flow involves an object moving through a fluid and experiencing opposing forces to its direction of motion. In such a case, the viscous forces are larger compared to inertial forces, and leads to very low fluid velocities. By studying the velocity of the moving object, the viscous forces and the viscosity of the fluid are obtained. The relationship between the viscous forces and viscosity is $F = 6\pi\eta r v$, with F being the viscous forces, η the viscosity, v the flow velocity of the object, and r the size of the object.

As per the Rouse description, the individual segments effectively acted as a local spring with a spring constant defined though the Kuhn length. Accordingly, the viscosity of the polymer solution was defined as [13, 16]:

$$[\eta] = \frac{\pi N^2 b^2 r c}{6} \tag{1.7}$$

where $[\eta]$ is the polymer chains' intrinsic viscosity, c is the number of polymers per unit volume, and r is the radius of each bead. As can be seen from the Fig 1.8, the molecular weight of the polymer was directly related to the chain length and number of segments N. The Rouse model was improved by Zimm [17], who included the fact that the beads of the polymer chains affect the solvent's velocity region. These disturbances travel through the solvent and affect the movement of the other beads. This results in the hydrodynamic interaction between the beads. As per Zimm's theory, the intrinsic viscosity at steady state could be described as [16, 17]:

$$[\eta] \propto (Nb^2)^{\frac{3}{2}} \tag{1.8}$$

where m is the mass of the polymer in the solution. The chain length (and number of segments N) provided the relationship between the viscosity and the molecular weight of the polymer. However, as the length of the polymer chain (and thus the number of beads in the chain) grew longer, the model became increasingly complicated. This involved a large number of individual models for each individual chain. As such, it was not feasible to describe the viscosity accurately.

1.4.2 Reptation model of Doi and Edwards

Doi and Edwards[18, 19, 20] developed a theory for the diffusion of rigid rods in a densely crowded environment. The assumptions made in this model were of the same nature as that for flexible chain motion in the theory of **reptation**. When flexible polymers acquire a coiled conformation, their behaviour in a network is dominated by steric interactions. This prevents them from occupying the same space at the same instant[14]. In such a network, the free movement of a single flexible polymer chain is restricted, essentially confining the polymer chain to smaller spaces between the other surrounding chains. The polymer is characterised by an effective segment length known as the blob size, which was defined previously as the correlation length ξ (Fig 1.6). This definition was obtained from the concept of entangled systems in the de Gennes' scaling theory[12]. The movement of the polymer chain was assumed to be through an approximately confined tube-shaped region. The dominant relaxation mechanism of this model was through changing of the tube, observed when the polymer chain completely retracts from a part of the tube, as shown in Fig 1.9. Reptation model therefore required that the concentration was

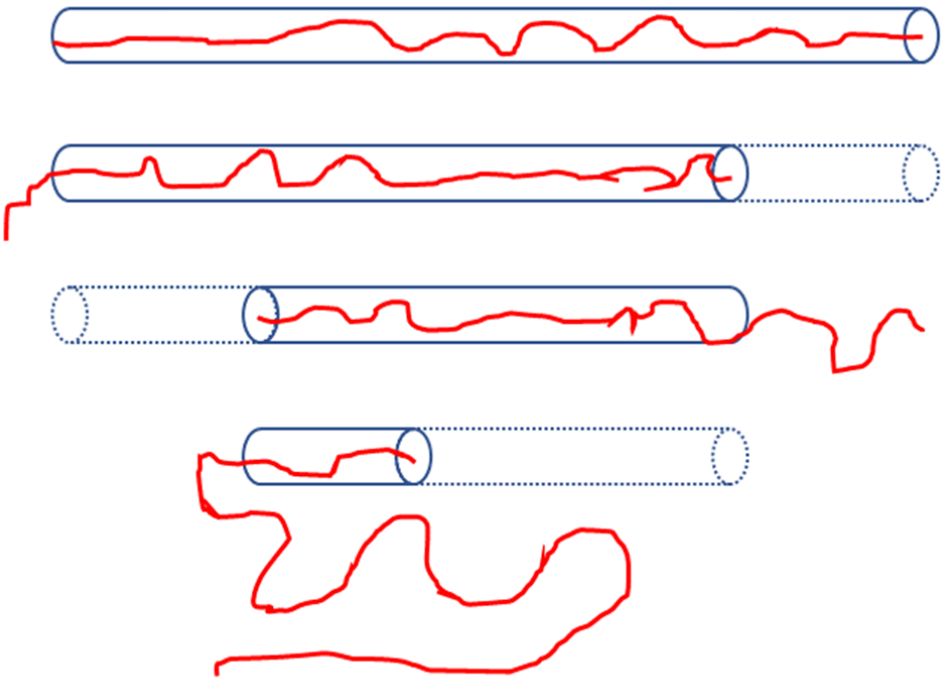

FIGURE 1.9: Reptation model: Decomposition of the tube resulting from the reptative motion of the polymer chain. The parts of the empty tube disappear.

large enough for neighboring polymer coils to overlap each other and form entanglements. As a result there is a lowest concentration c*, the overlap concentration,

below which tube model/reptation models are inaccurate. Lower solution concentrations of c < c* are defined as the dilute regime, while concentrations c > c* consists of the semidilute, entangled, and concentrated regimes.

In the thory of Doi-Edwards, all rods were assumed to have free rotations without any interactions with the other rods. When the finite diameter of a stiff polymer chain was taken into account, it resulted in a very dense system of elongated objects. Such objects with diameter d and length L exhibited an excluded volume interaction between them. This interaction resulted in the alignment of the objects. Doi [19] postulated that the finite length of the chain causes the length of the tube to fluctuate over a range L. The molecular weight M of the polymer chain is therefore related directly to the length L. The hydrodynamic volume here becomes that of the sphere spanned by the rod-like molecule in its Brownian rotation, hence growing with M^3. This effect when fitted against the experimental data on viscosity η as a function of M, gave a corrected form of the viscosity model as:

$$\eta \propto \eta_0(1 + f(M^{3.4})) \tag{1.9}$$

by relating the relaxation times of the chains experimentally to the molecular weight. In this model it was ensured that the radius of the effective constraining tube was much smaller than the contour length. However, this model was valid for a limited number of molecular weights. The effect of variations in tube length on the viscosity was not correctly identified. Corrections were claimed by Rubinstein [21] for the diffusion characteristics of the chains. He proposed a reptation model that was "discretized." A one-dimensional lattice was used to model the tube, and segments called as "reptons" were used to model the polymer. Each repton represented a link in the chain and was free to hop between sites, but the chain remained connected at all times. The length and molecular weight considerations were the same as that of Doi and Edwards theory. The diffusion characteristics varied accordingly as:

$$D \propto M^{-2}[1 + f(M^{-1})] \tag{1.10}$$

where D was the diffusion coefficient of the chains. This model was also signified by a relaxation time due to the disentanglement of the flexible chains. The viscosity was maintained of the same order as described by Eq 1.9. However, newer obstacles were formed with additional processes changing the orientation of the tube. The biggest drawback of this scaling model was that in a real system, especially in a polymer solution, a completely rigid rod is impossible to be realized. Thus this model was not as accurate for describing the viscosity characteristics of polymer solutions of varying parameters.

1.4.3 Extended Kirkwood-Riseman model for viscosity

This model applies to time scales that are long enough to ignore polymer inertia. The solvent is addressed as though it were a continuous fluid. Each polymer chain is modeled after a string of beads that interacts with the solvent through a series of point forces. The point forces allow the solvent to flow, resulting in hydrodynamic forces on the other polymer beads. The underlying hydrodynamic interactions depend on the interchain distances [22, 23, 24, 25, 26, 27]. Phillies et al [28, 29] made some modifcations to the theory of hydrodynamic interactions of the Kirkwood-Riseman model and made it applicable to predict the viscosity of the polymer solutions. They proposed that polymer beads are often in close proximity to other polymer beads in the same chain. Solvent molecules easily penetrate polymer coils

at concentrations below the overlap concentration, but interpenetration of polymer chains do not occur as much. As a result, adding polymer molecules to a dilute solution is more efficient at slowing the motion of free monomers than it is at slowing the motion of polymer chain monomer units. At polymer concentrations above the chain overlap concentration, the total polymer concentration is the same everywhere in solution. A chain's correlation length, on the other hand, ensures that the concentration of other chains close to it is often smaller than the average concentration of chains in solution. Consequently, interchain interactions have a smaller impact on the mobility of a polymer bead than they do on the mobility of a free monomer in solution. Using this modification, they predicted the viscosity model to be:

$$\frac{\eta}{\eta_0} = 1 + [\eta]c + k'[\eta]^2c^2 \tag{1.11}$$

where k' is the Huggins coefficient. The difficulty this model faced was that as concentrations increased, more and more terms were required to achieve accurate predictions. Simultaneously, the scale of the calculations needed to obtain additional forms grew rapidly.

1.5 Developed macroscopic viscosity scaling models

Polymer solutions have a wide variety of macroscopic viscosity scaling models, which can be found through literature studies. Huggins[30] suggested the first example of such a scaling model, developed for the specific viscosity of very dilute polymer solutions. Huggins' relationship may be summarized as follows:

$$\eta_{\text{macro}} = \eta_0 \left(1 + k'[\eta]c\right) \tag{1.12}$$

with k' being an empirically determined polymer-solvent constant and c being the concentration of polymer solutions. The intrinsic viscosity, $[\eta]$, is an indicator of the viscosity's concentration dependency. This model was developed by calculating viscosity at extremely low dilutions, and it was also backed up by others [31, 32, 33, 34, 35, 36] such as Baker:

$$\frac{\eta}{\eta_0} = (1 + [\eta]c)^{0.5\text{k}'} \tag{1.13}$$

Fikentscher and Mark:

$$\frac{\eta}{\eta_0} = \frac{[\eta]c}{1 - k'c} \tag{1.14}$$

and de Jong, Kruyt and Lens:

$$\frac{\eta}{\eta_0} = [\eta]c\exp(k'c) \tag{1.15}$$

All these different viscosity models were essentially of the same form as the one above by Huggins. The empirical constants k' had different values for each model, but of the same order. These models also contained some empirical constants specific to each model, but the form of each model were similar. Some other such models were proposed by Arrhenius [37]:

$$ln\frac{\eta}{\eta_0} = \frac{k'c}{2} \tag{1.16}$$

Hess and Philippoff [38]:

$$\frac{\eta}{\eta_0} = \left(1 + \frac{7k'c}{16}\right)^8 \tag{1.17}$$

and Bredee and de Booys [39]:

$$\frac{\eta}{\eta_0} = \left(1 + \frac{5k'c}{12}\right)^6 \tag{1.18}$$

again, with empirical constants k' having different values but of similar orders for each model. More importantly, these studies looked at how the viscosity of polymer solutions varies with their concentrations only in the dilute regime.

In polymer solutions of varying concentrations, crowding plays a massive effect on the resultant flow properties. If polymer coils are assumed to be spherical in size, the resultant solutions can be analogous to rigid spherical particles in an emulsion. Taking explicit notice of the interactions between neighboring spherical particles, a number of theories were developed to describe the viscosity of systems. These theories applied functional relationships for the dependence of the viscosity of rigid sphere suspensions to the volume fraction ϕ. The parameter ϕ is defined as the ratio of the volume of polymer used to prepare the solution to the total sum of the volumes of polymer and the solvent in the solution. Some of the proposed models were by Eilers [40]:

$$\frac{\eta}{\eta_0} = \left(\frac{1 + 0.5[\eta]\phi}{1 - \phi/\phi_m}\right)^2 \tag{1.19}$$

Mooney [41]:

$$ln\left(\frac{\eta}{\eta_0}\right) = \frac{[\eta]\phi}{1 - \phi/\phi_m} \tag{1.20}$$

and Krieger-Dougherty [42]:

$$\frac{\eta}{\eta_0} = (1 - \frac{\phi}{\phi_m})^{-[\eta]\phi_m} \tag{1.21}$$

where ϕ_m is the maximum packing volume of the system (the maximum volume of polymer that could be dissolved into a given volume of solvent), and $[\eta]$ is the intrinsic viscosity of the solution, related to the particle shape factor. As can be seen from these Eqs 1.19-1.21, the models described were accurate at defining the viscosity for a wide range of concentrations as well as the composition of the system. But they lacked in defining the effects of varying polymer molecular weight and chain sizes, internal dimensions of the polymer matrix, and crucially unsuitable for any length-scale dependence description.

Lyons and Tobolsky [43] had also proposed an empirical equation that has been shown to describe the viscosity of low molecular weight polymer solutions over the entire concentration range, i.e., from infinite dilution to bulk polymer. The Lyons model [44] was:

$$\frac{\eta}{\eta_0} = c[\eta] \exp \frac{k'[\eta]c}{1 - bc} \tag{1.22}$$

where k' is the Huggins' constant and b is some empirical parameter related to the concentration c. This model was amongst the first to describe the viscosity as an exponential function of the concentration. However, it also lacked in application to polymers of higher molecular weights. Another model of similar exponential

dependence was that developed by Martin [32]:

$$\frac{\eta}{\eta_0} = 1 + c[\eta]\exp(k_M c[\eta]) \tag{1.23}$$

where k_M was the Martin constant, an empirical paramter of the same order as the Huggins constant. It was also limited in applicability for solutions of low concentrations.

Of course, viscosity of polymers in solution does not depend only on the concentration. A lot of models tried to shed light on the dependence of viscosity on the molecular weight of the polymers [45], starting with Dreval et al [46]. In their relationships, they made assumptions for flexible polymers related to the intrinsic viscosity and concentrations (in the dilute solution ranges), where their function was of an exponential nature. Their model was later applied to the rigid, inflexible polymer chains, in particular poly(*p*-benzamide) (PBA)[47, 48]. They defined the viscosity η for a large number of flexible polymers in solution as:

$$ln\left(\frac{\eta}{\eta_0}\right) = KM^{\alpha}c^{\beta} \tag{1.24}$$

About the same time, Mark-Houwink[49, 50] formed a relationship that was similar to this one. The obtained dependency of viscosity to the molecular weight was:

$$[\eta] = KM^{a'} \tag{1.25}$$

where K was another empirical constant, similar to the empirical parameter developed by Huggins and a' is known as the Mark-Houwink parameter. The constants α, β and a' were related as a'=α/β. The difference was that in their definitions, they used intrinsic viscosity rather than specific viscosity. Further research by Barry [51], Korolev et al [52] and Warrick et al [53] established empirical viscosity scaling models that relate the dependence of viscosity on polymer molecular weight

Weissberg, Simha, and Rothman [54] used the dimensionless plots of $[\eta/\eta_0]$/c$[\eta]$ versus c$[\eta]$ to represent their viscosity-concentration data and noted molecular weight and solvent dependences in polystyrene solutions. Simha and Zakin [55], using similar variables, attempted to correct for the solvent dependence by considering the effect of concentration on the osmotic compression of expanded polymer coils in solution. Utracki and Simha [56, 57, 58] superimposed viscosity-concentration curves for different molecular weights by plotting $[\eta/\eta_0]$/c$[\eta]$ versus c/M^{-a1}, where $a1$ was of the same order as the Mark-Houwink exponent, and M was the molecular weight. Thereafter, Chou and Zakin [59, 60] showed that for good solvents, data for a number of linear flexible polymers above molecular weight 15,000 fitted a single curve $[\eta/\eta_0]$/c$[\eta]$ versus k'$[\eta]$c, where k' was the Huggins constant. However, all these models failed to describe relationships for broad distribution of molecular weights, effects of the the polymer coil sizes, and internal structure dependence of the viscosity.

Takahashi et al [61, 62, 63] also studied extensively the zero-shear viscosity data of different linear and branched polymers in good, poor, and θ solvents covering wide ranges of polymer concentration and molecular weight. They provided separate relationships for the scaling of polymer viscosity in the dilute and semi-dilute regions. The relationship for dilute solutions was of the same form as that of Huggins' (Eq 1.12) or Martin (Eq 1.23). However, for the semi-dilute solutions, they

proposed that:

$$\frac{\eta}{\eta_0} \propto \left(\frac{c}{c*}\right)^{\frac{4.4-3\nu}{3\nu-1}} \tag{1.26}$$

which gave:

$$\frac{\eta-\eta_0}{\eta_0} \propto M^{3.4} c^{\frac{3.4}{3\nu-1}} \tag{1.27}$$

They observed that the viscosity of polymers with various molecular weight distributions in good solvents could be expressed by the same scaling function as described above. However, such an observation was only for a narrow range of molecular weights where they could fit and use this model. Moreover, it was observed that for lower molecular weights, the experimental results did not conform to the theoretical model. Finally, their model also lacked in providing the dependence of the viscosity on the coil size changes and the activation energy required for the motion.

Through the study of concentrated protein solutions, Lefebvre designed a scaling model for large concentration ranges that also considered the effects of entanglement on the viscosity. This model was a combination of the Simha-Utracki visocity model [57] with the Graessley[64] expression for the polymer coil expansion at a given concentration in the semi-dilute region. Thus Lefebvre managed to design his model with regards to different regimes of polymer concentration, and described the two cross-over points c* and c** in them. The defined viscosity model was:

$$ln\left(\frac{\eta}{\eta_0}\right) = 2a'[\eta]c^*\left(\frac{c}{c^*}\right)^{\frac{1}{2a'}} - (2a'-1)[\eta]c^* \tag{1.28}$$

While the model was good in describing the concepts of entanglement and cross-over points, it did not consider the hydrodynamic scaling required for polymer chains. This model also did not provide information about the activation energy barriers of the flow process.

Scaling concepts were created by de Gennes [12, 65] using Huggins and Flory's [66] models, as previously mentioned. The principles of entanglements in polymer solutions, as well as their mathematical meanings, were obtained through these developments. In these models, the parameter ξ, which represents the correlation length, was created to depict the changes in the gradual entanglement of polymer chains in solutions. The dimensions of polymer chains due to their orientation in the solution, as well as polymer-solvent characteristics, were established. The use of the generalized Zimm models [67, 68] yielded the establishment of the power law equations relating the polymer coil dimensions to the molecular weight M of the polymers as:

$$R_g \sim M^{\nu} \tag{1.29}$$

The value of ν is determined from the mean-field theory and is indicative of the repulsive excluded-volume interactions. As shown by Flory [10] in the mean field model, ν is 0.6 for polymers in good solvents.

Yamakawa et al [69, 70, 71, 72] have also studied the excluded-volume effects on the viscosity of dilute polymer solutions. It allowed them to determine the viscosity-radius expansion factor dependence. Initially, they evaluated the intrinsic viscosity of polymer solution using a helical wormlike touched-bead model without excluded volume. It was found that the slope of the plot of intrinsic viscosity against molecular weight reduced as the helical nature became stronger. Their predicted model was:

$$log[\eta] = log(M[\eta]/\phi L) - log(\lambda^2 M_L) - 2.542 \tag{1.30}$$

with:

$$logM = logL + log(M_L/\lambda) \tag{1.31}$$

where M was the molecular weight, L the contour length of the polymer coil, λ the static stiffness parameter, and M_L the shift factor of the molecular weight due to the contour length. To address the inconsistencies of experimental findings from the predicted model, they described the viscosity model using a radius expansion factor as:

$$[\eta] = [\eta]_\theta \alpha^3 \tag{1.32}$$

where $[\eta]_\theta$ was the intrinsic viscosity of the polymer in a θ solvent at the θ temperature, and α^3 was the radius expansion factor, related to the excluded volume expansion coefficient. However, it was again observed that experimental results deviated from the theoretical model when applied to expansions for different internal size parameters.

The de Gennes scaling and related models [73, 74] were also able to detect changes in the dimensions as the concentration of the solutions increased, owing to excluded-volume effects at higher concentrations. While the concept of different concentration zones such as dilute, semi-dilute, and concentrated was observed, most experimental findings supporting the theory were restricted to semi-dilute polymer solutions. Later polymer scaling theories that included all three concentration regions, such as Sato et al's 'fuzzy-cylinder' method [75, 76], were able to provide good relationships between zero-shear polymer viscosity and concentration and molecular weight variations. However, this model was based on the Stokes-Sutherland-Einstein (SSE) viscosity relationship for particle diffusion. The same SSE equation (discussed later in Section 1.6) can fail by orders of magnitudes in many cases when applied to measurement of nanoviscosities, and so is not capable of providing a length-scale dependent description by itself.

More recently, Monkos [77] has studied the dependence of viscosity on the temperature using modified Arrhenius models. While studying aqueous solutions of bovine serum albumin, he predicted the viscosity-temperature dependence to be of the form:

$$\eta = \exp\left(-B + DT + \frac{E}{RT}\right) \tag{1.33}$$

where B and D were certain constant parameters, E was the activation energy for viscous flows, and R was the gas constant for a temperature T. This was a capable model for describing the dependence of viscosity on the activation energy and temperature. However, it required separate use of the Mooney (Eq 1.20) and Lefebvre models (Eq 1.28) to characterize the concentration dependence and the different cross-over points for the concentration regimes. It was not an universal model by any means.

Many scaling models have been implemented over the years, with the underlying theory being guided by some of the models described above. Concentration limits impose restrictions on some (usually applied in dilute or semi-dilute zones). When effects of dimensional changes versus concentration, temperature, activation energies for polymer-solvent systems, or the distribution pattern of molecular weights are taken into account, others are constrained in their applicability. Type of polymer and solvent also plays a part in such models, and often the practical application of such theory are limited. More importantly, such models cannot traverse different length-scales of the viscosity of complex systems, and therefore cannot be considered as universal.

A different approach was undertaken when studying the motion of nanoprobes

by Phillies [28, 29, 78, 79, 80, 81, 82, 83]. In such studies, extensive work was perfomed to identify the nanoviscosity due to hydrodynamic effects.The analysis of optical probe diffusion in polymer solutions was used to accomplish this. Quasielastic light scattering was used to determine probe motion. The probe diffusion coefficient D_p was found to follow the stretched exponential:

$$\frac{D_p}{D_{p0}} = \exp(-\alpha c^{\nu} M^{\kappa} {r_p}^{\delta}) \tag{1.34}$$

where r_p was the radius of the diffusing probes, D_{p0} was the self-diffusion coefficient of the the solution, α was a constant and the exponents κ and δ were theoretical constants of the order of unity. Phillies observed that such a model was incapable of correctly predicting the diffusion coefficient when the probe size and molecular weights increased. It was later discovered that the measurements of D_{p0} at elevated concentrations at the time uniformly fit stretched exponentials in c, but not the power laws predicted by some scaling models. However, this formed the basis for future extensive studies of viscosity at the nanoscale, in search for a combined length-scale based scaling model.

1.6 Nanoscale viscosity studies

Complex fluids are materials with a hierarchical structure that can be seen at different length scales. As a result, the properties of these heterogeneous materials are dependent on the length scale at which we probe them: length-scale-dependent dynamics have been observed in a variety of biological and physical systems, for example. Nanoparticle diffusion coefficients in an agarose gel are highly dependent on their size, approaching zero for sizes bigger than the typical pore diameter in the polymer network. A small probe diffusing near the glass transition temperature in supercooled liquids experiences viscosity three orders of magnitude lower than the macroscopic viscosity of the same liquid. Since macromolecules and lipids make up up to 40% of the volume of cells, the liquid that composes their interior has a high macroviscosity. Small proteins, on the other hand, diffuse freely in various cell compartments, including the nucleus, cytoplasm, endoplasmic reticulum, and mitochondria, at the molecular level. All of these findings suggest that at the molecular and macroscales, the crowded environment of cells exhibits a variety of rheological behaviors.

Capillary electrophoresis, sedimentation, and light scattering experiments (with a limited number of nanoprobes and low polymer concentrations in solutions) have been used to investigate the rheological nature of nanoscale objects. Currently, the most commonly used techniques for studying the micro-rheological properties of fluids involve some form of monitoring the motion of small probes inside the medium. One such crucial technique is the **Fluorescence Correlation Spectroscopy** (FCS), which can be used to study the flow and viscosity at the microscale simultaneously. In FCS, a statistical analysis of the fluctuations in fluorescence intensity is performed via time correlation. Such fluctuations occur due to the random Brownian motion of fluorescent particles in a solution. It provides information on the photophysics that cause the fluorescence intensity fluctuations, as well as diffusion behavior and absolute particle concentrations. The most obvious and visible cause for fluorescence fluctuations is due to the change in particle concentration in the observation volume. Single fluorophores passing through the detection volume cause temporal changes in fluorescence emission intensity, which are recorded by the method. By temporally

auto-correlating the recorded intensity signal, these intensity changes can be quantified in terms of their strength and duration. This results in the identification of the average number of fluorescent particles in the detection volume and their average diffusion time through the same volume. Eventually, important biochemical parameters as the concentration and size or shape of the particle (molecule) or viscosity of the environment are determined through this process.

Holyst et al[84, 85, 86] have performed extensive studies using FCS for the nanoscale motion of small probes in complex systems. In these studies, the starting point for describing such motion was the Stokes-Sutherland-Einstein (SSE) equation that uses simple diffusive motion for this purpose. The SSE equation is classified as a fluctuation–dissipation (FD) relation. According to the fluctuation–dissipation theorem the diffusion coefficient D is inversely proportional to the friction experienced by a particle during motion.

$$D = \frac{k_B T}{6\pi\eta r_p} \tag{1.35}$$

where η is the viscosity experienced by a nanoprobe of radius r_p, and k_B is the Boltzamann constant. As per this relationship, one would expect a simple relation between the different parameters such as:

$$\frac{D}{D_0} = \frac{\eta_0}{\eta} \tag{1.36}$$

However, it was observed[87] that small and large probes sedimenting in DNA solutions exhibited sedimentation coefficients significantly different from those expected by the use of Eq 1.36. Thus, it was proposed that there are three different regimes for particle diffusion in polymer solutions. Transitions between these regimes are not continuous. The regimes depend on the relation between the diameter of the probe particle d_p and characteristic length-scales in the polymer network. The first length-scale was the correlation length ξ as per the size of the mesh in the interpenetrating networks inside the complex system. Usually such a parameter could be obtained through the relationships between the radius of gyration, R_g, and the concentration region of the studied system. The second length-scale L was the distance between the entanglement points of the polymer chains. This parameter was also dependent on the concentration of the media, similar to the correlation length. In the first regime where a probe has a diameter $d_p < \xi$, the diffusion of the probe particle is not affected by the polymer mesh. When $\xi < d_p < L$, in short time scales, the motion of the probe particle is not affected by the presence of polymers. The long-time self-diffusion coefficient is affected by the presence of polymer chains. The probe in motion experiences an effective viscosity that scales with the d_p/ξ ratio. In the regime where $L < d_p$, the motion of the probe particle is affected by relaxation of the polymer chains and the probe experiences the macroscopic viscosity of the solution. Holyst et al[84, 85] performed FCS studies on the transport properties of complex liquids to observe this unusual length-scale dependence. They observed that the deviations from the SSE equation kept growing with reducing r_p/R_g ratios, with R_g being the radius of gyration of the polymer in the system. Based on such studies, an approximate model was proposed that described the effective viscosity experienced by probes undergoing motion in complex liquids, governed by the following key equation:

$$\eta = \eta_0 \exp\left[\left(\frac{\gamma}{RT}\right)\left(\frac{R_{eff}}{\xi}\right)^a\right] \tag{1.37}$$

where η is the effective viscosity, η_0 is the viscosity of the solvent or media, ξ is the correlation length, R_{eff} is the effective size of the particles in the system, a is a

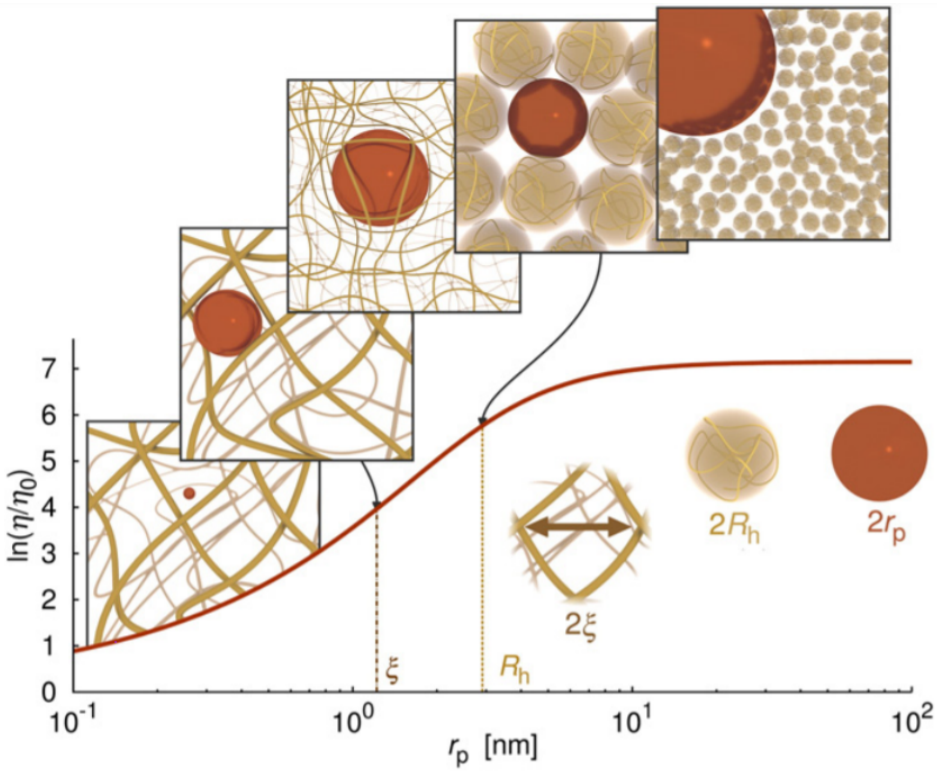

FIGURE 1.10: A plot of the effective viscosity experienced by nanoprobes moving in a solution of PEG in water. The diffusion coefficient or mobility of any probe particle can be obtained directly from this length-scale dependent viscosity curve [86]. This effective viscosity approaches the nanoviscosity for smaller probes as also studied by Phillies (1.6).

structural scaling parameter of the order of unity, γ is the activation energy of the flow process and R is the universal gas constant. The correlation length ξ is obtained by the following relation:

$$\xi = R_g(\frac{c}{c^*})^{-\beta} \tag{1.38}$$

where, c^* is the concentration at the crossover from dilute to semi-dilute regime and also known as the overlap concentration, R_g is the radius of gyration of the coils and β is a scaling exponent given by [12, 88]:

$$\beta = -\nu(1-3\nu)^{-1} \tag{1.39}$$

The parameter ν is defined from the mean-field theory and is indicative of the repulsive excluded-volume interactions. The overlap concentration c^* is obtained as:

$$c^* = \frac{M_w}{\frac{4}{3}\pi R_g^3 N_A} \tag{1.40}$$

where M_w is the polymer's molecular weight, and N_A is the Avogadro number.

A key step in the development of this model was the introduction of the parameter R_{eff}, which led the model to overcoming the issues of length-scale dependence.

The parameter R_{eff} was well defined by by Kalwarczyk et al[86] as:

$$R_{\text{eff}} = \sqrt{\frac{{r_p}^2 {R_h}^2}{{r_p}^2 + {R_h}^2}} \tag{1.41}$$

where R_h is the hydrodynamic radius of the polymer in the same solvent. Combining Eqs 1.35-1.41 into the model, it was proposed that the viscosity experienced by a broad range of probes over length-scales from nano to macro and millimeter could be expressed through this scaling model. The hydrodynamic size of the probe sets the scale at which the flow occurs. Thus instead of being the property of an object under motion, the viscosity experienced by the object is a property of the flow inside the fluid and the length-scale of that flow. The motion of a probe in any complex liquid generates hydrodynamic flow at a length-scale equal to R_{eff}. The Fig 1.10 developed by Kalwarczyk[86] was a representation of the smooth dependence of the viscosity on the length-scale of flow around the probing particle, when the results of Eqs 1.35-1.41 are plotted.

Extensive studies were performed on nano-objects and colloids using this proposed length-scale dependent viscosity model[84, 89, 85, 90, 91, 92, 93].However, not a lot of studies were made to cover the macroscopic viscosity for complex systems. The first conscious approach to study complex systems in macroscale was performed by Wisniewska et al[94], when polyethylene glycol (PEG/PEO) solutions in water were studied. The study involved obtaining further information on the activation energy for flow of complex systems, to complement the length-scale dependent viscosity model. A simple, qualitative physical explanation of the observed changes and crossover between concentration regimes was provided, along with a semi-empirical quantitative formulation based on extensive rheological measurements and literature data. In doing so, it was observed that the principles of the model could be valid for all kinds of polymer systems, but it was never fully explored. The idea that polymer coil sizes can vary at the macroscale with changing concentration of the complex system, was also not identified by the proposed length-scale dependent model, and required further investigation. A clearer idea about the different parameters of the model and their inter-dependent relationships at the macroscale was necessary.

1.7 Objective of this thesis

Rheology of polymer solutions suffers from the lack of a model of viscosity applicable across wide range of concentrations, temperatures, molecular weights and other processing variables. Previous scaling models lacked in one aspect or the other in terms of the number of variables they described. The core idea of this thesis was to apply to macroscale analysis the previously obtained scaling model from nanoprobe diffusion in different polymer systems. The nanoscale diffusion model defined the effective viscosity experienced by those probes as a function of: the probe size; the concentration of the system; the molecular weight of the polymers; and the temperature of the surroundings. In this work, we expanded the same model to macroscale analysis of viscosity by applying it to different common polymer systems:

- polydimethylsiloxane (PDMS) in ethyl acetate
- hydroxypropyl cellulose (HPC) in water
- polymethylmethacrylate (PMMA) in toluene, and

- polyacrylonitrile (PAN) in dimethyl sulfoxide (DMSO)

This work involved experiments for measuring the viscosities of the above mentioned polymer-solvent solution systems through rheometry at different concentrations and temperatures, hydrodynamic radii through dynamic light scattering (DLS), and molecular weight distributions and polydispersity index through gel permeation chromatography (GPC). Such measurements were crucial to obtaining data required to apply and fit to the previous nanoprobe diffusion model so that the length-scale dependent viscosity scaling model could be obtained. This model can fulfil the following areas of concern:

- to cover concentrations from dilute to concentrated in solution;
- obtain relations between the coil dimensions as a function of concentrations;
- describe how it can be used with commercial or standard polymers with a variety of molecular weight distributions;
- applicable for polymers with different polydispersities;
- be relevant for a wide range of temperatures at the normal operating range for most everyday polymer products.
- provide detailed information about all the different parameters in the model.

The developed scaling model can then be used as a length-scale based polymer characterization technique, developed on viscosity measurements. It is conventional to measure the viscosity at all polymer processing industries, and so a characterization technique through such measurements would be more comfortable compared to others. Finally, for research and development purposes, this scaling model can be applied for both nanoscale and macroscale analysis which would be unique.

Chapter 2

Experimental methodology

2.1 Viscometry

Viscosity is the study of the resistance to flow for any fluid. It is an essential quantity that is required for a large number of applications. A common example of dealing with fluid motion in everyday life is that of mixing honey in tea, or squeezing toothpaste onto a toothbrush. For the large scale production of the honey or toothpaste, it is vital to understand the viscosity characteristics of the different components. Viscosity measurements are commonly performed by two types of equipment, a **viscometer** or a **rheometer**.

A viscometer is a device used to calculate flow characteristics in Newtonian materials. A portable viscometer may be used for research in the field or at a distance. These instruments can usually measure in the range of 0.1 to 1000 s^{-1}. There are many different types of viscometers, usually based upon two different techniques of measurement. Both involves the relative motion of an object, such as a sphere or a rotor blade, through a medium. Usually one of the two components is stationary while the other component moves through it or past it. The different types of viscometers are categorized based on the type of motion of the studied object, such as **capillary, falling ball, falling sphere, rotational, vibrational or oscillating piston**. A commonly used technique is the Hoppler's falling ball viscometer. This device uses the Hoppler principle to measure the viscosity of Newtonian fluids. In this method, the time required for a ball to fall under gravity through an inclined sample-filled tube is measured. The tube is mounted on a pivot bearing which allows its quick rotation through a complete 180 degrees, thereby allowing the test to be repeated immediately. A means to improve the accuracy of the measurements is to perform the tests from both directions of the tube on the same sample. However, in our experimental studies, more complex rheometers were used for better characterization and are shown next.

Rheometers are more costly than viscometers, but they also have more versatility and offer a much broader variety of control and measurement parameters. A rheometer allows for much more detailed analysis of flow, deformation, and even material tackiness (for Newtonian and non-Newtonian materials). A rheometer can measure shear rates ranging from 0.000001 to 10,000 s^{-1}. A broader range enables more accurate data to be obtained which is crucial for the purpose of complex applications such as medical implants and devices. **Rotational (shear type) and capillary extrusion** rheometers are the two most commonly used varieties of such instruments. Capillary extrusion is typically utilised for highly concentrated suspensions/pastes, while the rotational varieties are often used for systems that are less concentrated (which could be either solutions, emulsions, or suspensions). For obtaining information about how molecular structures influence processing characteristics, rotational rheometers are chosen. They are relatively easy to use but their

measurement inaccuracy is around $\pm 10\%$. Various designs exist: all types have some form of element rotating inside the liquid at a constant rate. Most common rheome-

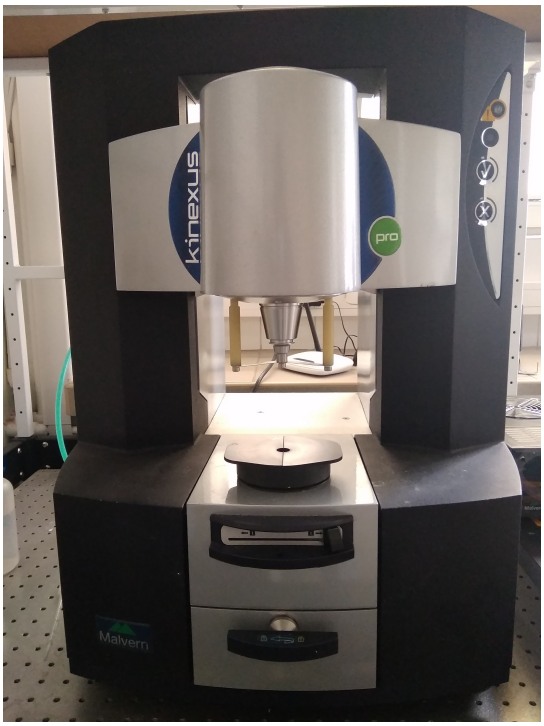

FIGURE 2.1: Malvern Kinexus Pro rotational rheometer used at the IChF, PAN.

FIGURE 2.2: Bohlin Gemini rotational rheometer used at the MPIP, Mainz.

FIGURE 2.3: Types of geometries used in our studies.

ters have either two coaxial cylinders with the fluid to be measured contained between them, or a cone-and-plate design, where the liquid is placed on horizontal plate and a shallow cone placed into it. The Figs 2.1-2.2 show the two types of rotational rheometers used for our studies, while Fig 2.3 shows the geometries used for the same. Common to all such equipment is the method of control for obtaining the desired viscosity information depending upon the type of rheological fluid analyzed. Such controls are usually of four types - constant stress, constant strain, constant frequency or constant amplitude, and provide a wide range for characterizing polymers based on the type of application.

2.2 Dynamic Light scattering (DLS)

We required a method to obtain the hydrodynamic radius of the polymers used in our studies. For this reason, we used dynamic light scattering (DLS), a common measurement technique for particle size analysis in the nanometer range. It uses the principles of the Brownian motion of scattered particles in a solution, where they move randomly in all directions. This principle states that there is constant collisions between the solute particles and the solvent molecules due to their random motions. As particles collide, a certain amount of energy is transferred, causing particle movement. Since energy transfer is more or less continuous, smaller particles are affected more. Smaller particles diffuse at a higher rate than larger particles as a result. By knowing all other parameters influencing the particle movement, the hydrodynamic radius of the particles can be obtained from their diffusion characteristics.

The relation between the diffusion rate of the particles and their size is given by the Stokes-Sutherland-Einstein (SSE) equation. The translational diffusion coefficient D can be used to calculate the particle diffusion rate. Furthermore, since both

the viscosity of the dispersant and the temperature have a significant impact on particle movement, they are included in the equation.

$$D = \frac{k_B T}{6\pi\eta R_h} \tag{2.1}$$

where k_B is the Boltzmann constant, T is the temperature, η is the medium's viscosity, and f = $6\pi\eta$RH is the frictional coefficient for a hard sphere in a viscous medium. One of the most important requirements for the Stokes-Einstein equation

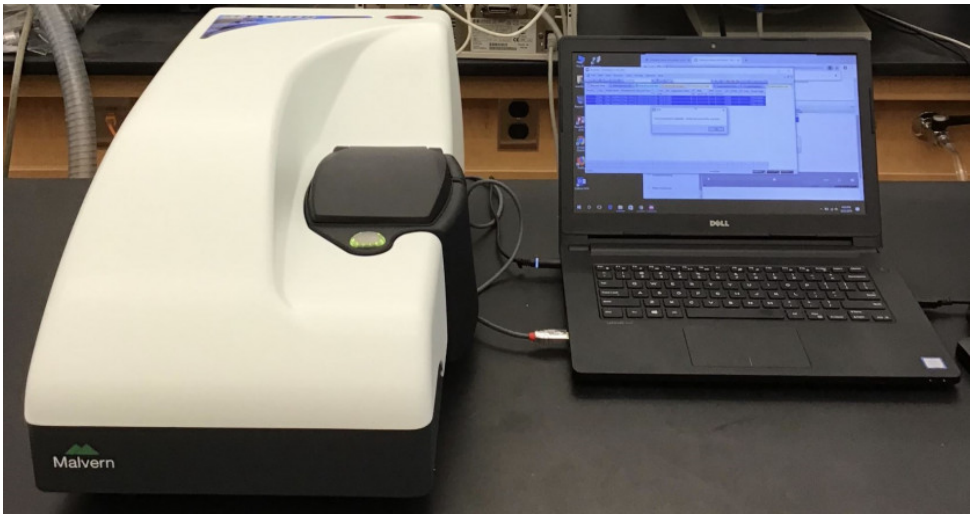

FIGURE 2.4: Malvern Zetasizer Nano setup used at the IChF.

is that the particles must travel only in Brownian motion. There is no random movement if there is sedimentation, which would contribute to misleading results. As a result, the initiation of sedimentation denotes the DLS measurement's upper size limit. The lower size limit, on the other hand, is determined by the signal-to-noise ratio. Since small particles scatter less light, the measurement signal is inadequate. To track the movement of the particles, the scattered light is observed over a period of time. The scattered light's intensity does not remain constant over time, but it will change.Smaller particles diffuse at a quicker rate than larger particles, resulting in faster fluctuations. Larger particles, on the other hand, produce larger amplitudes between the maximum and minimum scattering intensities. This initial intensity trace is then used to create a correlation function, which is a mathematical representation of the scattered light's fluctuations. The translational diffusion coefficient is calculated using it. This is the primary weighting model shown in DLS software since the effects of DLS measurements are intensity-based (intensity variations over time are detected). The volume- and number-based distribution can be recalculated from the intensity-based distribution. The material refractive index and absorbance of the measured sample at the laser wavelength must be determined for this. The diffusion coefficient is calculated using the cumulant algorithm, which is included in most software packages for measuring the various delay times of intensity fluctuations; the hydrodynamic diameter (i.e. particle size) is estimated using the Stokes-Einstein equation. DLS provides information not only about the mean particle size, but also about the particle size distribution. Only low sample volumes are required and the sample can be re-used after the measurement, which is a big advantage from such a setup. The Malvern Zetasizer DLS setup used in our studies is shown in Fig 2.4.

2.3 Gel permeation chromatography (GPC)

We required a technique to obtain the molecular weight distribution, and the polydispersity of the polymers studied. For this purpose, we used gel permeation chromatography (GPC). Normally, all chromatography are separation methods used for chemical analysis. A column, capillary, or other container containing a mobile and stationary process is used in almost all chromatography equipment. Gel permeation chromatography (GPC), also known as size exclusion chromatography (SEC), is a type of liquid chromatography (LC). It consists of moving polymer solutions through a column of chemically modified inorganic silicas or polymeric beads. The size of the polymer molecules inside the solution determines the separation mechanism. The various lengths of polymer chains in a sample are isolated and their relative abundance is determined using this method. For this purpose, the instrument uses a pump for forcing the solvent through it, an injection port for inserting the test sample onto the column, a column for retaining the stationary phase, some detectors for detecting the components exiting from the column, and software for monitoring the various parts of the instrument. The software is also used for measurement information and to show the corresponding results. The components are identified in different ways as they exit the column, and the sample's elution activity is shown in a graph, or chromatogram. The chromatogram depicts the amount of material that has departed the column at any given time. Higher molecular weight (larger) polymer coils elute first, followed by lower molecular weight (and hence smaller) chains. Elution volume is the principal criterion for separation. The chromatogram's data is then compared to a calibration that depicts the elution activity of a collection of polymers with known molecular weights. This enables the sample's critical molecular weight distribution to be determined. After that, the data is used to classify polymers and divide mixtures into discrete fractions. Different separated components include polymers, oligomers, monomers and any non-polymeric additives. GPC/SEC is the most readily used technique for obtaining the molecular weight distribution of polymers. Furthermore, the polymer mixture can be separated into individual components as necessary for any experiments or applications. GPC/SEC is commonly used in conjunction with other techniques that classify polymers based on their acidity, basicity, charge, or affinity.

Chapter 3

Development of a universal macroviscosity scaling model

3.1 Typical characteristics of a viscosity scaling model

The main limitation for a proper universal viscosity scaling model have been discussed before in section 1.3. Conversely, a model that overcomes those limitations will have the ability to effectively describe the various structure-property relationships associated with polymers. Thus a typical viscosity scaling model should have interdependent relationships of:

- Concentration ranges
- Molecular weight ranges
- Hydrodynamic radius R_h, gyration radius R_g, correlation length ξ
- Temperature variations
- Molecular weight distribution
- Crossover points based on chain solvent interactions
- Polymer-solvent compatibility
- Activation energies for the process

Apart from these, there are limitations of the capacity to measure the viscosity effectively, the physical property of the polymers and solvents, etc., that determines the applicability of the scaling model. Based on the above considerations, a few critical parameters are available that are often used to construct any scaling model for viscosity of polymer solutions. These parameters are described in detail in the following section.

3.2 Proposed scaling model parameters

3.2.1 Hydrodynamic radius, R_h

The hydrodynamic radius, R_h, of any molecule in a solution is it's effective radius, measured by assuming that it is a body diffusing through the solution while feeling resistance from the solution's viscosity. The correlation curve is the measured data in a dynamic light scattering (DLS) experiment. All of the information about particle diffusion inside the sample being measured is contained within the correlation curve. D is the diffusion coefficient, which is determined by fitting the correlation

curve to an exponential equation, with D proportional to the exponential decay's lifetime. The SSE equation is then used to measure the hydrodynamic radius, R_h, from the diffusion coefficient.

The size calculated by DLS is defined as the radius of a conceptual hard sphere that has a similar diffusion rate as the particle under study. Since such conceptual or hypothetical hard spheres do not exist, this description is only valid for visualization purposes. In practice, non-spherical, dynamic (tumbling), and solvated macromolecules exist in solution. Consequently, the apparent size of the dynamic hydrated/solvated particle is determined by the radius measured from the particle's diffusional properties. As a result, the word "hydrodynamic" radius was coined. In general, empirical dimensionless power law equations relating the coil size (in nm) and molecular weights M (in g/mol) for long chains are of the form:

$$\frac{R_c}{R_0} = K\left(\frac{M}{M_0}\right)^y \tag{3.1}$$

where the parameter R_c is usually described as the the gyration or hydrodynamic radius, R_0 and M_0 are some standard reference sizes, and K and y are dimensionless constants with values unique to a polymer-solvent system [95, 96, 97]. Commonly, such an equation as described in Eq 5.11 is simplified to the form [98]:

$$R_c = KM^y \tag{3.2}$$

These power law equation are used to define the different size parameters. The results for the hydrodynamic radius obtained in our DLS measurements are fit to the power law Eq 3.2, and corresponding parameters are shown in the Table 3.1.

TABLE 3.1: Power law parameters for defining hydrodynamic radius, R_h (nm), of our different polymer systems, according to Eq 3.2, M being in g/mol.

Equation $R_h = K'M^{y'}$		
Polymer system	K′	y′
HPC-water	0.0120	0.580
PMMA-toluene	0.0106	0.570
PAN-DMSO	0.0110	0.563
PDMS-ethyl acetate	0.0113	0.570

3.2.2 Gyration radius, R_g

For any object, the radius of gyration is the distance from its center of mass at which the entire mass could be concentrated without changing its moment of rotational inertia about an axis through that center of mass. This is also the root-mean-square distance of the segments of a polymer chain from its center of mass. The radius of gyration is a metric for the size of the random coil shape that many synthetic polymers obtain in solution or in their amorphous bulk state. The size properties of a polymer in solution are influenced by the molecular weight of a macromolecule, its structure (whether or not it is branched, and how it is branched), and the degree of swelling caused by the solvent. Similar to the hydrodynamic radius, it can be estimated from power law equations relating it to the molecular weight of the polymers as expressed through Eq 3.2. Unlike the R_h which is measured through DLS measurements, the R_g can be measured through Static light scattering (SLS), as well as through neutron

and X-ray scattering techniques. However, in our studies, the R_g values have been estimated from reported literature values of similar polymer-solvent systems. The R_g data were then fit through Eq 3.2 to obtain the different power law parameters, which are shown in the table 3.2. Both R_g and R_h can be used to learn about the inter-

TABLE 3.2: Power law parameters for defining gyration radius, R_g (nm), of our different polymer systems, according to Eq 3.2, M being in g/mol.

Equation $R_g = K'' M^{y''}$		
Polymer system	K″	y″
HPC-water	0.0278	0.553
PMMA-toluene	0.0270	0.535
PAN-DMSO	0.0255	0.533
PDMS-ethyl acetate	0.0265	0.530

nal structure of polymer chains, which is an important aspect of their analysis. R_g's value is slightly more dependent on the structure of the molecule of interest than R_h's value because of the way it is calculated. The ratio of R_g and R_h, on the other hand, is what really gives shape information about a polymer chain in any system.

3.2.3 Correlation length ξ

A crucial parameter related to the concentration of the polymer solutions is the correlation length ξ or the distance between the chain interlink points inside the polymer matrix. Also know as the mesh size, it is a characteristic length in polymer systems that affects their viscosity. The most intuitive mesh size in a polymer matrix for most researches is probably the distance between crosslinking points. It is mostly estimated by theoretical calculations (e.g., tree-like approximation, real space renormalized effective medium approximation), or certain light scattering experiments. For any entangled system, ξ is the average distance between the entanglement points of polymer chains [12, 99, 100] or in general it is a distance between the center of masses of polymer coils. It is a characteristic length within which a monomer from the same polymer chain is more likely to be found than monomers from other chains. The screening length of the excluded volume effect is also known as the correlation length. Owing to the presence of other polymer chains, the excluded volume effect (intramolecular interaction) vanishes easily for a length scale larger than the correlation blob. Blob size is another term for this correlation length (from de Gennes blob theory) [12, 99]. It is determined experimentally through light scattering techniques [101, 102, 86], and it depends on the concentration c as follows:

$$\xi = R_g \left(\frac{c}{c^*}\right)^{-\beta} \tag{3.3}$$

where, c^* is the concentration at the crossover from dilute to semi-dilute regime and also known as the overlap concentration, and β is a scaling exponent given by [12, 88]:

$$\beta = -\nu(1 - 3\nu)^{-1} \tag{3.4}$$

The parameter ν is defined from the mean-field theory and is indicative of the repulsive excluded-volume interactions. As shown by Flory [10] in the mean field model, ν is 0.6 for polymers in good solvents. Typically, it provides information about the solvent quality for a particular polymer inside a solution. However, ξ is typically

available for polymer solutions up to the semi-dilute concentrations, and loses significance in the concentrated solutions or polymer melts. Therefore, in our studies, the ξ values were kept constant beyond the semi-dilute regime.

3.2.4 Overlap concentration, c*

Polymer chains in dilute solutions are far apart from one another and act as isolated hard spheres [10]. Further subdivisions of the dilute regime at lower limits have been proposed in principle [103, 104, 105, 106], but such concentrations ultimately approach infinite dilution and are not easily accessible using traditional experimental setups. At concentrations where polymer coils overlap, the semi-dilute regime begins. The chains gradually interpenetrate each other as the concentration rises, forming a uniform mesh-like structure. [94, 73]. At a critical concentration c^*, when the coils simply reach each other, the transition between isolated coils (dilute regime) and interpenetrating coils (semi-dilute regime) occurs [12, 99, 100]:

$$c^* = \frac{M_w}{\frac{4}{3}\pi R_g^3 N_A} \tag{3.5}$$

where M_w is the molecular weight of the polymer, R_g is the radius of gyration, and N_A is the Avogadro number. Dynamic properties of macromolecules for both random coils and rodlike chains tend to change rather abruptly in crossing over from dilute to semidilute regimes. The crucial criterion that is considered through the estimate of c* is the magnitude of the volume occupied by a random coil at that concentration. This allows to further identify the changes in the other related dynamic parameters.

3.2.5 Activation energy parameter, γ

Viscosity represents the internal friction among the chains of a polymer melt or solution due to their motion. Such internal frictional forces are a source of energy barriers for motion. These barriers are caused by intra-chain and inter-chain effects, or some other interactions between the different molecules in the system. The Eyring theory [107] assumes that viscous flow is therefore an activated-rate process, i.e., it involves the overcoming of a potential energy barrier of height E_a. This energy barrier is overcome when temperature changes cause random variations of the energy of an atom or molecular segment with time, leading to a finite possibility of exceeding the value E_a. As a result, there are minimum energy points created inside the molecular structure which was termed as **holes**, surrounded by larger cages of molecules with higher energy barriers. For the viscous flow of most polymers in molten or solution forms, the activation energy is this minimum energy E_a required for the flow unit (chain segment, usually a monomer). To do so, the monomer transits from the current position to the neighbouring hole during the flow process, leaving behind a hole in its place. A monomer can theoretically move between any point inside the structure, but the thermodynamics of the system favour motion to that of a minimum energy. This also leads to the fastest possible flow rates, and the lowest possible viscosity and frictional losses, corresponding to the activated-rate process. The viscosity as per the Eyring theory can be expressed through the following relation:

$$\eta = \frac{N_a h}{V} \exp \frac{E_a}{RT} \tag{3.6}$$

where N_a is the Avogadro's number, h is the Planck constant, V is the molal volume, R is the gas constant, T the absolute temperature and E_a the activation energy of the process. The schematic is shown in Fig 3.1. It means that for ordinary viscous flow

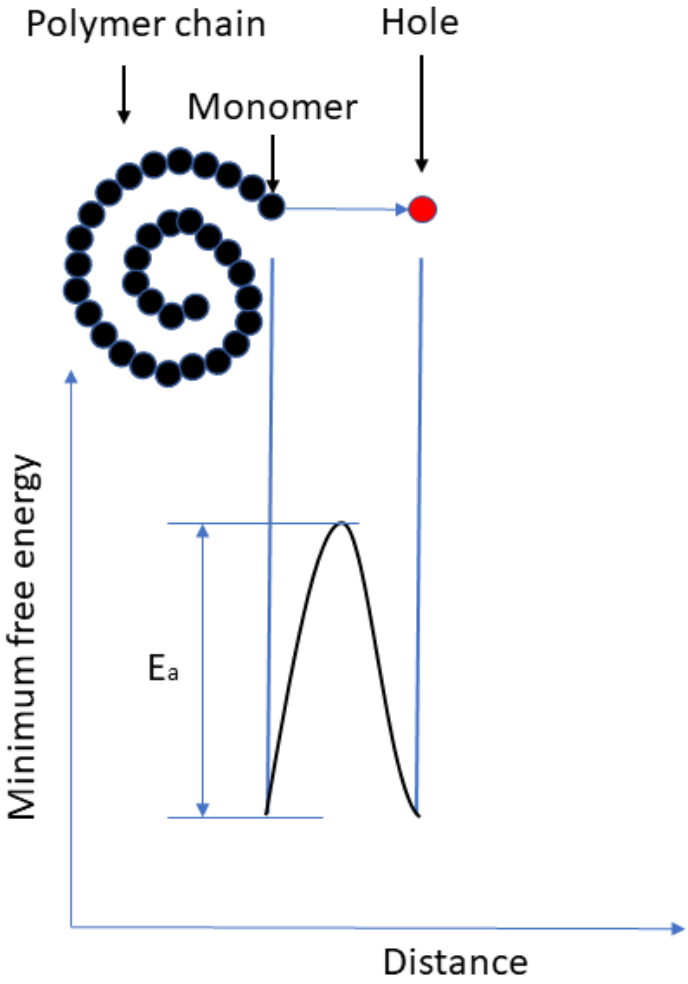

FIGURE 3.1: Activation energy, and associated hole in the flow process, as per Eyring.

we expect the polymer chains layers to slip over each other into a small hole. The viscous flow activation energy can therefore be used to judge the degree of difficulty in the material's fluidity and evaluate its processing performance. In any scaling model, the activation energy plays a crucial part in proper characterization of the polymer-solvent system.

3.2.6 Scaling parameter, a

Every polymer-solvent system is characterized by a parameter a of order unity, which provides details on the internal structure of any complex liquid. Crossovers between the dilute, semi-dilute, and concentrated solution concentration regimes cause differences in the internal structures, and hence changes in the value of a. It was observed that $a = \beta^{-1}$ for the dilute regime and $a = R_h {R_g}^{-1} \beta^{-1}$ for semi-dilute regime of concentrations [85, 94]. As shown by Kalwarczyk et al [86], a varied from 1.29 for hard sphere-like objects in dilute polymer solutions and colloids to 0.78 in entangled systems. Of course, in their studies[86, 94], the entangled systems did

not extend to the concentrated zone, and so the value of a for highly entangled systems could be even lower. Chemically different polymers demonstrate universal enhancement of various molecular properties with increase in the chain length or molecular weight M, such as coil dimensions and relaxation times. When analyzing a wide range of polymer solutions, there are differences when identifying the scale at which entanglement sets in. Some expect it to be effective at the scale of monomeric contact, whereas experimentally it is characterised by a molecular weight between entanglements M of the order of 100-200 monomer units. On shorter scales in polymer melts the simple scaling due to hydrodynamic screening is observed. For all these reasons, a uniform scaling parameter that allows expression of the viscosity of the polymer solution is essential, and provided by the parameter a here. The values for a determines the quality of the solvent for a polymer as well as the the type of entanglements present inside the system. This in turn provides information regarding the other parameters defining the viscosity.

Chapter 4

Experimental conditions and results

4.1 Materials

We have chosen polymers based on their widespread use and applicability, and determined good solvents for the polymers based on the solubility parameter values. Four different systems were selected with polymers varying in their polydispersity. The information about the selected systems are shown in the table below.

TABLE 4.1: Polymer-solvent systems studied in this thesis.

Polymer	Solvent	Company	Mol. wt.(g/mol)	Polydispersity
HPC	Water	Sigma Aldrich	80000	4.71
			100000	4.82
PDMS	Ethyl Acetate	Alfa Aesar	9000	1.93
			28000	2.15
			63000	2.78
			139000	2.14
PAN	DMSO	Sigma Aldrich	150000	2.45
PMMA	Toluene	In-House MPIP, Mainz	24000	1.08
			70000	1.14

The solvents were also obtained from the same companies as the polymers and with purity of 99.2%. The polydispersity is the ratio of the weighted average and number average molecular weights obtained from the GPC measurements for the weight distribution, shown in Section 4.3.

4.2 Viscosity measurements

Polymer solutions were prepared in a wide range of concentrations, depending upon the type of system and applicable solution concentrations in the Newtonian viscosity ranges. We prepared solutions of PDMS in ethyl acetate at 12 different concentrations ranging from 0.001 – 8.000 g/cm^3. HPC, PMMA and PAN were powdered polymers with limited solubility ranges in the solvents unlike PDMS in ethyl acetate. Different concentration ranges for the solutions for these three polymers were prepared from 0.005 – 1.000 g/cm^3. We stirred the solutions at 800 rpm for 1-2 days, and 3 days for the highest molecular weight of PDMS.

We measured the viscosity of these solutions at temperature intervals of 5 K, over a temperature range of 283-303 K. The first criteria was to show the Newtonian nature exhibited by each polymer-solvent system, as discussed previously in Chapter 1 and shown for PDMS-ethyl acetate. For this purpose, the measurements for PDMS

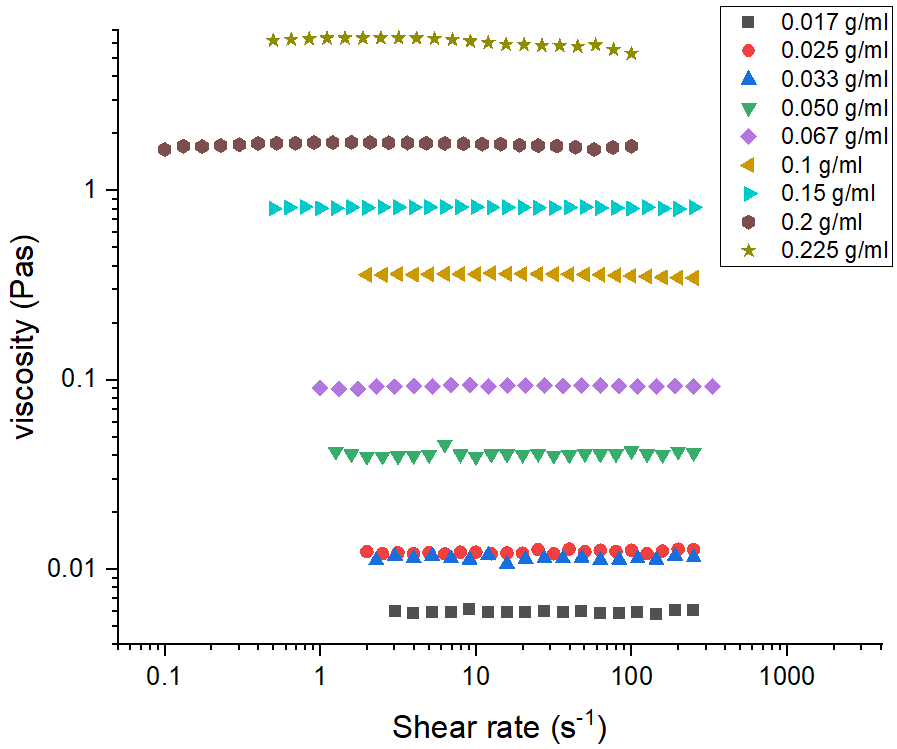

FIGURE 4.1: Newtonian nature of our studied HPC-water system, some examples.

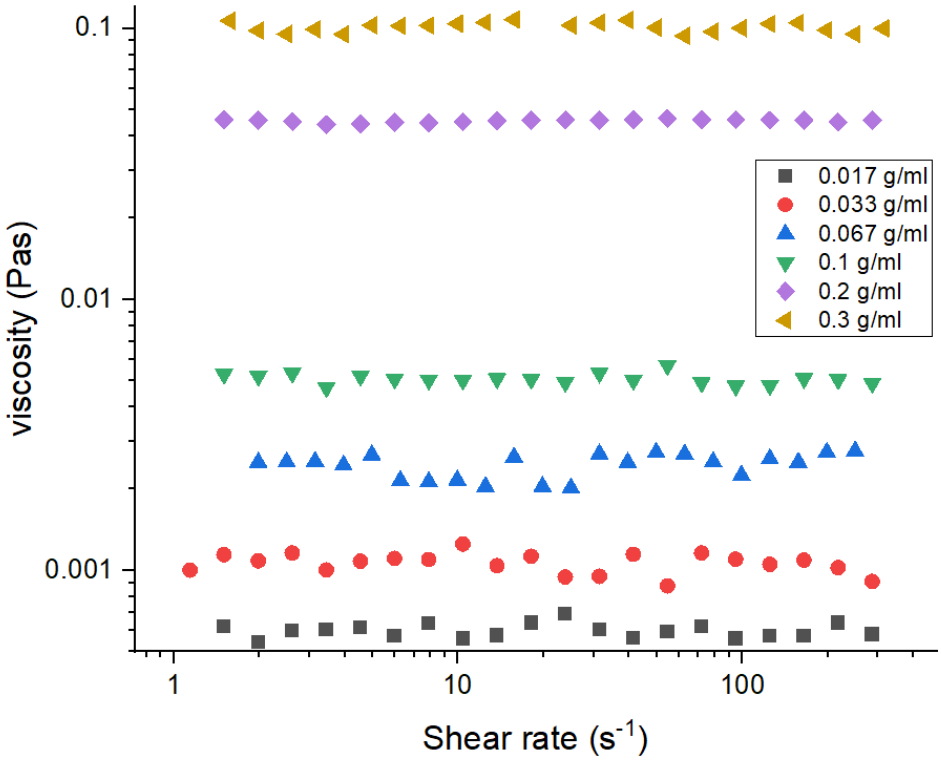

FIGURE 4.2: Newtonian nature of our studied PMMA-toluene system, some examples.

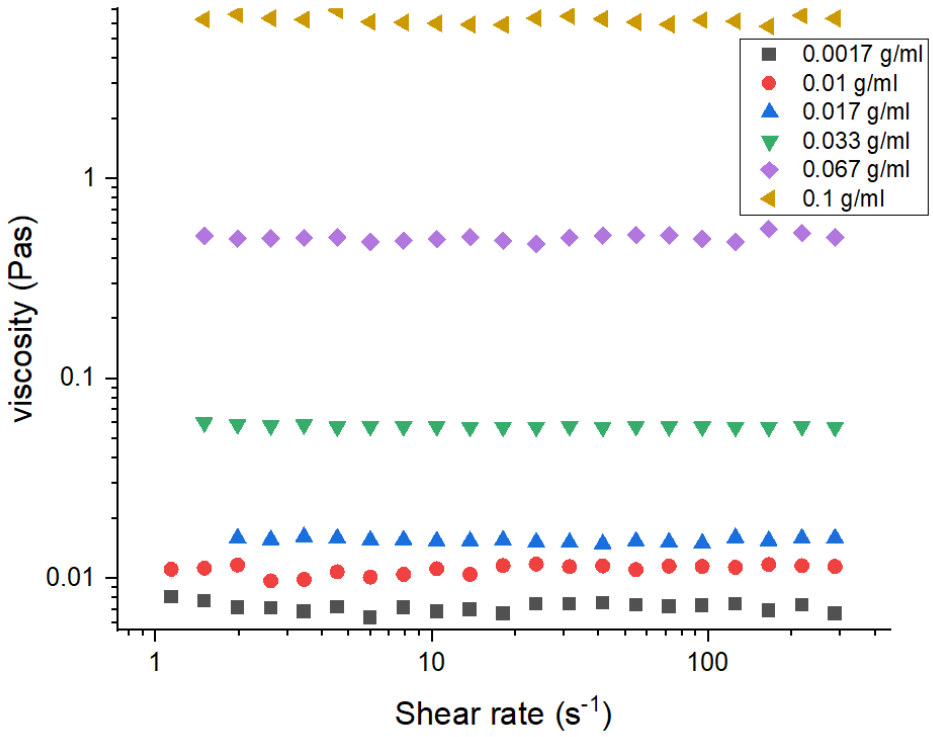

FIGURE 4.3: Newtonian nature of our studied PAN-DMSO system, some examples.

and PAN solutions were completely performed on a Malvern Kinexus Pro rheometer using cone-plate geometry. Viscosity measurements for HPC and PMMA solutions were performed using a Bohlin Gemini rheometer using the same geometries with same configurations. The geometry chosen had a 0.02 radian angular gradient. The temperature was kept to within ± 0.1 K. The viscosity of dilute polymer solutions was similar to that of the solvent. We conducted experiments using coaxial cylinder geometries to provide more accurate data in this area. Depending on the type of polymer analyzed, the shear rate was kept between 0.1-1000 s^{-1}, and the shear stress range was varied accordingly. All of the measurements were carried out at constant shear rates. PAN measurements in DMSO were carried out up to 288 K, but not below, because DMSO freezes below that temperature. The zero-shear viscosity was calculated using the linear viscosity data collected. The Figs 4.1-4.3 show the linear Newtonian nature of the zero-shear viscosity of HPC, PMMA and PAN solutions. This was similar to the Newtonian nature seen in our results for PDMS solutions, shown previously in Fig 1.2. This zero-shear viscosity represented the viscosity of the polymer solution. The corresponding information is provided in the two Figs4.4-4.5, to provide clarity between the much higher concentrations of PDMS than the other polymers.

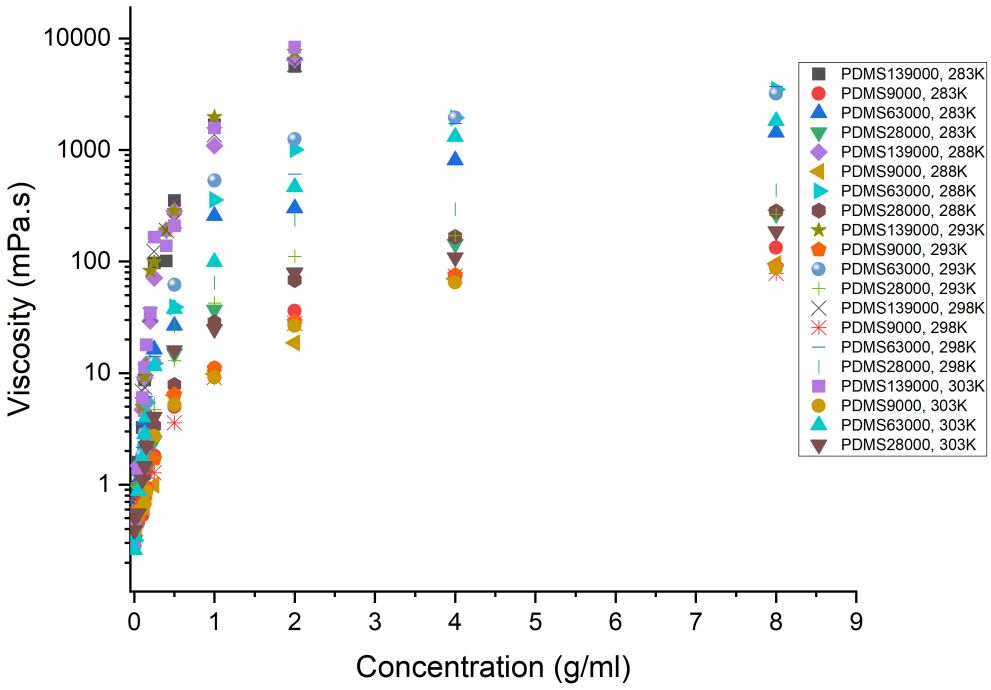

FIGURE 4.4: Viscosity data for all studied concentrations of PDMS at temperature range of 283-303K.

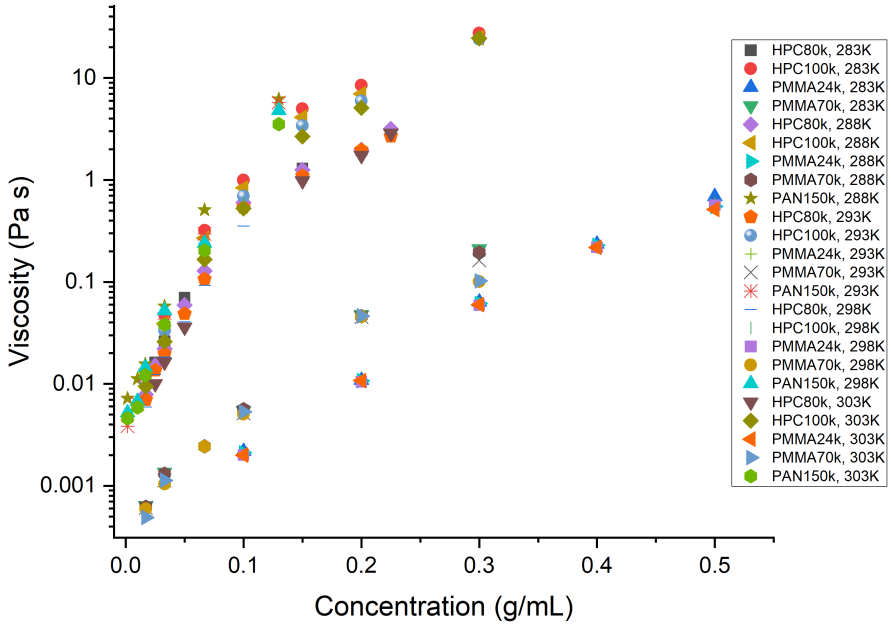

FIGURE 4.5: Viscosity data for all studied concentrations of HPC, PMMA and PAN at temperature range of 283-303K.

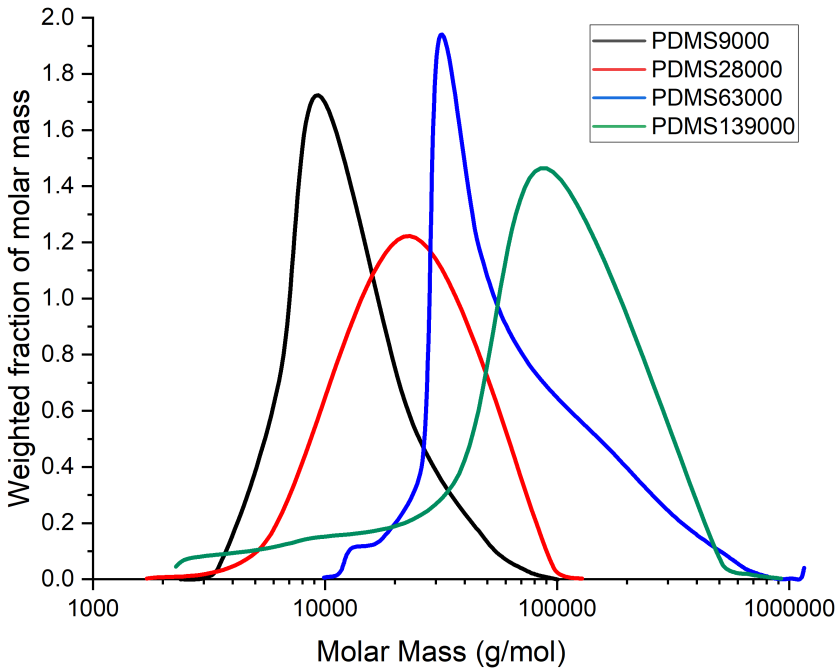

FIGURE 4.6: Molecular weight distributions of PDMS measured at 298K by GPC.

4.3 GPC measurements

Gel permeation chromatography (GPC) measurements were performed to obtain the molecular weight distribution and thereby the polydispersity index of each polymer. GPC for PDMS were performed with a Viscotek dosing and pumping module GPCmax VE 2001, triple detection module (RI, RALS / LALS, IV) Viscotek TDA 305, Viscotek detector UV Detector 2600, Jordi Resolve DVB Medium MB gel column (300 x 7.8 mm), eluent - dichloromethane HPLC, flow 1 ml / min, separation temperature and measurement 303 K. For calculations by conventional calibration, set 12 is used narrow patterns PS ReadyCal set Mp 400-2 000 000.

Similarly, GPC measurements were performed for HPC, PAN and PMMA with an Agilent Series 1260 device equipped with a PSS SECcurity pump and a PSS SECcurity RI refractive index detector. For the cellulose, 0.1M NaCl-water solution was used as an eluent at a flow rate of 1.0 mL/min and at a temperature of 303 K . For the PAN and PMMA, dimethyl formamide (DMF) and toluene, respectively, were used as an eluent at a flow rate of 1.0 mL/min and at a temperature of 333 K and 303 K respectively. Some of the obtained chromatography information is shown in Fig 4.6.

4.4 DLS measurements

Hydrodynamic radius, R_h, of the polymer coils were measured through dynamic light scattering technique (DLS). Dilute polymer solutions of a specific concentration were used for each polymer molecular weight, and measurements were performed at 293 K for all of them. A Malvern Zetasizer Nano equipment was utilized for this purpose. the obtained mean size distribution for some polymer varieties variety are shown in Fig 4.7. The setup was calibrated with standard PDMS and PMMA of narrow molecular distribution and the sizes compared against literature. The measurements for the polydisperse samples were performed after that. Sizes calculated from light scattering is analyzed and reported as such.

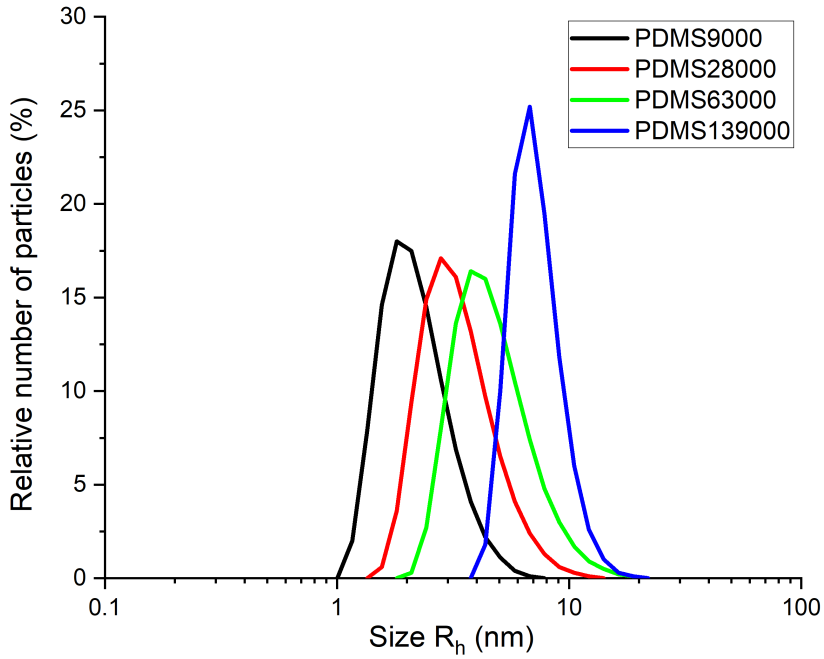

FIGURE 4.7: Hydrodynamic radius, R_h, measured at 293 K for all different molecular weights of PDMS through DLS.

Chapter 5

Macroscopic viscosity analysis for polymer solutions

5.1 Previously developed equation and its limitations

The viscosity of a solution is determined by a variety of internal characteristics (which vary depending on the chemical composition of the solution) as well as some key lengthscales in the system, such as size of the polymer coils (R_h and R_g respectively), and the correlation length ξ [89, 101]. The correlation length is strongly influenced by the polymer concentration in solution. As a result, polymer solutions are typically divided into three types based on polymer concentration: dilute, semi-dilute, and concentrated. [12, 99, 73]. The idea of viscosity for different length-scales was first explored during the previous studies of nanoprobe diffusion in hexaethylene-glycol-monododecyl-ether and PEG/PEO solutions in water for a wide range of nanoprobes' sizes (0.28-190.00 nm) [84, 89]. The size of the probe sets the length-scale at which we probe the viscosity. As already discussed in Chapter 1, we determined the effective viscosity experimentally as a function of the probe size, r_p, from the diffusion coefficient of nanoprobes, D:

$$\eta(r_p) = \frac{k_B T}{6\pi D r_p} \tag{5.1}$$

The effective viscosity was calculated using the following theoretical equation:

$$\eta(r_p) = \eta_0 \exp\left[\left(\frac{\gamma}{RT}\right)\left(\frac{R_{eff}}{\xi}\right)^a\right] \tag{5.2}$$

Here, $\eta(r_p)$ is the effective viscosity experienced by the nano-probes (in units of Pa.s), η_0 is the solvent viscosity (also in units of Pa.s), R is the gas constant, T the temperature in the absolute scale, k_B is the Boltzmann constant, a is a structural parameter of the order of unity, γ is the effective activation energy of the solution (in kJ/mol), and ξ is the correlation length (in nm). R_{eff} is the length-scale given by [85, 92, 94]:

$$R_{eff}^{-2} = r_p^{-2} + R_h^{-2} \tag{5.3}$$

where R_h is the polymer's hydrodynamic radius in solution. In the case of large probes, $R_h << r_p$, Eq 5.2 reduces to the macroscopic viscosity η_{macro} of the polymer solution:

$$\eta_{macro} = \eta_0 \exp\left[\left(\frac{\gamma}{RT}\right)\left(\frac{R_h}{\xi}\right)^a\right] \tag{5.4}$$

where η_{macro} is the viscosity observed at the macroscale. This method has been successfully applied to a variety of complex liquids: colloidal solutions, protein solutions, micellar solutions, cytoplasm of HeLa cells and *E.coli*. Afterwards, a lot of work was performed on analysis of the viscosity of polyethylene glycol (PEG) solutions in water for dilute and semi-dilute concentration regimes, as elucidated in a series of papers[89, 86, 102, 108]. As a consequence, a model for length-scale-dependent viscosity in solutions was proposed, initially for a system comprising two polymer species. The use of aqueous PEG/PEO solutions, whose single-component solutions had already been well expressed in the form of viscosity scaling, offered an easily interpretable comparison. The focus during development of the model was entirely on double-entangled systems, which featured two characteristic length-scales that were distinguishable to two different polymers, while ensuring that their solution concentrations were such that they remained within the entangled zone. For further identification of the individual contributions of each component, investigations were performed on systems that contained two PEG/PEO species with molecular weights that vary by, at the very minimum, an order of magnitude. The viscosity of all these systems were studied at both the macroscale (using rotational rheometry) and nanoscale (through fluorescence correlation spectroscopic measurement of molecular probe diffusion, similar to the previous nanoprobe diffusion studies). This approach allowed the development of the single equation, Eq 5.4 that was thought of being capable for describing the viscosity of different types of polymer solutions across all length-scales.

Previous approaches, on the other hand, were only valid in a modest parameter space of concentrations (dilute, semi-dilute, or within some limits of these regimes), molecular masses, and temperatures. One of the key issues with strong viscosity models is the absence of results for various dependencies such as radius of gyration as a function of concentration and temperature for various polymer-solvent systems [73, 98] or activation energy for flow at various thermodynamic conditions. Although the thermodynamics of polymer solutions is well understood [109], polymer rheology is not. Another important underlying aspect integral to all these parameters is the molecular weight of the polymers, obtained from its distribution functions. From the standpoint of theoretical developments, standard polymers with well-characterized narrow chain distributions are ideal. On the other hand, practical applications are limited to faster manufacturing processes and techniques that result in polymers with wider weight distributions. It's also critical that the model can be used on a larger scale, and that it can handle a wide range of polymers and solvents, which was a limitation of the previous PEG/PEO-water model.

5.2 Applying overlap concentration, c*

To develop our model, our first consideration was expansion of the concentration regimes to beyond the dilute-semi dilute studies for most well-developed scaling theories, including our own model as described in Section 5.1. The classification of concentration zones into non-entangled and entangled zones, as used in the PEG/PEO systems, is based on the perspective of the polymer inside the solution. It allows us to identify whether the polymers are well separated from each other (non-entangled, or dilute), or their chain penetrate and intertwine with each other (entangled). Such an approach can be effectively described by Fig 5.1.

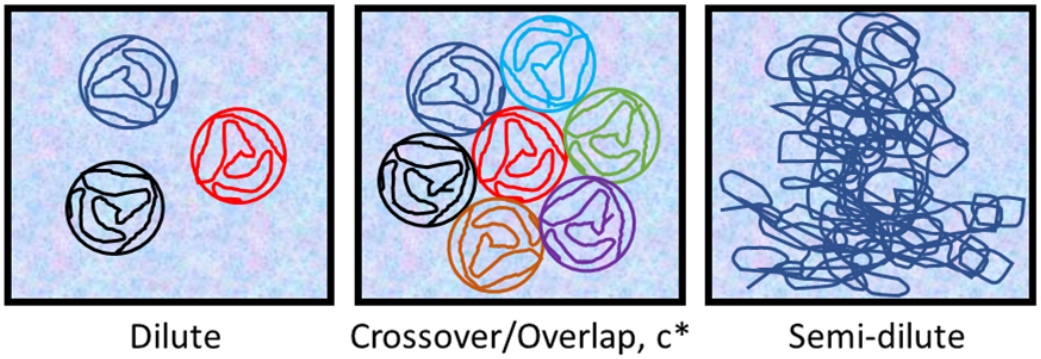

FIGURE 5.1: Concentration zones based on whether systems are non-entangled (dilute) or entangled (semi-dilute).

The crossover or overlap concentration c* was described previously in Eq 3.5. Initially, the obtained viscosity data were plotted as a function of the c to c* ratio, where both the concentration parameters c and c* were expressed in terms of the mass of the polymer per unit volume of the solvent, according to de Gennes' proposed general scaling theory. The de Gennes' theory states that such scaling plots start to plateau off beyond the semi-dilute concentrations, after an initial linear rise. As can be seen from Figs 5.2-5.3, a similar dependence was observed for our polymer systems as in theory.

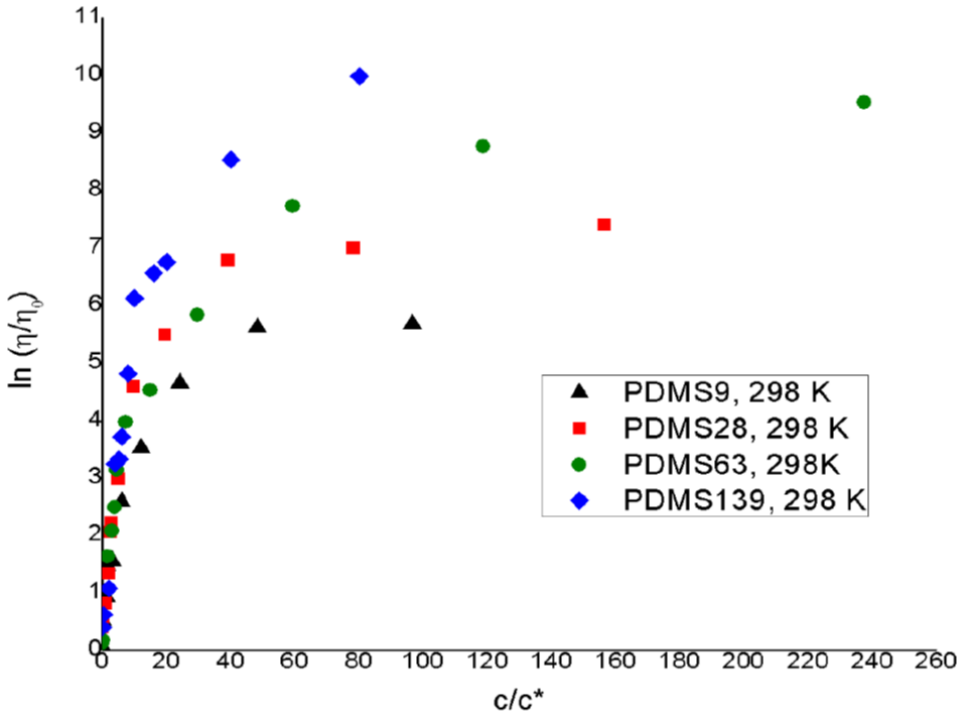

FIGURE 5.2: Results of relative viscosity measurements for PDMS-ethyl acetate solutions plotted against ratio of concentration c to overlap concentration c^*

However, such a theory is not enough to obtain a complete linear scaling across different variables. This is because at higher concentrations, the plots plateau off instead of collapsing on a single line. To take care of this, the viscosity scaling

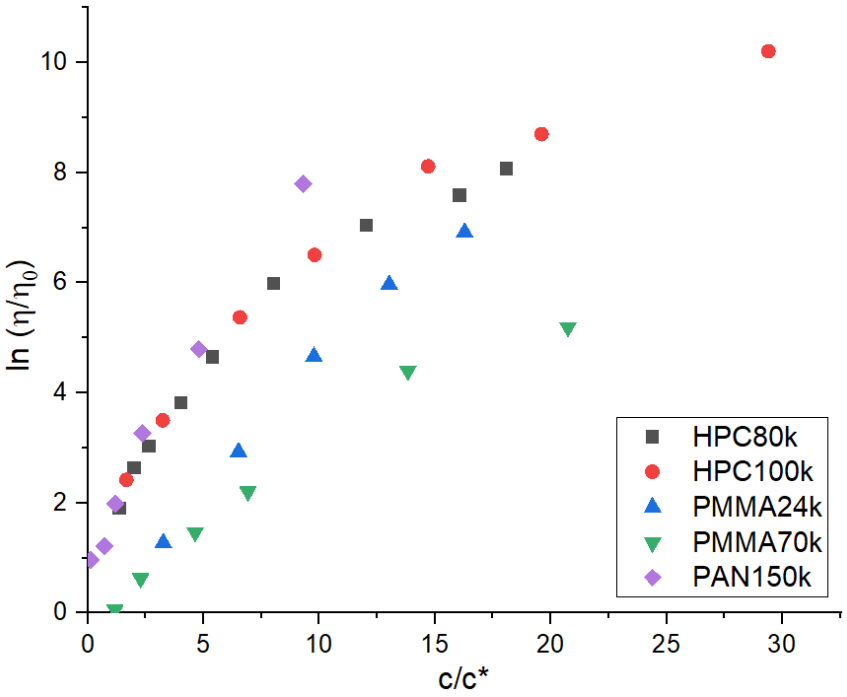

FIGURE 5.3: Results of relative viscosity measurements for HPC, PMMA and PAN solutions plotted against ratio of concentration c to overlap concentration c^*

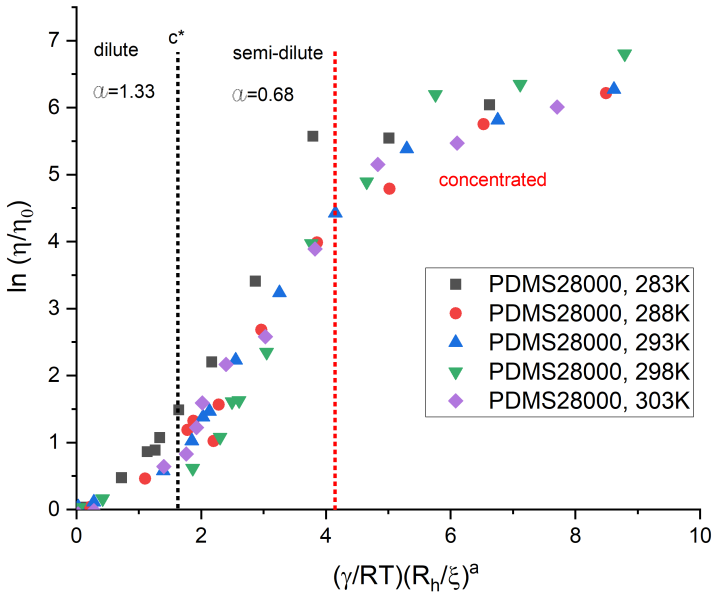

FIGURE 5.4: Initial scaling of viscosity data for PDMS of molecular weight 28kg/mol at different temperatures. Only one crossover point c^* was applied (black vertical dotted line). The red vertical dotted line indicated another change in properties from semi-dilute regime, alluding to the presence of a second crossover c^{**} and the concentrated zone. As per the fitting results, here we fixed c^*.

paradigm was developed initially by Wisniewska et al for PEG/PEO systems upto semi-dilute concentrations, as mentioned before. The same scaling paradigm, Eq 5.4 was applied at first to our PDMS-ethyl acetate systems without making any changes during fitting for any of the parameter values from the PEG/PEO-water system. The results of such an approximate fitting are provided in Fig 5.4. It can be seen from the Fig 5.4 that the low-concentration solutions complied with this relationship to a greater extent than the samples with higher concentrations. Even though the basic c/c^* scaling of Fig 5.2 is also correct, the representation of Eq 5.4 scales the data better. The deviation of this scaling results in Fig 5.4 from perfect linearity was due to variations in the different fitting parameters of Eq 5.4 for a completely different polymer-solvent system. However, the most crucial factor for such a deviation was that there existed a second crossover at higher concentrations which was not considered. Such a crossover occurs within the entangled zone when the concentration can no longer be classified as semi-dilute, but it is known as concentrated.

5.3 Introduction of cross-over from semi-dilute to concentrated solutions, c**

To identify this crossover point, we decided to approach the nomenclature of the entangled zones from the perspective of the amount of solvent present in the system, and the number of interactions of the solvent molecules with the monomer chains in solution. Literature reviews provided a solution to calculating this unknown second crossover point. As described by Cheng et al [98], and Daoud et al [73], with increasing polymer concentration, coil dimensions begin to shrink. This is due to a decrease in the number of solvent-monomer contacts as the molar fraction of polymers in solution increases. The pure polymer melt is the extreme limit of the concentrated regime of polymer solutions. Cheng et al [98] presented an equation for the concentration at the onset of the transition between semi-dilute and concentrated regime:

$$c^{**} = \frac{R_g}{R_g(\theta)}^{2(3\nu-1)/(2\nu-1)} c^* \tag{5.5}$$

where $R_g(\theta)$ is R_g for the pure polymer melt [110]. The parameter $\nu = 0.6$ is from the Flory model for polymers in good solvent [10]. This model, however, does not always match experimental data. For linear PDMS chains, we looked to the radius of gyration, R_g description by Gagliardi et al[111] to obtain the required weighted average values from:

$$R_g = (0.0265 \pm 0.005) M_w^{0.53\pm0.02} \tag{5.6}$$

Thus in the case of PDMS solutions, we applied $\nu = 0.53$ instead of 0.6 in Eq 5.5 to calculate the prospective c** values. As we progress into the concentrated region, this is the point at which the composition of the complex liquid changes quantitatively. We interpreted the various local molecular interactions between the monomer and the solvent based on those quantitative values to widely classify the solution into three concentration zones. Consequently, via the molecular proportion of the interacting molecules, we were able to determine the shift from semi-dilute to concentrated zone at:

$$\text{molecular fraction of monomers in solution} > 0.5$$
$$\implies \text{c} \geq \text{c}^{**}$$

We could explain this by the fact that the number of solvent molecules interacting per monomer unit of the polymer chains in the solution was less than 1-2 at such large concentrations. Fig 5.5 depicts this definition of the semi-dilute - concentrated crossover point c**.

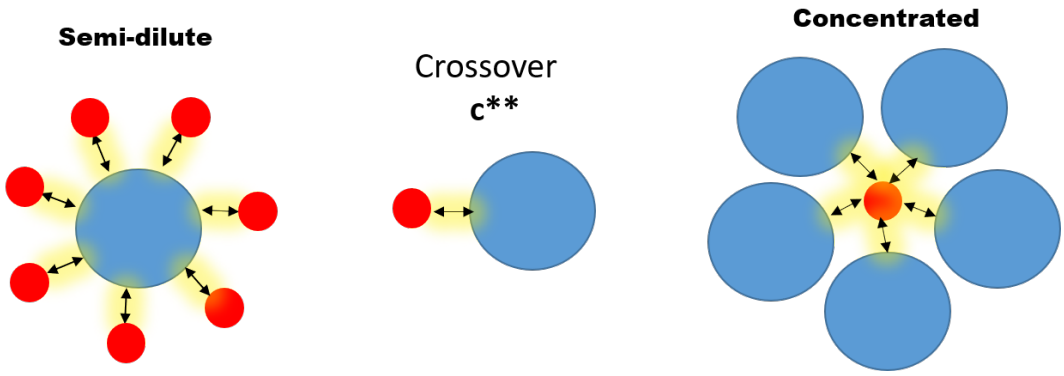

FIGURE 5.5: Crossover point *c*** from semi-dilute to concentrated regime based on molecular interactions. The ● denotes the solvent molecules, while the bigger ● denotes the monomers.

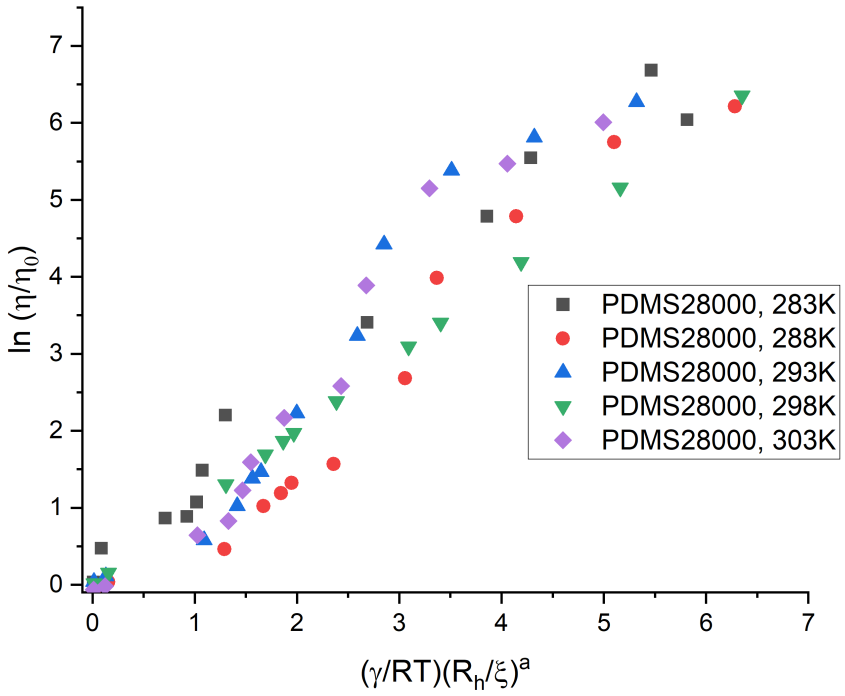

FIGURE 5.6: Initial scaling of viscosity data for PDMS of molecular weight 28 kg/mol at different temperatures with both crossover points c* and c**. It was observed that further scaling with regards to other parameters was necessary. As per the fitting results, here we fixed c** and *a*.

The effect of the solvent on the polymer is determined by the intermolecular interactions oberserved for polymer chains in solution [76]. Since the number of

interacting solvent molecules is far greater at lower concentrations, the correlation length, as measured by Eq 5.3 (the junction of hard-sphere polymer coil interactions to entangled coil interactions), governs the change from dilute to semi-dilute. It should be noted that the size of the monomer and solvent molecules in Fig 5.5 is merely a representation of the transitional phase or crossover point, and not to scale according to their actual sizes. The corresponding Fig 5.6 shows the results with the same parameter values as in Fig 5.4, with the addition of c** values. It could be clearly seen that while there was an improvement in the linearity of the scaling function, it needed better analysis of the other parameters influencing the viscosity.

The same viscosity scaling paradigm, Eq 5.4 was applied to our other three polymer systems of HPC-water, PMMA-toluene and PAN-DMSO as well. The approach was kept similar to that of PDMS-ethyl acetate, without changing any of the fitting parameter values from the PEG/PEO-water results [108] for the applied intial scaling. However, because these three were powdered polymers with a saturation limit of dissolution in the solvents within our temperature range, calculations of c^{**} revealed that, unlike with PDMS-ethyl acetate, the applied concentrations did not venture into the theoretical concentration ranges above c^{**}. As a result, all fitting was applied in the dilute and semi-dilute concentration ranges as done by Wisniewska et al [108] on PEG/PEO-water solutions. Another reason for having lower concentration ranges for these three polymers was their Non-newtonian behaviour in solution at higher concentrations, especially for HPC. At around 313 K approximately, the HPC in water solutions starts to separate out and form precipitates, making it imperative that all solutions are prepared and stored at ambient temperatures bewteen 283-303 K. Beyond 5% by weight concentrations in solution, HPC exhibits non-Newtonian behavior. HPC has a maximum solubility in water of about 30% by weight, after which it exhibits totally non-Newtonian behavior. As such, theoretically it was possible to obtain c** values for HPC in water solutions by applying Eq 5.5, however prepared solution concentrations for viscosity analysis were always lower than the established c** values. Theoretical c** values was around 27-30% concentrations by polymer weight. The same limits were found for PAN-DMSO and PMMA-toluene, with similar explanations for higher theoretical c** values, so all experimental concentrations were restricted to the semi-dilute concentration areas.

5.4 Coil dimensions R_h and R_g variations with concentration

There are different parameters that define the dimensions of polymer coils inside the solution, providing different representations of structure-property relationships. The exponent ν (Eq (5.4)) from Flory's mean-field theory [10] allows us to obtain the parameter β=3/4 which is essential for the correlation length ξ estimation. The correlation length ξ exists only in the entangled zone, and is different to the parameter gyration radius, R_g. As mentioned before in section 3.2 R_g describes the isolated polymer coil blob size at all concentrations, whereas ξ defines the distance between the interconnection points of the polymer networks. When the polymer coils are well-separated in dilute zone of the solution concentrations, they are ideally treated as perfectly spherical objects. It is assumed in such a zone that any changes in concentration does not impact the size of the coils, since they remain apart from each other regardless of local monomer density fluctuations. Therefore, for dilute solutions where there is no interconnected networks, it is more accurate to define ξ as the mean distance between the centre of masses of different nearby coils. Correspondingly, this allows to identify the position of all coils of the polymer in solution, a

characteristic that is valid for defining ξ across all regimes of solution concentration classification. In this way, estimates of mesh sizes and blob sizes can be obtained even in semi-dilute and concentrated solution regimes (as postulated by Rubinstein [112]).

A different coil dimensional parameter - the hydrodynamic radius, R_h, of the polymer coils (defined previously in section 3.2, were measured at dilute concentrations through dynamic light scattering technique. The data obtained, when combined with available empirical values of R_h obtained from literature for our studied different polymer-solvent systems, was subsequently used to fit in the scaling equation (Eq 5.4). For long chains, empirical power law equations of the type [98] R_c=KM_v^y connect coil size (in terms of nm) and molecular weights (in terms of g/mol), as shown in Eq 3.2. The constants K and y have values unique to a polymer-solvent system [95, 96, 97], and the parameter R_c is typically defined as the gyration or hydrodynamic radius. However, such relationships are not adequate enough to obtain fluctuations in coil sizes due to higher concentrations, where there are much higher effects of chain stiffness for instance. Based upon the work of Gagliardi et al [111], Eq 5.6 was used to calculate the gyration radius R_g for PDMS, with minor changes in the power law coefficient to account for the change in solvent and fit the experimental data. It was more difficult to obtain emipirical power law relationships for the hydrodynamic radius R_h in the case of PDMS-ethyl acetate systems, due to lack of previous research data for this specific polymer-solvent system. Therefore, we used dynamic light scattering measurements to obtain information about the R_h for PDMS-ethyl acetate at dilute concentrations. To ensure that power law would be valid, we fit the measured data within limits of other empirical power law equations available for different polymer systems [94] including other solvent systems for PDMS [97, 96]. The fitting of R_h with Eq 5.4 resulted in the following power law relation for PDMS-ethyl acetate:

$$R_h = (0.0113 \pm 0.001) M_w^{0.57 \pm 0.01} \tag{5.7}$$

where R_h is determined in nanometers (nm). Power law relationships for R_h for the other three polymer-solvent systems- HPC-water, PMMA-toluene, and PAN-DMSO, were also obtained similarly from the DLS measurements. Similar to PDMS, they were combined with available literature data [96, 97, 113, 114, 115, 116, 117, 118], and the resultant coefficients and exponents of the different power law relations for both R_h and R_g of our studied polymer-solvent systems have been presented earlier in Tables 3.1-3.2.

When analyzing the structure within the polymer solutions, the coil dimensions are considered constant, as formerly stated, even as concentrations increase. Usually it is because previous studies of polymer solutions were focused on either the dilute region of concentrations, or in the semi-dilute zones very close to the dilute regime. The polymer coils are separated and far apart in the dilute solutions [73]. With such a small number of coils in the solution, interchain or intrachain interaction effects are irrelevant, and the coil dimensions are unaffected by even small concentration changes. As such, the ratio of the coil dimensions R_h and R_g remain fixed at the values obtained from power-law relationships. In the case of PDMS-ethyl acetate for instance, the ratio in the dilute regime is given by:

$$\frac{R_h}{R_g} = A, c < c^* \tag{5.8}$$

where, the parameter A is obtained from Eqs(5.6,5.7) as:

$$A = \frac{(0.0113 \pm 0.001) M_w^{0.57 \pm 0.01}}{(0.0265 \pm 0.005) M_w^{0.53 \pm 0.02}} \tag{5.9}$$

The corresponding R_h/R_g ratios for HPC-water, PMMA-toluene and PAN-DMSO in the dilute solution regimes can be similarly obtained by dividing their power law relationships available in Tables 3.1-3.2. Considering that previously established values of R_h/R_g are approximately around 0.6 numerically for most polymers in good solvents [119, 120, 121], the relationship for all our polymer-solvent systems maintain the same numerical state in the dilute regime.

As we move further into higher concentration regimes, it is vital to consider the effect of the local monomer fluctuations on the size of the polymer coils, to obtain a clearer characterization of polymer solutions. R_h and R_g provide us information not only about the effective size and orientation of polymer coils in solution, but also regarding the hydrodynamic and static screening lengths that occur [122, 73]. Daoud and Jannink [73], and later on Cheng et al [98] proposed that due to increasing screening effects of repulsive intrachain interactions being far greater than that of interchain interactions, the coil dimensions should decrease with increasing concentrations in the semi-dilute and concentrated regimes. Bennett et al [122] utilized the same approach to make it applicable for higher concentration regimes beyond c^*, while predicting that the variations of hydrodynamic screening length would lead to fluctuations of polymer coil sizes as well. However this approach, which was applied for PDMS solutions with other good solvents such as toluene and benzene, predicts a decrease in the static and hydroydynamic screening length with increasing concentration. The ratio of the hydrodynamic to the static screening lengths therefore increase with increasing concentration. But this approach was developed by having measurements of solutions with concentrations up to 0.2 g/ml, which is slightly lower than the end of the predicted semi-dilute zone in our data for PDMS-ethyl acetate systems. It is also the same situation when using dynamic light scattering measurements to obatining information for R_h, where we are limited to using concentrations within the dilute or lower semi-dilute zone. In order to obtain any information about further effects of coil dimension changes, we are usually limited to thoretical assumptions based on neutron scattering experiments. Our viscosity paradigm scaling theory instead provides information about coil dimension fluctuations with concentration changes in the same principle as that of Bennett, upto the semi-dilute zone. This leads to a slight increase in the coil dimensions in the semi dilute zone, and we initially determined the following relationship in the case of PDMS-ethy acetate systems:

$$\frac{R_h}{R_g} = A x^{0.053 \pm 0.005}, c^{**} > c > c^* \tag{5.10}$$

with x being the mole fraction of the monomer in the solution, and parameter A as obtained from Eq 5.14 above. Our predicted exponent for x (approximately 0.053) is slightly lower than that developed by Bennett et al [122] (approximately 0.15) for other PDMS-solvent systems. Following this, we applied the same theory for our other three polymer-solvent systems, and by fitting all the relevant data through Eq 5.4, we arrived at the following general relationship for polymer coil size variations in the semi-dilute regime:

$$\frac{R_h}{R_g} \sim x^r, c^{**} > c > c^* \tag{5.11}$$

where r is the value of the exponents for the mole fractions in the case of each different polymer system. The values of A can be determined using Tables 3.1-3.2 as mentioned before. All our predicted exponents r for the polymer mole fractions are provided in Table 5.1. The exponents for HPC are far lower than for the other

TABLE 5.1: Exponent r defining the dependence of coil sizes on mole fractions x

Polymer system	r
HPC-water	0.005
PMMA-toluene	0.043
PAN-DMSO	0.053
PDMS-ethyl acetate	0.053

polymers [118, 123, 124], as HPC has a far stiffer chain and resists deformations. Consequently, it leads to far lower increase in sizes as compared to the other polymers.

The interactions between the monomer and the solvent are reduced to a greater degree in the concentrated zone than in the semi-dilute zone. The screening effect explained by Bennett [122] or Cheng [98] extends to the concentrated zone, possibly before the onset of the second crossover. However, we assume that the intrachain repulsive interactions in the semi-dilute zone are much greater than those in the concentrated zone. Interchain attractive interactions significantly outnumber intrachain repulsions at large polymer concentrations, and this accumulation of chains within the solution matrix decreases the hydrodynamic to static screening ratio as concentration rises. Correspondingly, a decrease in the R_h/R_g ratio follows. For the sake of convenience, we suggest that beyond the second crossover, at higher concentrations, the coil dimensions shrink:

$$\frac{R_h}{R_g} = Ax^{-0.047\pm0.001}, c > c^{**} \tag{5.12}$$

The coil dimensions become similar to the original unperturbed sizes as the solution approaches melt properties. The above Eqs 5.8-5.16, and fitting of the experimental viscosity data to the values of the constants allows us to gain a better understanding of the effect of concentration on coil dimensions. This is extremely crucial to the analysis of the structure and behavior of polymer coils in good solvents.

The three powdered polymers HPC, PMMA and PAN did not have solution concentrations that could reach the concentrated zones, and so, their ceoncentration-size dependence in the cocentrated regime was not determined, unlike for PDMS-ethyl acetate [2]. This is a general issue with most polymers in that their effective concentration zones usually lie in the semi-dilute concentration regions by theory. This also explains why most available scaling theories in literature were usually developed for semi-dilute concentration regimes. The parameter R_h is crucial for obtaining the specific polymer-solvent relationship. The R_h/R_g ratio is calculated using our fitted model, and it implicitly relates to hydrodynamic volume changes relative to viscosity as described under shear flow (obtained through Eqs 5.1, 5.3, and 3.3). Most importantly, we have attempted to offer a simpler model that explicitly provides the size changes due to various stiffness effects, rather than the different variables that affect chain stiffness.

5.5 Scaling parameter a

The scaling exponent a in Eq 5.4 is a parameter of order unity that changes discontinuously at the crossover to the different concentration regimes. When the initial scaling paradigm was developed in PEG/PEO-water solutions, it was observed that $a = \beta^{-1}$ for the dilute regime and $a = R_h {R_g}^{-1} \beta^{-1}$ for semi-dilute regime of concentrations [108]. This parameter a is clearly a feature of a particular polymer-solvent system, and it provides details on the internal configuration of any complex liquid [101]. Changes in the internal properties (as illustrated by the differences in coil sizes) result from switching between the three regimes of dilute, semi-dilute, and concentrated solutions, and hence leads to changes in the value of a. [12, 64, 125, 126]. Fitting of the Eq 5.4 allows us to obtain the different values of a within acceptable deviations as provided in the Table 5.2 for all polymer systems investigated so far [94, 2, 127].

TABLE 5.2: Scaling parameter a values for different polymer systems, in different concentration regimes - dilute (Dil), semi-dilute (SDL) and concentrated (Conc).

Scaling parameter a values				
Polymer system	Dil	SDL	Conc	Error
HPC-water	1.28	0.85	-	$\pm$ 0.02
PMMA-toluene	1.25	0.75	-	$\pm$ 0.02
PAN-DMSO	1.25	0.86	-	$\pm$ 0.02
PDMS-ethyl acetate	1.28	0.85	0.59	$\pm$ 0.02

The values are in line with the available literature values for other polymer systems [128, 129, 130, 131] in dilute and semi-dilute systems. It can also be seen from Table 5.2 that the values of a for dilute and semi-dilute regimes maintains the same form, as shown in the polymer systems developed by Wisniewska et al [94, 108] for PEG/PEO-water. Fitting also allows us to obtain the a values for the concentrated zone as well in the case of PDMS-ethyl acetate solutions. The obtained data for a remain applicable for all different molecular weights of these polymer-solvent systems. Our scaling parameter a is very similar to and of the same order as the well-defined Mark Houwink parameter. As observed for the Mark Houwink parameter, typical values are around 0.8 for a good solvent for polymers, with variations between 0.5-0.8. As the polymer flexibility in the solution reduces, this parameter value rises to beyond 1.0. Similarly, in our case, the scaling parameter a is dependent on the chain entanglements, with purely inflexible spherical approximation in the dilute zone (a = 1.25-1.30), and according to variation in semi-dilute (a = 0.75-0.86) and concentrated zones (only for PDMS solutions) (a = 0.58-0.61).

5.6 Activation energy parameter, γ, and its components

Viscosity is a rate activated entity for flow processes, similar to that of chemical reactions. Every motion requires an overcoming of the barrier or threshold, below which the motion stays inactive and above which the it proceeds. For any fluid to flow, it needs to arrest the various frictional forces existing between the molecular layers. Thus there exists a parameter in our scaling paradigm for identifying the amount of threshold energies required for negating before the the viscous flow is activated. Our developed activation energy parameter γ [94] is related through the rate theory of Eyring [107, 132], as already discussed in section 3.2. The basis of parameter γ

is overcoming the molecular layer frictional energies so that the layers start to slip over each other by one molecule at a time. This slippage of one molecular layer past the surrounding molecules though a small hole results in the flow of the solution. We further expanded the study of this parameter to identify the exact nature of its components [2]. Depending on the solution concentrations, the amount of frictional interactions inside the system varies, and so does the energy required for the flow of the viscous solution. Since there is always a certain amount of polymer present in our solutions, the total interaction parameter, γ, is assumed to be a sum of the weighted fractions of the different molecules inside the system. Thus γ is defined as:

$$\gamma = \gamma_{1,2}X_1 + \gamma_{2,2}X_2 \tag{5.13}$$

where the subscripts 1 denote solvent and 2 denotes monomer, and X denotes the mole fraction of the corresponding component. Through the fitting procedure applied to Eq 5.4, we obtain estimates of the different activation energy parameters in the same way as we obtained for the coil size fluctuations and scaling parameter before. The results of the fitting for γ parameters are provided in the Table 5.3.

TABLE 5.3: Activation energy parameters for all polymer-solvent systems studied in Eq 5.13

All γ are in units of kJ/mol		
Polymer-solvent	$\gamma_{1,2}$	$\gamma_{2,2}$
HPC-water	4.20±0.50	2.70±0.30
PMMA-toluene	4.60±0.70	3.10±0.60
PAN-DMSO	4.30±0.30	2.90±0.25
PDMS-ethyl acetate	4.00±0.50	2.75±0.50

The subscripts 1, 2 denote the solvent-monomer activation parameter, which is the prevalent one in the semi-dilute zone, as previously mentioned. Accordingly, any variations in the total energy are affected by $gamma_{1,2}$ values during the fitting process, while the other components are considered constant. This is maintained in the same manner for the concentrated zone with $\gamma_{2,2}$. Both components are kept constant during the fitting for the dilute zone, since such situations involve activation energies primarily due to the frictional forces of the solvent molecules. The pure solvent viscosity parameter, η_0, provides the necessary solvent molecular interactions for consideration. From the information of Table 5.3, it can be seen that the overall γ varies around 4.00 kJ/mol (± 0.50 kJ/mol) across all range of mole fractions for all the molecular weights. Activation energies for different systems as reported in various literature [94, 108] are of the same magnitude for the viscous motion of such polymer solutions. The activation energies for the systems are very similar, even though there are differences in the monomer sizes of the different polymers. The expected HPC monomer size is almost 7-8 times larger than that of PMMA, PEG, PDMS or PAN monomers. It implies that the activation energy of polymer solutions is not very dependent on the monomer size. Most analysis for polymer solutions utilize the well-known Flory-Huggins interaction parameter for identifying the internal interaction values inside them. From literature reviews, we observed that the values of the Flory-Huggins parameter for each of our four polymer-solvent systems also has very close values around 0.48 for all. They vary by 5-10% in their values depending upon the types of solvents. It is similar to our observations that simple molecular interactions are not the exact source for the activation energies, regardless of the concentration of the solution. This is contrary to our original assumptions for

describing the nature of the activation energies for viscous flow of solutions. Initially we felt that the amount of the three internal interactions in a two-component system - monomer-monomer, monomer-solvent and solvent-solvent interactions - would determine the effective activation energy required for the viscous flow. However, in such an assumption the size of the monomer would indeed play a big part, which does not seem to be the case when we consider the derived activation energies for the HPC-water solutions. It could be due to the fact that water-soluble polymers often develop hydrophobic interactions, which strikingly lead to phase separation or a demixing on heating. This rather complex cooperative interaction induces an additional ordering of the water molecules in the immediate vicinity of hydrophobic groups. With semi-flexible chains like the cellulose derivatives, long chains may be soluble, but short ones of the same substitution pattern unexpectedly become insoluble and tend to crystallize [133]. We assume that such tendencies lead to lowered activation energies for the HPC monomers in water solutions, even though their sizes are larger.

5.7 Molecular weight averaging function in polydisperse samples

We have shown previously that through GPC measurements, we obtain the molecular weight distribution of our polymers which provides their weight average molar mass, M_w. This mass is used as the molecular weight in the scaling model to obtain the different scaling parameters. When the scaling model was developed initially for PEG/PEO-water solutions or for nanoprobe diffusion, highly standard polymers with narrow molecular weight distributions were used. For this reason, there was no reason to consider any polydispersity effects in the scaling method. In our studies, we have tried to ensure that the model can be used for a wide variety of polymers with different variables, including the ability to use it for non-standard industrial polymer grades. The easiest way to do that is to ensure that the molecular weight distribution covers the differences in individual chain masses due to polydispersity. We initially tried to apply the weighted average M_w for the scaling model, and observed that the scaling obtained for our polymer systems were not as linear as it could be. In the Figs 5.7-5.9, we show the results of scaling for some of our polydisperse polymer systems - HPC-water and PAN-DMSO. We also combined it with the scaling for monodispersed PMMA-toluene solutions, and the results confirmed that a rectification of the averaging function employed for the polydispersed samples was necessary.

Different forms of averaging functions of the generated chromatographic weight distributions may be used to determine the molecular weight of polymer chains. Within any polymer, the chains are seldom of equal length and weight, resulting in a weight distribution. Because of the kinetics or thermodynamics of the reactions, polymerization techniques cause molecular weights to be scattered across various polymer chains. This distribution of molecular weights (MWD) determines the behavior of a polymer in solution or melt form. It is important to obtain a definition of mean or average of these MWDs in order to link the polymer's behavior to its typical molecular weight. Theoretically, different methods are available in literature for determining this average molecular weight [134, 135, 136, 137], and they are employed through fractionation techniques such as GPC to obtain information about the different fractions. In reality, however, the separated fractions are only somewhat narrower in distribution than the rest of the polymers. These fractions

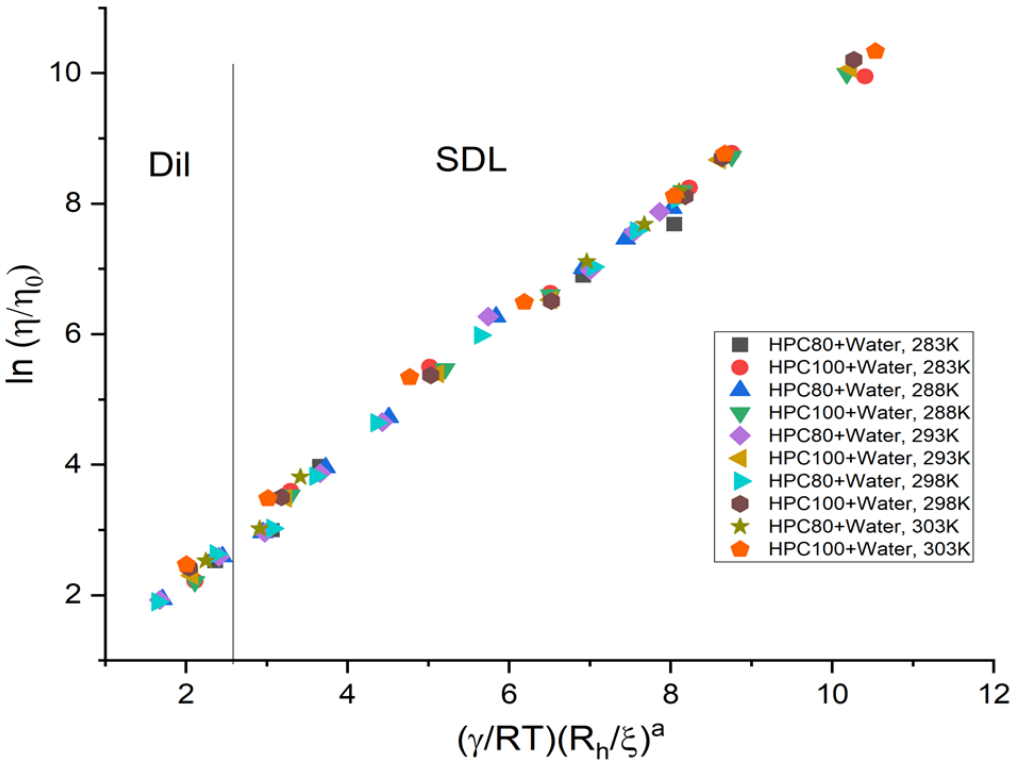

FIGURE 5.7: Viscosity scaling plots for HPC-water at all temperatures (283-303 K), plotted for calculations made with M_w.

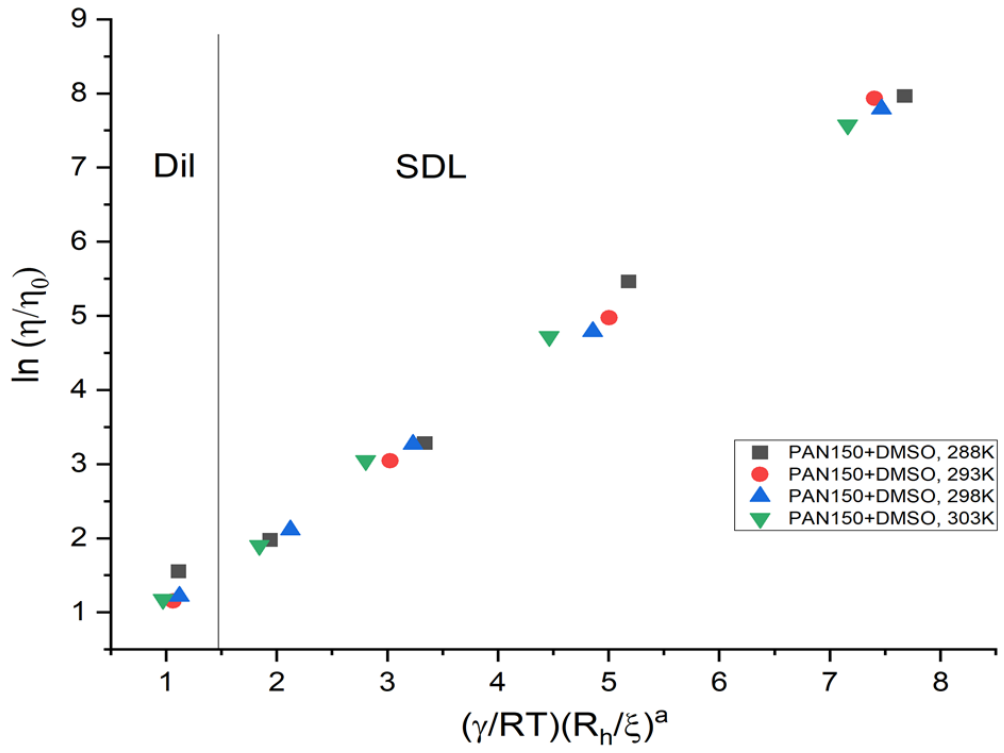

FIGURE 5.8: Viscosity scaling plots for PAN-DMSO at all temperatures (283-303 K), plotted for calculations made with M_w.

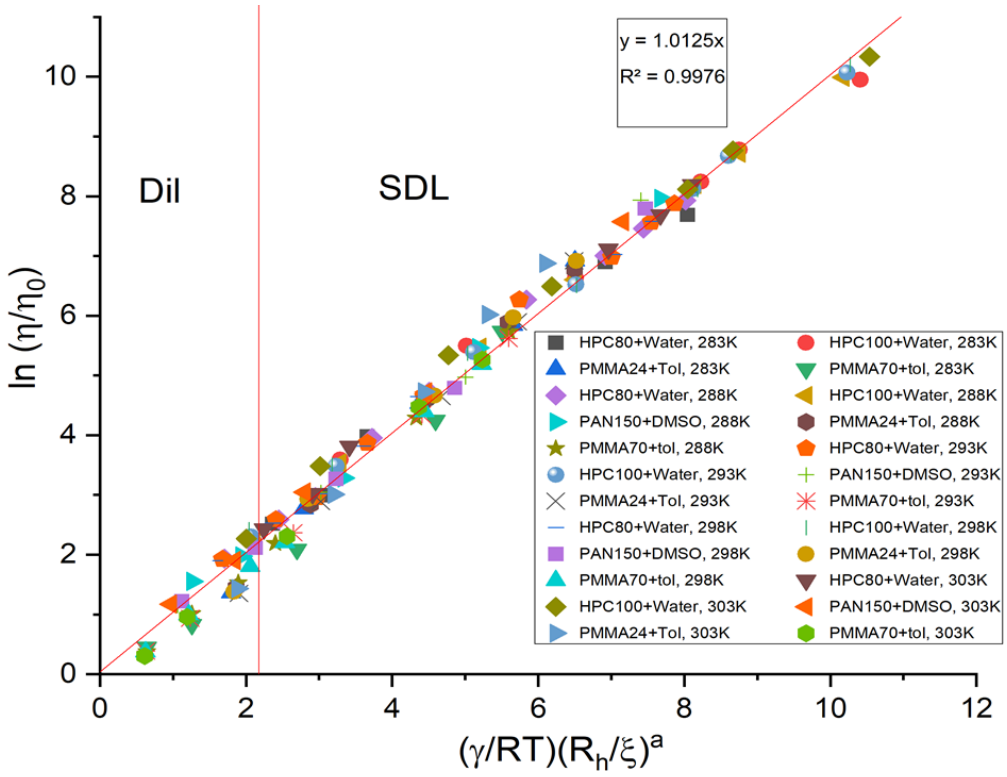

FIGURE 5.9: Combined viscosity scaling plots for all molecular weights of HPC-water, PAN-DMSO and PMMA-toluene at all temperatures (283-303 K), plotted for calculations made with M_w. As per the fitting results, here we fixed the coil dimension changes and γ.

are imagined as perfect and reported as such. Mathematically, the simplest method for obtaining the average molecular weight is simply an arithmetic mean of the molar masses of each macromolecule, and is know as the number average molecular weight, M_n. It is of the form:

$$M_n = \frac{\sum_{i=1}^{\infty} M_i N_i}{\sum_{i=1}^{\infty} N_i} \tag{5.14}$$

The weight average molecular weight, M_w, is the second and most widely used averaging term. It considers the sum of the product of the weight fraction and the molar mass of each species. It is usually calculated by:

$$M_w = \frac{\sum_{i=1}^{\infty} M_i^2 N_i}{\sum_{i=1}^{\infty} M_i N_i} \tag{5.15}$$

The M_n predicts the number of particles in each species present inside a system. The M_w however informs not only about the number of molecules in each species, but also their masses The polydispersity index, or PDI, of a polymer sample is calculated using the ratio of the above two mass indices. Therefore:

$$\text{PDI} = \frac{M_w}{M_n} \tag{5.16}$$

The closer this index approaches to 1, the more similar the fractions within the polymer are in terms of length and weight, and the narrower their distribution function

becomes. However, polymers synthesized using standard industrial manufacturing methods are seldom flawless in terms of polymer chain uniformity. As a result, the PDI of polymers is always greater than 1, and $M_n < M_w$. It also indicates that using M_w or M_n to define the mass of polydisperse samples isn't appropriate, since two individual polymer chains of greatly differing weights may be described by a mean unrelated to their characteristics.

There is another function that can also be used to obtain the molecular weight of the polymers by using a relative method, as developed by Chee et al [138]. It involves measuring the intrinsic viscosities of dilute polymer solutions, and using the Mark-Houwink-Sakurada (Eq 5.5) relationship to obtain the viscosity average molar mass as:

$$M_v = \left[\frac{\sum_{i=1}^{\infty} M_i^{1+a'} N_i}{\sum_{i=1}^{\infty} M_i N_i} \right]^{\frac{1}{a'}} \tag{5.17}$$

where a' is the Mark-Houwink (MH) parameter available for specific polymer-solvent systems. The Mark-Houwink (MH) equation can also be obtained when our Eq 5.4 is reduced to a generalized form. In fact, the scaling parameter a in our Eq 5.4 is of the same form as the MHS exponent a', and replaces it in all of our calculations, as already discussed in section 5.5. M_v always takes up values in between M_n and M_w [136, 139, 140]. The distribution of molar masses can be depicted as in Fig 5.10. It

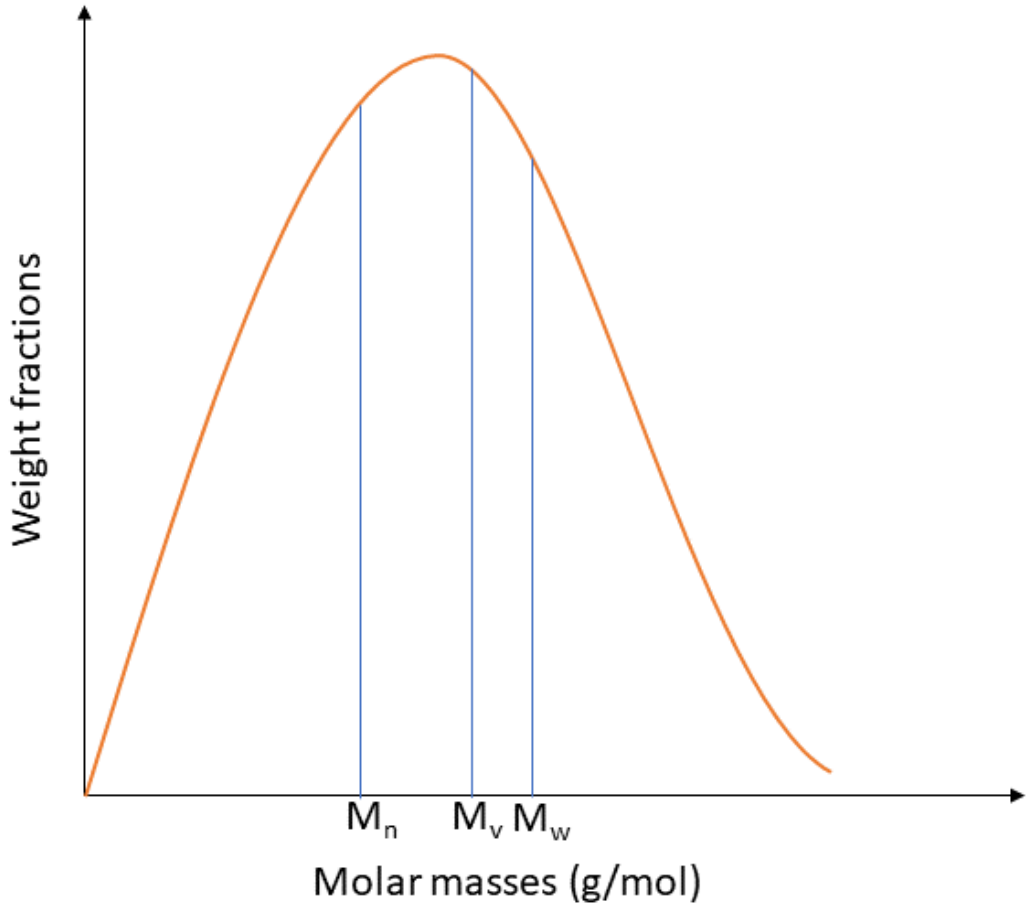

FIGURE 5.10: Molar Mass distributions.

can be seen that for all situations, $M_n < M_v < M_w$. Using Taylor series expansion of

Eq 5.17, and disregarding the higher expansion terms of a, a simple linear equation relating M_w and M_v can be obtained as:

$$M_v = M_w + S(a-1) \tag{5.18}$$

where S is quantified as:

$$S = \frac{\sum_{i=1}^{\infty} M_i{}^2 N_i}{\sum_{i=1}^{\infty} M_i N_i} ln M_i - M_w ln M_w \tag{5.19}$$

On further investigation, it can be observed that the parameter S and M_w can be related through a digamma function of PDI, and it is of the form:

$$\frac{S}{M_w} = \psi(b+2) - ln(b+2) \tag{5.20}$$

Here $\psi(x)$ is the digamma function in (x), which in this scenario is the parameter b, and b itself is related to the PDI as:

$$b = \frac{\text{PDI} - 2}{1 - \text{PDI}} \tag{5.21}$$

It demonstrates that, despite the fact that most literature uses M_w and M_v interchangeably for molecular weight data, this is not always the case. The values will differ greatly depending on the polydispersity in a lot of situations. Crucially, it can be observed that the Eqs 5.20-5.21 cannot describe the case when the PDI = 1 exactly, since b becomes undefined. Taking limits of Eq 5.20, we find that:

$$\begin{gathered} \text{for PDI} \longrightarrow 1 \\ \implies S/M_w \longrightarrow 0 \\ \& \; M_v \longrightarrow M_w \end{gathered}$$

in Eq 5.18. The Schulz distribution function, on which the above Eqs 5.20-5.21 are based on, was derived from real systems, and in all such cases, $M_n \leq M_w$. For the ideal perfect scenario where $M_w = M_n$, there is no need for any model or relevant equations and the distribution function shown in Fig 5.10 collapses to a single straight line. Consequently, M_v is the same in this case as the other molecular weight averaging methods. Therefore, the aforementioned equations are significant because they provide a method for obtaining various averaging indices of molecular weights dependent on their features in real systems. This is more beneficial.

TABLE 5.4: M_v and M_w relations for the polymer systems

Polymer	M_w g/mol	PDI	S/M_w	M_v g/mol
HPC80k	107336	4.71	-0.442	95475
HPC100k	146690	4.82	-0.446	130346
PMMA24k	25063	1.08	-0.037	24831
PMMA70k	73416	1.14	-0.381	66418
PAN150k	333257	2.45	-0.324	306266
PDMS9000	12167	1.93	-0.260	11375
PDMS28000	27615	2.15	-0.291	25607
PDMS63000	55870	2.78	-0.353	50936
PDMS139000	92895	2.14	-0.290	86168

Commercial polymers' polydispersity has a major impact on their applicability. All previous scaling models were created for highly monodispersed standardized

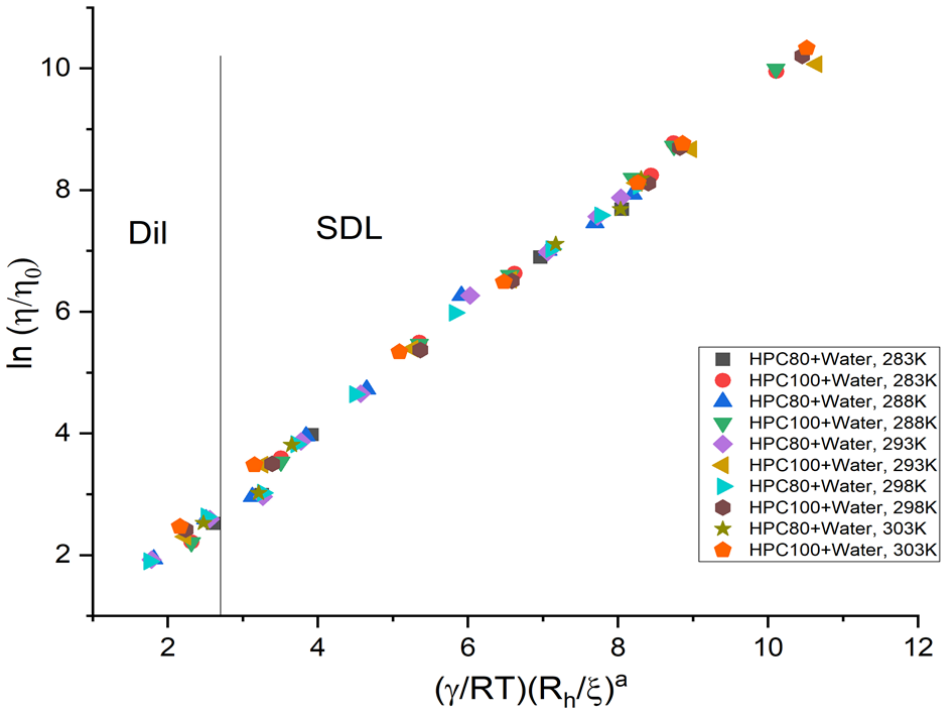

FIGURE 5.11: Viscosity scaling plots for HPC-water at all temperatures (283-303 K), plotted for calculations made with M_v.

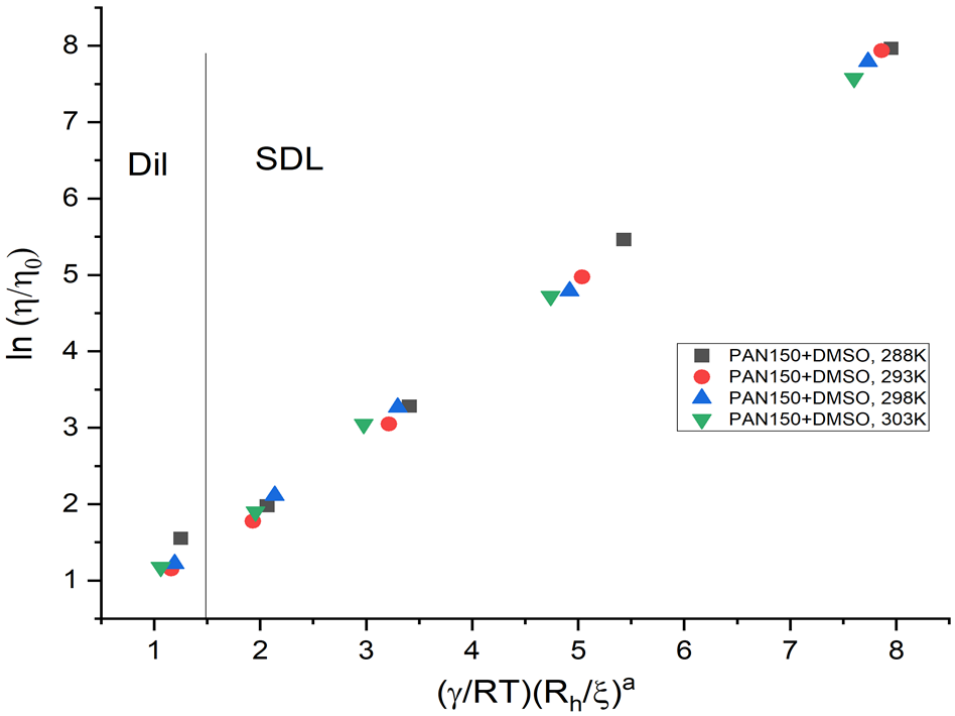

FIGURE 5.12: Viscosity scaling plots for PAN-DMSO at all temperatures (283-303 K), plotted for calculations made with M_v.

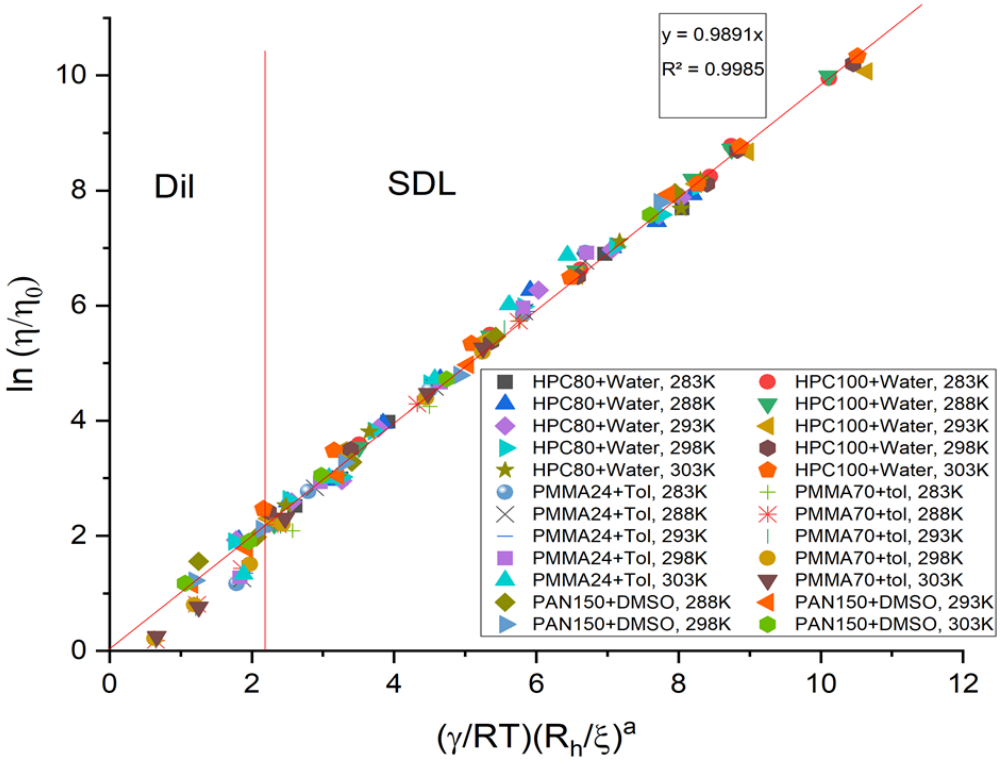

FIGURE 5.13: Combined viscosity scaling plots for all molecular weights of HPC-water, PAN-DMSO and PMMA-toluene at all temperatures (283-303 K), plotted for calculations made with M_v. As per the fitting results, here we fixed M_v, and replaced all M_w.

polymers, as mentioned earlier. Mass production of monodispersed polymers is uncommon in reality. Through Eqs 5.15-5.21, we show the capacity to use our base Eq 5.4 for all types of polymer molecular weight distributions, whether wide or narrow. As can be seen from our GPC results, the HPC polymers had high polydispersities of over 4, and even the polyacrylonitriles had a relatively higher polydispersity. Judging from Eq 5.18, it can be seen that for monodisperse samples and PDI close to 1, the different molecular weight averages, M_w and M_v, are identical and it does not matter which is used for quantitave measurements through the model. In this scenario, it's more popular to use a distribution that can be accessed more quickly by testing, such as GPC. However, once the PDI reaches a certain level, the distance between the distributions widens, making M_v a more accurate option for polydisperse samples. It takes various chain weight fractions into account and gives an averaging method that is closest to the peak. As such, applying Eqs 5.15-5.21, we can obtain the M_v for the different polymer fractions with different molecular weights and it is shown in the Table 5.4. It can be seen from the Table 5.4 that in case of PMMA systems, the PDI is very low, and can always be approximated as monodispersed sample. However, there is still certain variations in the different molecular weight distributions, and the low effect of it is observed through the S/M_w ratios.

The scaling parameter a used in these equations is the same as the scaling parameter a used in our modelling of the dilute solution zones. All of these calculations for M_w or intrinsic viscosity per the Mark-Houwink equations are done at dilute solution ranges, which is consistent with theory. It keeps our study on point with the theory and moves the averaging value to a more accurate estimate. As can also be seen from Table 5.4, the difference in M_w and M_v for the highly monodisperse

samples is extremely low (less than 5%) and therefore maintains the theory that they can be used interchangeably in all such calculations.

Applying M_v for M_w for HPC and PAN calculations provides us with an overall linear fitting as can be seen in Figs 5.11-5.13. All the fitting curves are compared with the use of M_w (Fig 5.9) and M_v (Fig 5.13) separately, and the linearity of the curves noted. It informs us that fitting with M_v is clearly a better choice than M_w, and therefore should be considered in the case of polydisperse samples to obtain a more accurate picture.

5.8 Final fitting results

The final accurate curve of the scaling paradigm was obtained by proper interpretation and implementation of the various parameters in Eq 5.4. Having applied the appropriate values of all the different parameters mention in sections 5.1-5.7, we arrived at the Fig 5.14 for PDMS-ethyl acetate systems. Since the PDMS system was the only one containing the concentrated regime in its scaling, it is necessary to show its fitting separately to give a better idea, as shown in Fig 5.14.

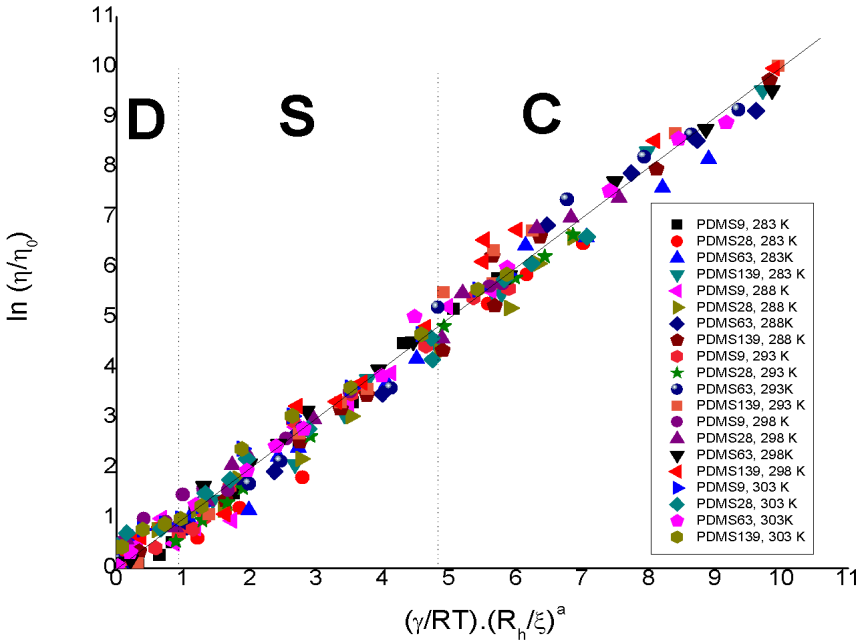

FIGURE 5.14: Complete viscosity scaling for PDMS-ethyl acetate solutions at all moleular weight ranges, including the temperature dependence and the change of parameters at different crossovers. The labels 'D' represents the dilute regime, 'SD' the semi-dilute regime and 'C' the concentrated regime, with the dotted lines in-between representing the cross-over points c* and c** respectively. All fitting parameters were verified before.

Individual scaling curves for HPC, PAN and including PMMA were already shown in Figs 5.13, which contained the proper application of all the different scaling parameters as per Eq 5.4. The following Fig 5.15 is just a combination of the results from Fig 5.13 and Fig 5.14 to provide a complete picture of the total linear scaling. Taking into account the proposed model's simplicity as well as the assumptions and estimations used in the descriptions of ξ, crossover points c^* and c^{**}, coil dimensions R_h and R_g, viscosity average molecular weight distribution M_v, and scaling

and activation energy parameters a and γ, we deem the linear model's consistency to the experimental data to be really successful. This can be seen in Figs 5.14-5.15.

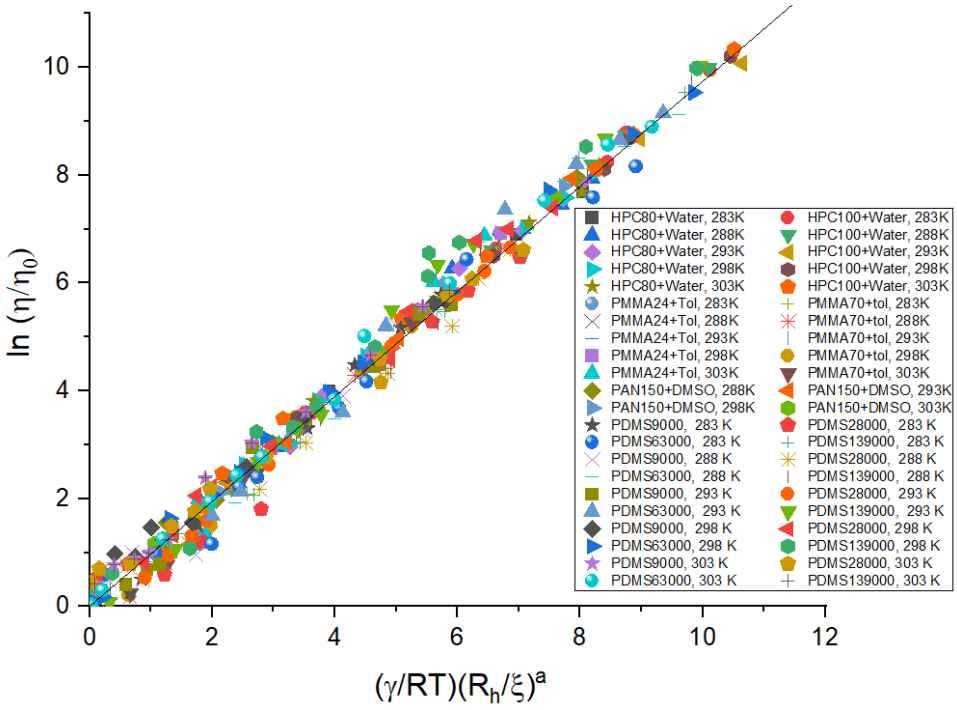

FIGURE 5.15: Continuation of the complete viscosity scaling including the temperature dependence and the change of parameters at different crossovers. Measurements were performed on PDMS-ethyl acetate, HPC-water, PAN-DMSO and PMMA-toluene, for different molecular weights (9-300 kg/mol), concentrations (0.001-8.000 g/cm^3 for PDMS, 0.005-0.300 g/cm^3 for HPC, PAN and PMMA), and temperatures (283-303 K). All fitting parameters were verified before.

5.9 Connectivity to established scaling laws

We probed further into the applicability of the linear scaling model from Eq 5.4 than the viscosity scaling models provided in literature by the general Kirkwood-Riseman [120], Martin [32], Huggins [30], Baker [36], and others [34, 35, 38, 39, 141, 43, 28, 42, 41, 72, 77]. There have also been equations specific to certain polymer-solvent systems as developed by Warrick et al [53] and Kolorlev et al [52]. These equations have the basic form of the relationship for viscosity of polymer solutions as:

$$\eta = \eta_0(1 + c[\eta]) \tag{5.22}$$

where $[\eta]$ is the intrinsic viscosity. As mentioned before, for the non-entangled regime (dilute solutions), a=β^{-1}, and the general form of Eq 5.4 reduces to:

$$\eta = \eta_0[1 + \frac{\gamma_{1,2}}{RT}(\frac{R_h}{R_g})^a \frac{c}{c^*}] \tag{5.23}$$

where we consider only the first term of the series when the exponential function in Eq 5.4 is expanded. This shows that our scaling equation has the same form as Eq 5.22 when considered in the same limits of low concentrations for solutions. Eq 5.22

and Eq 5.23 are of the same general form, and the intrinsic viscosity is expressed as:

$$[\eta] = \frac{\gamma_{1,2}}{RT}(\frac{R_h}{R_g})^a \frac{1}{c^*} \tag{5.24}$$

The inverse relationship between intrinsic viscosity and overlap concentration c^* is also observed in this form , as per the Mark-Houwink equation [66, 142, 143]. Easy estimations of the intrinsic viscosity for polymer dilute solutions can be made through Eq 5.24. More expansion terms of the exponential series in Eq 5.4 will show more precise equations that are similar to the Huggins equation in its most widely used form [30].

If we replace the concentration in g/mL in our Eq 5.4 by the volume fraction ϕ occupied by the polymers in the solution, then the general equation can assume a different form similar to that of Krieger-Dougherty. For a constant molecular weight, the size parameters would be a constant, and instead of c*, we would obtain a maximum packing volume fraction ϕ_m when the viscosity approaches infinite values. With γ, R and T being constants as well, The Eq 5.4 would then take up the form:

$$\frac{\eta}{\eta_0} = exp\left[\left(\frac{\gamma_{1,2}}{RT}\right)\left(k''\frac{\phi}{\phi_m}\right)\right] \tag{5.25}$$

where k'' is a constant obtained from the calculations of radius and molecular weights. Depending on whether we use a stretched exponential function or not, the equation can accordingly reach the form of Mooney [41] or Krieger-Dougherty [42].

If we replace the radius parameters in Eq 5.24 with their power law forms as shown in Eq 3.2 ($R \propto M^y$), and the form of c* in Eq 3.5, we can arrive at the following general form:

$$[\eta] = A\left(\frac{\gamma_{1,2}}{RT}\right) M^{a''} \tag{5.26}$$

where A is a constant obtained by replacing the coefficients in the different equations, and a'' is the accordingly obtained exponent of the order of unity. For other parameters remaining constant, this is the form exhibited by models such as that of Lyons-Tobolski [43] or Mark-Houwink [49] ($[\eta]=KM^{a'}$]. Of course all our plots are dimensionless stretched exponential curves related to the concentration, and it conforms to the models of Simha [58], Utracki [57], Zakin [60], etc.

The Monkos model (Eq 1.33) can be obtained directly if we substitute our parameters to obtain similar form to the constants in his model. This way we obtain the general form:

$$\eta \propto \exp\left(\frac{\gamma}{RT}\right) \tag{5.27}$$

where we obtain direct relation between the viscosity to the activation energies.

As a result, the relationship defined by Eq 5.4 can be suggested for a broad range of scenarios involving the characterization and analysis of polymer solutions in all regimes.

Chapter 6

Summary and Conclusions

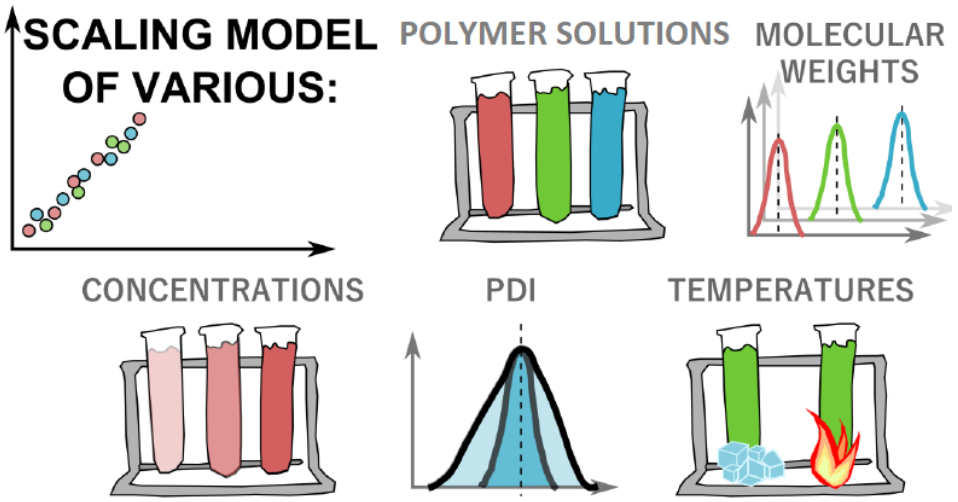

FIGURE 6.1: Summary of macroscopic viscosity scaling model.

In this work, we have developed the previously established nanoscale viscosity scaling paradigm for suitable application to macroscale viscosity analysis as a polymer characterization technique. Utilizing previous studies of PEG/PEO-water solutions as the base, we investigated and modified all the different model parameters, and applied it to multiple different polymer solutions systems. We have ensured that proper definitions of variables that affect the viscosity of a polymer solution have been obtained so that this scaling model can function as an universal characterization technique.

- Our scaling provides a method for characterizing the macroscale viscosity of polymer solutions. It is applicable for a broad range of concentrations, molecular weights, temperatures and polydispersities.

$$\eta_{\text{macro}} = \eta_0 \exp\left[\left(\frac{\gamma}{RT}\right)\left(\frac{R_\text{h}}{\xi}\right)^a\right] \tag{6.1}$$

$$\eta(r_\text{p}) = \frac{k_\text{B}T}{6\pi D r_\text{p}} \tag{6.2}$$

$$R_\text{eff}{}^{-2} = r_\text{p}{}^{-2} + R_\text{h}{}^{-2} \tag{6.3}$$

- Our studies involved measurable parameters, not simply fitted parameters.

$$R_c = KM^y \tag{6.4}$$

$$\xi = R_g(\frac{c}{c^*})^{-\beta} \tag{6.5}$$

- Two distinct crossovers between the concentration regimes were found in our overall studies, as represented by the c^* and c^{**}. The scaling parameters as well as the concentration dependent coil dimensions are altered at these crossover points. The equations for crossover points were:

$$c^* = \frac{M_w}{\frac{4}{3}\pi R_g^3 N_A} \tag{6.6}$$

$$c^{**} = \frac{R_g}{R_g(\theta)}^{2(3\nu-1)/(2\nu-1)} c^* \tag{6.7}$$

- Scaling parameter a changes were of the same order as for the previously reported polymer systems.

- Coil dimension model was carefully developed and applied here appropriately [2]. This allows to guarantee that the effects of concentration changes, interchain and intrachain interations, repulsions and screenings are portrayed in the resulting size and structure of the polymer-solvent systems. These findings reaffirm that the volume occupied by macromolecules, as well as the dynamic molecular structures created by them, greatly influence the rheological properties of complex systems.

$$\frac{R_h}{R_g} \sim x^r, c^{**} > c > c^* \tag{6.8}$$

- Previously developed notions of viscous flow as an activated energy process [92, 108, 94, 2] have been successfully reevaluated to obtain information regarding the various components influencing the flow of complex systems.

$$\gamma = \gamma_{1,2}X_1 + \gamma_{2,2}X_2 \tag{6.9}$$

- The proposed approach has been developed based on common polymer characterization notions: Flory exponents, correlation length and hydrodynamic and gyration radii. All parameters were carefully interpreted and calculated while taking into consideration every variations due to concentration and temperature changes.

- Furthermore, through Eqs 5.18-5.21, We use it for a wide range of standardized and non-standard polymers.

$$M_\mathrm{v} = M_\mathrm{w} + S(a-1) \tag{6.10}$$

This allows for a greater application of the technique from pure academic research to useful industrial processing applications, with an emphasis on commercially used polymers. The majority of studies use samples that are extremely monodispersed. However, large-scale synthesis of such monodispersed

polymers is impractical, and the resulting theories are of limited use in large-scale applications. The ultimate effect of obtaining a general scaling model applicable for large numbers of commercially available polymers is highly important since they are used more regularly.

- Our scaling model is not directly applicable for polymer melts. The use of the solvent viscosity and the solvent component of the interaction energy are vital to this form of scaling, but these parameters do not exist for a pure polymer melt. Our model can be approximated to reach the form of $\eta \propto M^{3.4}$ relationship for polymer melts as proposed by various models [19, 144], however, the exponent would not be the same. For a specific temperature, the different parameters used in our Eq 5.4 such as η_0, ξ, and $\gamma_{1,2}$ are constants. In fact, ξ is maintained as a constant for the concentrated solution regime and does not change beyond the semi-dilute regime as it has no physical meaning in such a regime. Therefore, the Eq 5.4 can be treated as:

$$\eta = A \exp\left[\left(\frac{\gamma_{1,2}X_1 + \gamma_{2,2}X_2}{RT}\right)\left(\frac{R_h}{B}\right)^a\right] \tag{6.11}$$

  where A and B are constants relating to the entanglements present inside a system. In fact, the first term in the brackets of the above Eq 6.11 would also become 0 for a polymer melt. Since the coil sizes would still be a function of the molecular weight of the polymer, the entire equation can be rewritten to the form:

$$\eta = A' \exp\left[\left(\frac{\gamma_{2,2}}{RT}\right) M^m\right] \tag{6.12}$$

  where A' is an overall constant and m exponent relates the molecular weight dependence of the viscosity for polymer melts. This has the same form as proposed in literature [19, 144]. Of course, polymer melts are rarely Newtonian in nature, and require far in-depth rheological studies to determine their viscosity as well as other properties. Since polymer solutions have different form compared to polymer melts, we conclude that our scaling model requires more investigation into identifying the constants mentioned in Eqs 6.11-6.12 so that it can also be applied to polymer melts.

- We developed our conclusions after performing precise viscosity measurements through accurate techniques for a number of model good solvent systems: HPC in water, PMMA in toluene, PAN in DMSO, and PDMS in ethyl acetate. Based on previously well established scaling model, this investigation shows that it can be further enhanced to cover more extensive complex systems. Literature data [86, 94, 108, 2, 98, 122, 111] supports the validity of our proposed physical approach, in conjunction with curves obtained from our own experimental results. We have therefore shown through extensive studies that such a model that was developed from the diffusive motion studies of nanoscale objects in complex systems [89, 85, 102] can be used to analyze and characterize polymer solutions for all purposes. This completes our approach to establishing a uniform length-scale characterization method for different types of polymer systems with different purpose of application.

Bibliography

[1] R Eisenschitz, B Rabinowitsch, and K Weissenberg. "Zur Analyse des formänderungswiderstandes". In: *Mitteilungen der deutschen Materialprüfungsanstalten*. Springer, 1929, pp. 91–94.

[2] Airit Agasty et al. "Scaling equation for viscosity of polydimethylsiloxane in ethyl acetate: From dilute to concentrated solutions". In: *Polymer* 203 (2020), p. 122779.

[3] Tim Osswald and Natalie Rudolph. "Polymer rheology". In: *Carl Hanser, München* (2015).

[4] Wolfgang Ostwald. "About the velocity function of the viscosity "a t disperse systems. i". In: *colloid journal* 36.2 (1925), pp. 99–117.

[5] A de Waele. "The manifestation of interfacial forces in dispersed systems". In: *Journal of the American Chemical Society* 48.11 (1926), pp. 2760–2776.

[6] Pierre J Carreau, Ian F MacDonald, and R Byron Bird. "A nonlinear viscoelastic model for polymer solutions and melts—II". In: *Chemical Engineering Science* 23.8 (1968), pp. 901–911.

[7] KY Yasuda, RC Armstrong, and RE Cohen. "Shear flow properties of concentrated solutions of linear and star branched polystyrenes". In: *Rheologica Acta* 20.2 (1981), pp. 163–178.

[8] Malcolm M Cross. "Rheology of non-Newtonian fluids: a new flow equation for pseudoplastic systems". In: *Journal of colloid science* 20.5 (1965), pp. 417–437.

[9] Roger Pynn and Arne Skjeltorp. *Scaling phenomena in disordered systems*. Vol. 133. Springer Science & Business Media, 2013.

[10] Paul J. Flory. *Principles of polymer chemistry*. Cornell University Press, 1953.

[11] Sam F Edwards. "The statistical mechanics of polymers with excluded volume". In: *Proceedings of the Physical Society (1958-1967)* 85.4 (1965), p. 613.

[12] Pierre-Gilles De Gennes and Pierre-Gilles Gennes. *Scaling concepts in polymer physics*. Cornell university press, 1979.

[13] Prince E Rouse Jr. "A theory of the linear viscoelastic properties of dilute solutions of coiling polymers". In: *The Journal of Chemical Physics* 21.7 (1953), pp. 1272–1280.

[14] Philipp Sebastian Lang. "Reptation in entangled polymer networks". PhD thesis. lmu, 2015.

[15] Werner Kuhn. "über die gestalt fadenförmiger moleküle in lösungen". In: *Kolloid-Zeitschrift* 68.1 (1934), pp. 2–15.

[16] V Lisy, J Tothova, and AV Zatovsky. "The Rouse-Zimm-Brinkman theory of the dynamics of polymers in dilute solutions". In: *arXiv preprint cond-mat/0509398* (2005).

[17] Bruno H Zimm. "Dynamics of polymer molecules in dilute solution: viscoelasticity, flow birefringence and dielectric loss". In: *The journal of chemical physics* 24.2 (1956), pp. 269–278.

[18] Masao Doi and Sam F Edwards. "Dynamics of rod-like macromolecules in concentrated solution. Part 2". In: *Journal of the Chemical Society, Faraday Transactions 2: Molecular and Chemical Physics* 74 (1978), pp. 918–932.

[19] M Doi. "SF Edwards The theory of polymer dynamics". In: *Clarendon, Oxford* (1986).

[20] Mand Doi and SF Edwards. "Dynamics of rod-like macromolecules in concentrated solution. Part 1". In: *Journal of the Chemical Society, Faraday Transactions 2: Molecular and Chemical Physics* 74 (1978), pp. 560–570.

[21] Michael Rubinstein. "Discretized model of entangled-polymer dynamics". In: *Physical review letters* 59.17 (1987), p. 1946.

[22] John G. Kirkwood and Jacob Riseman. "The Intrinsic Viscosities and Diffusion Constants of Flexible Macromolecules in Solution". In: *The Journal of Chemical Physics* 16.6 (1948), pp. 565–573. DOI: 10.1063/1.1746947. eprint: https://doi.org/10.1063/1.1746947. URL: https://doi.org/10.1063/1.1746947.

[23] HC Brinkman. "The viscosity of concentrated suspensions and solutions". In: *The Journal of Chemical Physics* 20.4 (1952), pp. 571–571.

[24] Jacob Riseman and Robert Ullman. "The concentration dependence of the viscosity of solutions of macromolecules". In: *The Journal of Chemical Physics* 19.5 (1951), pp. 578–584.

[25] Nobuhiko Saitô. "Concentration dependence of the viscosity of high polymer solutions. I". In: *Journal of the Physical Society of Japan* 5.1 (1950), pp. 4–8.

[26] Hiromi Yamakawa. "Concentration dependence of polymer chain configurations in solution". In: *The Journal of Chemical Physics* 34.4 (1961), pp. 1360–1372.

[27] Karl F Freed and SF Edwards. "Polymer viscosity in concentrated solutions". In: *The Journal of Chemical Physics* 61.9 (1974), pp. 3626–3633.

[28] George DJ Phillies. "Quantitative prediction of. alpha. in the scaling law for self-diffusion". In: *Macromolecules* 21.10 (1988), pp. 3101–3106.

[29] George DJ Phillies. "Low-shear viscosity of nondilute polymer solutions from a generalized Kirkwood–Riseman model". In: *The Journal of chemical physics* 116.13 (2002), pp. 5857–5866.

[30] Maurice L. Huggins. "The Viscosity of Dilute Solutions of Long-Chain Molecules. IV. Dependence on Concentration". In: *Journal of the American Chemical Society* 64.11 (Nov. 1942), pp. 2716–2718. DOI: 10.1021/ja01263a056.

[31] George DJ Phillies. "Hydrodynamic scaling of viscosity and viscoelasticity of polymer solutions, including chain architecture and solvent quality effects". In: *Macromolecules* 28.24 (1995), pp. 8198–8208.

[32] A.F. Martin. In: *Paper presented at the Memphis meeting of the American Chemical Society, April, 1942* ().

[33] G.W. Schulz and F Blaschke. In: *J. prakti. Chem.* 158.1-8 (1941), pp. 130–135.

[34] H Fikentscher and H Mark. "Ueber die Viskosität lyophiler Kolloide". In: *Kolloid-Zeitschrift* 49.2 (1929), pp. 135–148.

[35] HG de Jong, HR Kruyt, and W Lens. "Zur Kenntnis Der Lyophilen Kolloide". In: *Kolloid Beihefle* 36 (1932), p. 429.

[36] F Baker. "The viscosity of cellulose nitrate solutions". In: *J. Chem. Soc.* 103 (1913), p. 1653.

[37] Svante Arrhenius. "The viscosity of solutions". In: *Biochemical Journal* 11.2 (1917), p. 112.

[38] Wladimir Philippoff. "The viscosity characteristics of rubber solutions". In: *Rubber Chemistry and Technology* 10.1 (1937), pp. 76–104.

[39] HL Bredée and J de Booys. "Kritische Auswertung der Viskositäts-Konzentrationsformeln kolloider Lösungen. I". In: *Kolloid-Zeitschrift* 79.1 (1937), pp. 31–43.

[40] von H Eilers. "Die viskosität von emulsionen hochviskoser stoffe als funktion der konzentration". In: *Kolloid-Zeitschrift* 97.3 (1941), pp. 313–321.

[41] Melvin Mooney. "The viscosity of a concentrated suspension of spherical particles". In: *Journal of colloid science* 6.2 (1951), pp. 162–170.

[42] Irvin M Krieger and Thomas J Dougherty. "A mechanism for non-Newtonian flow in suspensions of rigid spheres". In: *Transactions of the Society of Rheology* 3.1 (1959), pp. 137–152.

[43] PF Lyons and AV Tobolsky. "Viscosity of polypropylene oxide solutions over the entire concentration range". In: *Polymer Engineering & Science* 10.1 (1970), pp. 1–3.

[44] M Rink, A Pavan, and S Roccasalvo. "Concentration dependence of zero-shear viscosity for polymer solutions: A test of the lyons-tobolsky equation". In: *Polymer Engineering & Science* 18.10 (1978), pp. 755–766.

[45] Tohru Kawai. "Viscosity of solution of rigid macromolecules". In: *Die Makromolekulare Chemie, Rapid Communications* 1.3 (1980), pp. 187–191. DOI: https://doi.org/10.1002/marc.1980.030010311. eprint: https://onlinelibrary.wiley.com/doi/pdf/10.1002/marc.1980.030010311. URL: https://onlinelibrary.wiley.com/doi/abs/10.1002/marc.1980.030010311.

[46] VE Dreval, A Ya Malkin, and GO Botvinnik. "Approach to generalization of concentration dependence of zero-shear viscosity in polymer solutions". In: *Journal of Polymer Science: Polymer Physics Edition* 11.6 (1973), pp. 1055–1076.

[47] Shigeharu Onogi et al. "Dependence of viscosity of concentrated polymer solutions upon molecular weight and concentration". In: *Journal of Polymer Science Part A-2: Polymer Physics* 5.5 (1967), pp. 899–913.

[48] Shigeharu Onogi et al. "Effects of molecular weight and concentration on flow properties of concentrated polymer solutions". In: *Journal of Polymer Science Part C: Polymer Symposia*. Vol. 15. 1. Wiley Online Library. 1967, pp. 381–406.

[49] R Houwink. "On the Structure of Rubber." In: *The Journal of Physical Chemistry* 47.6 (1943), pp. 436–442.

[50] AI Goldberg, WP Hohenstein, and H Mark. "Intrinsic viscosity-molecular weight relationship for polystyrene". In: *Journal of Polymer Science* 2.5 (1947), pp. 503–510.

[51] A.J. Barry. "Viscometric Investigation of Dimethylsiloxane Polymers". In: *J. App. Phys.* 17 (1946), p. 1020.

[52] A Ya Korolev et al. "Molekularnyi ves i kharakteristicheskaya vyazkost fraktsii polidimetilsiloksana". In: *Doklady Adademii Nauk SSSR* 89.1 (1953), pp. 65–68.

[53] EL Warrick, WA Piccoli, and FO Stark. "Melt viscosities of dimethylpolysiloxanes". In: *Journal of the American Chemical Society* 77.19 (1955), pp. 5017–5018.

[54] SG Weissberg, Robert Simha, and S Rothman. "Viscosity of dilute and moderately concentrated polymer solutions". In: *Journal of Research of the National Bureau of Standards* 47.3 (1951), pp. 2257–2274.

[55] Robert Simha and Jacques L Zakin. "Solution viscosities of linear flexible high polymers". In: *Journal of Colloid Science* 17.3 (1962), pp. 270–287. ISSN: 0095-8522. DOI: https://doi.org/10.1016/0095-8522(62)90042-9. URL: https://www.sciencedirect.com/science/article/pii/0095852262900429.

[56] L Utracki and Robert Simha. "Corresponding state relations for the viscosity of moderately concentrated polymer solutions". In: *Journal of Polymer Science Part A: General Papers* 1.4 (1963), pp. 1089–1098.

[57] LA Utracki and R Simha. "Viscosity of polymer solutions: scaling relationships". In: *Journal of Rheology* 25.3 (1981), pp. 329–350.

[58] Robert Simha and Lechoslaw Utracki. "Corresponding state relations for the Newtonian viscosity of polymer solutions. II. Further systems and concentrated solutions". In: *Journal of Polymer Science Part A-2: Polymer Physics* 5.5 (1967), pp. 853–874.

[59] Lung-Yu Chou and Jacques L Zakin. "The effect of concentration on the viscosities of solutions of linear flexible high polymers". In: *Journal of Colloid and Interface Science* 25.4 (1967), pp. 547–557.

[60] JL Zakin et al. "Generalized correlations for molecular weight and concentration dependence of zero-shear viscosity of high polymer solutions". In: *Journal of Polymer Science: Polymer Physics Edition* 14.2 (1976), pp. 299–308.

[61] Yoshiaki Takahashi et al. "Zero-shear viscosity of linear polymer solutions over a wide range of concentration". In: *Macromolecules* 18.5 (1985), pp. 1002–1008.

[62] Yoshiaki Takahashi et al. "Zero-shear viscosity of branched polymer solutions". In: *Polymer journal* 18.1 (1986), pp. 89–94.

[63] Yoshiaki Takahashi et al. "Effects of molecular weight distribution on zero-shear viscosity of linear polymers in dilute and semidilute regions". In: *Polymer journal* 24.9 (1992), pp. 987–990.

[64] W Graessley. "Polymer chain dimensions and the dependence of viscoelastic properties on concentration, molecular weight and solvent power". In: *Polymer* 21.3 (Mar. 1980), pp. 258–262. DOI: 10.1016/0032-3861(80)90266-9.

[65] F Brochard and PG De Gennes. "Dynamical scaling for polymers in theta solvents". In: *Macromolecules* 10.5 (1977), pp. 1157–1161.

[66] P. J. Flory and T. G Fox. "Treatment of Intrinsic Viscosities". In: *Journal of the American Chemical Society* 73.5 (May 1951), pp. 1904–1908. DOI: 10.1021/ja01149a002.

[67] JJ Hermans. "Polymer Solution Properties, Part II: Hydrocynamics and Light Scattering". In: *Dowden, Hutchinson, and Ross, Stroudsburg, Pa* (1978).

[68] Hans Christian Öttinger. "Generalized Zimm model for dilute polymer solutions under theta conditions". In: *The Journal of chemical physics* 86.6 (1987), pp. 3731–3749.

[69] Fumiaki Abe et al. "Excluded-volume effects on the mean-square radius of gyration of oligo-and polystyrenes in dilute solutions". In: *Macromolecules* 26.8 (1993), pp. 1884–1890.

[70] Ken Horita et al. "Excluded-volume effects on the intrinsic viscosity of oligo-and polystyrenes. Solvent effects". In: *Macromolecules* 26.19 (1993), pp. 5067–5072.

[71] Fumiaki Abe et al. "Excluded-volume effects on the mean-square radius of gyration and intrinsic viscosity of oligo-and poly (methyl methacrylates)". In: *Macromolecules* 27.3 (1994), pp. 725–732.

[72] Ken Horita et al. "Excluded-volume effects on the transport coefficients of oligo-and poly (dimethylsiloxane) s in dilute solution". In: *Macromolecules* 28.13 (1995), pp. 4455–4463.

[73] M. Daoud et al. "Solutions of Flexible Polymers. Neutron Experiments and Interpretation". In: *Macromolecules* 8.6 (Nov. 1975), pp. 804–818. DOI: 10.1021/ma60048a024.

[74] M. Daoud and G. Jannink. "Temperature-concentration diagram of polymer solutions". In: *Journal de physique* 37.7-8 (1976), pp. 973–979.

[75] Takahiro Sato and Akio Teramoto. "Dynamics of stiff-chain polymers in isotropic solution: zero-shear viscosity of rodlike polymers". In: *Macromolecules* 24.1 (1991), pp. 193–196.

[76] Takahiro Sato, Yuji Jinbo, and Akio Teramoto. "Intermolecular interaction of stiff-chain polymers in solution". In: *Macromolecules* 30.3 (1997), pp. 590–596.

[77] Karol Monkos. "Viscosity analysis of the temperature dependence of the solution conformation of ovalbumin". In: *Biophysical Chemistry* 85.1 (2000), pp. 7–16.

[78] George DJ Phillies et al. "Phenomenological scaling laws for "semidilute"macromolecule solutions from light scattering by optical probe particles". In: *The Journal of chemical physics* 82.11 (1985), pp. 5242–5246.

[79] George DJ Phillies. "The hydrodynamic scaling model for polymer self-diffusion". In: *The Journal of Physical Chemistry* 93.13 (1989), pp. 5029–5039.

[80] George DJ Phillies. "Chain architecture in the hydrodynamic scaling picture for polymer dynamics". In: *Macromolecules* 23.10 (1990), pp. 2742–2748.

[81] George DJ Phillies. "The hydrodynamic scaling model for polymer dynamics". In: *Journal of non-crystalline solids* 131 (1991), pp. 612–619.

[82] George DJ Phillies. "Range of validity of the hydrodynamic scaling model". In: *The Journal of Physical Chemistry* 96.24 (1992), pp. 10061–10066.

[83] George DJ Phillies. "The hydrodynamic scaling model for the dynamics of non-dilute polymer solutions: A comprehensive review". In: *arXiv preprint arXiv:1606.09302* (2016).

[84] Jedrzej Szymański et al. "Diffusion and viscosity in a crowded environment: from nano-to macroscale". In: *The Journal of Physical Chemistry B* 110.51 (2006), pp. 25593–25597.

[85] Tomasz Kalwarczyk et al. "Comparative analysis of viscosity of complex liquids and cytoplasm of mammalian cells at the nanoscale". In: *Nano letters* 11.5 (2011), pp. 2157–2163.

[86] Tomasz Kalwarczyk et al. "Motion of nanoprobes in complex liquids within the framework of the length-scale dependent viscosity model". In: *Advances in colloid and interface science* 223 (2015), pp. 55–63.

[87] Howard K Schachman and William F Harrington. "On Viscosity Measurement in the Ultracentrifuge1". In: *Journal of the American Chemical Society* 74.15 (1952), pp. 3965–3966.

[88] Yu Cheng, Robert K Prud'Homme, and James L Thomas. "Diffusion of mesoscopic probes in aqueous polymer solutions measured by fluorescence recovery after photobleaching". In: *Macromolecules* 35.21 (2002), pp. 8111–8121.

[89] Robert Holyst et al. "Scaling form of viscosity at all length-scales in poly (ethylene glycol) solutions studied by fluorescence correlation spectroscopy and capillary electrophoresis". In: *Physical Chemistry Chemical Physics* 11.40 (2009), pp. 9025–9032.

[90] Tomasz Kalwarczyk, Marcin Tabaka, and Robert Holyst. "Biologistics—diffusion coefficients for complete proteome of Escherichia coli". In: *Bioinformatics* 28.22 (2012), pp. 2971–2978.

[91] Marcin Tabaka, Tomasz Kalwarczyk, and Robert Hołyst. "Quantitative influence of macromolecular crowding on gene regulation kinetics". In: *Nucleic acids research* 42.2 (2013), pp. 727–738.

[92] Krzysztof Sozanski et al. "Activation energy for mobility of dyes and proteins in polymer solutions: from diffusion of single particles to macroscale flow". In: *Physical review letters* 111.22 (2013), p. 228301.

[93] Krzysztof Sozański et al. "Small crowders slow down kinesin-1 stepping by hindering motor domain diffusion". In: *Physical review letters* 115.21 (2015), p. 218102.

[94] Agnieszka Wisniewska et al. "Scaling of activation energy for macroscopic flow in poly (ethylene glycol) solutions: entangled–non-entangled crossover". In: *Polymer* 55.18 (2014), pp. 4651–4657.

[95] Ken Horita et al. "Excluded-Volume Effects on the Transport Coefficients of Oligo-and Poly (dimethylsiloxane) s in Dilute Solution". In: *Macromolecules* 28.13 (1995), pp. 4455–4463.

[96] Ryan C. Hayward and William W. Graessley. "Excluded Volume Effects in Polymer Solutions. 1. Dilute Solution Properties of Linear Chains in Good and θ Solvents". In: *Macromolecules* 32.10 (1999), pp. 3502–3509.

[97] William W. Graessley, Ryan C. Hayward, and Gary S. Grest. "Excluded-volume effects in polymer solutions. 2. Comparison of experimental results with numerical simulation data". In: *Macromolecules* 32.10 (1999), pp. 3510–3517.

[98] Gang Cheng, W. W. Graessley, and Y. B. Melnichenko. "Polymer dimensions in good solvents: crossover from semidilute to concentrated solutions". In: *Physical review letters* 102.15 (2009), p. 157801.

[99] Iwao Teraoka. *Polymer solutions: an introduction to physical properties*. John Wiley & Sons, 2002.

[100] Masao Doi. *Introduction to polymer physics*. Oxford university press, 1996.

[101] Tomasz Kalwarczyk et al. "Comparative Analysis of Viscosity of Complex Liquids and Cytoplasm of Mammalian Cells at the Nanoscale". In: *Nano Letters* 11.5 (2011). PMID: 21513331, pp. 2157–2163. DOI: 10.1021/nl2008218. eprint: https://doi.org/10.1021/nl2008218. URL: https://doi.org/10.1021/nl2008218.

[102] Tomasz Kalwarczyk et al. "Length-scale dependent transport properties of colloidal and protein solutions for prediction of crystal nucleation rates". In: *Nanoscale* 6.17 (2014), pp. 10340–10346.

[103] Chi Wu. "Light-Scattering evidence of a "critical" concentration for polymer coil shrinking in dilute solution". In: *Journal of Polymer Science Part B: Polymer Physics* 32.8 (June 1994), pp. 1503–1509. DOI: 10.1002/polb.1994.090320822.

[104] Rongshi Cheng. "On the concentration regimes of a flexible-chain polymer solution". In: *Macromolecular Symposia* 124.1 (Oct. 1997), pp. 27–34. DOI: 10.1002/masy.19971240106.

[105] Anastasios Dondos, Constantinos Tsitsilianis, and George Staikos. "Viscometric study of aggregation phenomena in polymer dilute solutions and determination of the critical concentration c**". In: *Polymer* 30.9 (Sept. 1989), pp. 1690–1694. DOI: 10.1016/0032-3861(89)90332-7.

[106] Anastasios Dondos and Constantinos Tsitsilianis. "Viscometric study of extremely dilute macromolecular solutions: Critical concentration c and the intrinsic viscosity of the polystyrene through scaling laws. The values of the Huggins constant". In: *Polymer International* 28.2 (1992), pp. 151–156. DOI: 10.1002/pi.4990280209.

[107] Henry Eyring. "Viscosity, Plasticity, and Diffusion as Examples of Absolute Reaction Rates". In: *The Journal of Chemical Physics* 4.4 (Apr. 1936), pp. 283–291. DOI: 10.1063/1.1749836.

[108] Agnieszka Wisniewska et al. "Scaling equation for viscosity of polymer mixtures in solutions with application to diffusion of molecular probes". In: *Macromolecules* 50.11 (2017), pp. 4555–4561.

[109] Johannes Brandrup et al. *Polymer handbook*. Vol. 89. Wiley New York, 1999.

[110] William W Graessley. *Polymeric liquids & networks: structure and properties*. Garland Science, 2003.

[111] Simona Gagliardi et al. "Conformation of cyclic and linear polydimethylsiloxane in the melt: a small-angle neutron-scattering study". In: *Applied Physics A* 74.1 (2002), s469–s471.

[112] Michael Rubinstein, Ralph H Colby, et al. *Polymer physics*. Vol. 23. Oxford university press New York, 2003.

[113] Youngho Eom and Byoung Chul Kim. "Solubility parameter-based analysis of polyacrylonitrile solutions in N, N-dimethyl formamide and dimethyl sulfoxide". In: *Polymer* 55.10 (2014), pp. 2570–2577.

[114] Youngho Eom and Byoung Chul Kim. "Effects of chain conformation on the viscoelastic properties of polyacrylonitrile gels under large amplitude oscillatory shear". In: *European Polymer Journal* 85 (2016), pp. 341–353.

[115] Robert Evans and Adrian FA Wallis. "Cellulose molecular weights determined by viscometry". In: *Journal of applied polymer science* 37.8 (1989), pp. 2331–2340.

[116] Mohammad R Kasaai. "Comparison of various solvents for determination of intrinsic viscosity and viscometric constants for cellulose". In: *Journal of applied polymer science* 86.9 (2002), pp. 2189–2193.

[117] Josua Timotheus Oberlerchner, Thomas Rosenau, and Antje Potthast. "Overview of methods for the direct molar mass determination of cellulose". In: *Molecules* 20.6 (2015), pp. 10313–10341.

[118] Goksu Cinar Ciftci et al. "Tailoring of rheological properties and structural polydispersity effects in microfibrillated cellulose suspensions". In: *Cellulose* 27.16 (2020), pp. 9227–9241.

[119] Chong Meng Kok and Alfred Rudin. "Relationship between the hydrodynamic radius and the radius of gyration of a polymer in solution". In: *Die Makromolekulare Chemie, Rapid Communications* 2.11 (1981), pp. 655–659.

[120] John G Kirkwood and Jacob Riseman. "The intrinsic viscosities and diffusion constants of flexible macromolecules in solution". In: *The Journal of Chemical Physics* 16.6 (1948), pp. 565–573.

[121] A Ziya Akcasu and Charles C Han. "Molecular weight and temperature dependence of polymer dimensions in solution". In: *Macromolecules* 12.2 (1979), pp. 276–280.

[122] A Bennett et al. "Concentration dependence of static and hydrodynamic screening lengths for three different polymers in a variety of solvents". In: *Polymer* 45.25 (2004), pp. 8531–8540.

[123] Saumil Sudhir Vadodaria and Robert John English. "Aqueous solutions of HEC and hmHEC: effects of molecular mass versus hydrophobic associations on hydrodynamic and thermodynamic parameters". In: *Cellulose* 23.2 (2016), pp. 1107–1121.

[124] W Brown, D Henley, and J Öhman. "Studies on cellulose derivatives. Part II. The influence of solvent and temperature on the configuration and hydrodynamic behaviour of hydroxyethyl cellulose in dilute solution". In: *Die Makromolekulare Chemie: Macromolecular Chemistry and Physics* 64.1 (1963), pp. 49–67.

[125] Richard P. Wool. "Polymer entanglements". In: *Macromolecules* 26.7 (Mar. 1993), pp. 1564–1569. DOI: 10.1021/ma00059a012.

[126] Michael Rubinstein, Ralph H. Colby, and Andrey V. Dobrynin. "Dynamics of Semidilute Polyelectrolyte Solutions". In: *Physical Review Letters* 73.20 (Nov. 1994), pp. 2776–2779. DOI: 10.1103/physrevlett.73.2776.

[127] Liang Ying, Chen Hou, and Wang Fei. "Diffusion coefficient of DMSO in polyacrylonitrile fiber formation". In: *Journal of applied polymer science* 100.6 (2006), pp. 4447–4451.

[128] Christian Clasen and W-M Kulicke. "Determination of viscoelastic and rheooptical material functions of water-soluble cellulose derivatives". In: *Progress in polymer science* 26.9 (2001), pp. 1839–1919.

[129] Coralie Brumaud et al. "Cellulose ethers and water retention". In: *Cement and Concrete Research* 53 (2013), pp. 176–184.

[130] Thipphaya Cherdhirankorn et al. "Diffusion in Polymer Solutions Studied by Fluorescence Correlation Spectroscopy". In: *The Journal of Physical Chemistry B* 113.11 (Mar. 2009), pp. 3355–3359. DOI: 10.1021/jp809707y.

[131] SO Ilyin et al. "Viscosity of polyacrylonitrile solutions: The effect of the molecular weight". In: *Polymer Science Series A* 57.4 (2015), pp. 494–500.

[132] R. E. Powell, W. E. Roseveare, and Henry Eyring. "Diffusion, Thermal Conductivity, and Viscous Flow of Liquids". In: *Industrial & Engineering Chemistry* 33.4 (Apr. 1941), pp. 430–435. DOI: 10.1021/ie50376a003.

[133] Walther Burchard. "Solubility and solution structure of cellulose derivatives". In: *Cellulose* 10.3 (2003), pp. 213–225.

[134] Henri Benoit, Alfred M Holtzer, and Paul Doty. "An experimental study of polydispersity by light scattering". In: *The Journal of Physical Chemistry* 58.8 (1954), pp. 635–640.

[135] Thomas Carl Ward. *Molecular weight and molecular weight distributions in synthetic polymers*. 1981.

[136] P Manaresi et al. "A general intrinsic viscosity-molecular weights relationship for polydisperse polymers". In: *European polymer journal* 24.6 (1988), pp. 575–578.

[137] Yu-Ping Chin, George Aiken, and Edward O'Loughlin. "Molecular weight, polydispersity, and spectroscopic properties of aquatic humic substances". In: *Environmental science & technology* 28.11 (1994), pp. 1853–1858.

[138] KK Chee. "Estimation of molecular weight averages from intrinsic viscosity". In: *Journal of applied polymer science* 30.4 (1985), pp. 1359–1363.

[139] Walter E Gloor. "The numerical evaluation of parameters in distribution functions of polymers from their molecular weight distributions". In: *Journal of Applied Polymer Science* 22.5 (1978), pp. 1177–1182.

[140] Walter E Gloor. "Extending the continuum of molecular weight distributions based on the generalized exponential (Gex) distributions". In: *Journal of Applied Polymer Science* 28.2 (1983), pp. 795–805.

[141] J Lefebvre. "Viscosity of concentrated protein solutions". In: *Rheologica Acta* 21.4 (1982), pp. 620–625.

[142] Shoei Fujishige. "Intrinsic Viscosity-Molecular Weight Relationships for Poly(N-isopropylacrylamide) Solutions". In: *Polymer Journal* 19.3 (Mar. 1987), pp. 297–300. DOI: 10.1295/polymj.19.297.

[143] E.R. Morris et al. "Concentration and shear rate dependence of viscosity in random coil polysaccharide solutions". In: *Carbohydrate Polymers* 1.1 (Sept. 1981), pp. 5–21. DOI: 10.1016/0144-8617(81)90011-4.

[144] Ralph H Colby, Lewis J Fetters, and William W Graessley. "The melt viscosity-molecular weight relationship for linear polymers". In: *Macromolecules* 20.9 (1987), pp. 2226–2237.